

University of Alberta

**Membrane and Mitochondrial Responses
to Cryobiological Conditions**

by

Anthony John Reardon

A thesis submitted to the Faculty of Graduate Studies and Research
in partial fulfillment of the requirements for the degree of

Master of Science

Medical Sciences - Laboratory Medicine and Pathology

©Anthony John Reardon

Spring 2013

Edmonton, Alberta

Permission is hereby granted to the University of Alberta Libraries to reproduce single copies of this thesis and to lend or sell such copies for private, scholarly or scientific research purposes only.

Where the thesis is converted to, or otherwise made available in digital form, the University of Alberta will advise potential users of the thesis of these terms.

The author reserves all other publication and other rights in association with the copyright in the thesis and, except as herein before provided, neither the thesis nor any substantial portion thereof may be printed or otherwise reproduced in any material form whatsoever without the author's prior written permission.

Abstract

The success of cellular cryopreservation is indicated by the state of post-thawed cells. Using human umbilical vein endothelial cells as a model, the cryobiological response to interrupted cooling protocols was evaluated with a combination of fluorescence microscopy and flow cytometry. Cryoinjured cells were identified using fluorescence intensity with flow cytometry, where light scatter gating strategies were shown to have limitations. Plasma membrane integrity has become the standard assay for post-thaw cell survival. This investigation provided a direct comparison of the integrity of the plasma membrane with the functional state of mitochondria in frozen-thawed cells. A disconnect was found between these two sites of cryoinjury: at specific low temperature conditions cells with depolarized mitochondria still had an intact plasma membrane. This result indicates that different mechanisms may affect each of these sites of cryoinjury. These findings are of interest in understanding the mechanisms of cryoinjury required to minimize cell damage during cryopreservation.

Acknowledgements

I would like to express my appreciation to several individuals for their contributions to this thesis.

To my supervisors, Drs. Locksley McGann and Janet Elliott: I am grateful to have had two of the most dedicated and supportive mentors a student could ask for. Thank you for the encouragement, knowledge, and enthusiasm that made me a better researcher and a better person.

To my committee members, Drs. Jason Acker and Thomas Churchill: Thank you for your contributions, feedback, and advice.

To the past and present members of the McGann/Elliott and Acker Cryolabs, especially Dr. Lisa Ross-Rodriguez, Michal Zielinski, Garson Law, and Billal Sultani: Thank you for your insightful discussions and easy-going conversations.

To my parents, Mark and Mary-Lynne: Thank you for providing the foundation to base my life on. And to my brothers, Patrick, Matthew and Peter: Thank you for sometimes shaking that foundation.

To my wife Shari: Thank you for being there. None of this would have been possible without your motivation and unwavering support.

Table of Contents

CHAPTER 1 – INTRODUCTION	1
1.1 Cryobiology and its applications	1
1.2 Cryoinjury	3
1.3 Methods in cryopreservation	6
1.3.1 Conventional cryopreservation procedures	6
1.3.2 Interrupted cooling protocols	8
1.4 Assessments of cryoinjury	10
1.4.1 The integrity of the plasma membrane	10
1.4.2 Subcellular alterations	11
1.4.3 Tools for investigating cryoinjury	12
1.5 Aim of thesis	13
1.6 Hypotheses	14
1.7 Objectives, tools and approach	14
1.7 References	17
CHAPTER 2 - CHARACTERIZING HUVEC CRYOBIOLOGICAL RESPONSES USING INTERRUPTED COOLING PROTOCOLS	22
2.1 Introduction	22
2.2 Materials and methods	27
2.2.1 Cell cultures	27

2.2.2 Interrupted cooling protocols	28
2.2.3 Assessment of cell recovery	30
2.2.4 Statistical Analysis	31
2.3 Results and discussion	32
2.3.1 Investigating the impact of cooling rate on the HUVEC response to interrupted slow cooling	32
2.3.2 A detailed investigation of HUVEC responses to changes in hold time at -9 °C and -12 °C for interrupted rapid cooling	36
2.3.3 Investigating the HUVEC response to decreasing hold temperatures during interrupted rapid cooling	39
2.4 Conclusions	42
2.5 References	55

CHAPTER 3 - FLUORESCENCE AS AN ALTERNATIVE TO LIGHT SCATTER GATING STRATEGIES TO IDENTIFY FROZEN-THAWED CELLS WITH FLOW CYTOMETRY 58

3.1 Introduction	58
3.2 Materials and methods	62
3.2.1 Cell cultures	62
3.2.2 Assessment of cell recovery	63
3.2.3 Flow cytometry analysis	64
3.3.4 Statistical Analysis	66
3.3 Results	66
3.3.1 Effectiveness of forward light scatter gating	66

3.3.2 Effectiveness of fluorescence gating with a membrane integrity assay – SytoEB	68
3.3.3 Effectiveness of fluorescence gating with a mitochondrial polarization assay – JC-1	71
3.4 Discussion	74
3.5 Conclusions	78
3.6 References	88
CHAPTER 4. INTERRUPTED SLOW COOLING OF HUVEC: A COMPARATIVE ANALYSIS OF MITOCHONDRIAL AND MEMBRANE CRYOINJURY	93
4.1 Introduction	93
4.2 Materials and methods	96
4.2.1 Cell cultures	96
4.2.2 Interrupted cooling protocol	97
4.2.3 Assessment of cell recovery	98
4.2.4 Flow cytometry assessment	99
4.2.5 Statistical Analysis	100
4.3 Results and discussion	101
4.3.1 Controls and contour plots: measurements of mitochondrial membrane potential with flow cytometry	101
4.3.2 Investigating the effect of decreasing temperature on the polarization state of HUVEC mitochondria during interrupted slow cooling	103

4.3.3 Mitochondria and the membrane: a comparison of HUVEC mitochondrial polarization and membrane integrity during interrupted slow cooling	105
4.4 Conclusions	108
4.5 References	116
CHAPTER 5 – GENERAL DISCUSSION AND CONCLUSIONS	119
5.1 Review of aim and hypotheses	119
5.2 Summary of thesis results	119
5.3 Significance in cryobiology	122
5.4 References	124
APPENDIX A.	125
A verification of controls: membrane integrity with fluorescence microscopy and flow cytometry	125

List of tables

Table		Page
2-1	Membrane integrity response of HUVEC to interrupted slow cooling at different cooling rates.	51
2-2	Membrane integrity response of HUVEC to interrupted rapid cooling as a function of hold temperature for different hold times.	54

List of figures

Figure		Page
2-1	Representative light microscopy photograph depicting appearance of adhered HUVEC culture prior to trypsinization for experimentation.	44
2-2	Schematic of interrupted slow cooling at a rate of 1.0 °C/min.	45
2-3	Schematic of interrupted rapid cooling with a 3 minute hold time.	46
2-4	Fluorescent microscope images of HUVEC stained with SytoEB	47
2-5	Plot of hydraulic conductivity (L_p) as a function of temperature for HUVEC and TF-1 cells	48
2-6	Arrhenius plot of natural logarithm of L_p ($\mu\text{m}/\text{min}/\text{atm}$) for HUVEC and TF-1 cells as a function of inverse temperature (K^{-1})	49
2-7	Response of HUVEC to interrupted slow cooling at different cooling rates	50
2-8	Response of HUVEC to interrupted rapid cooling as a function of hold time for two different hold temperatures	52
2-9	Response of HUVEC to interrupted rapid cooling as a function of hold temperature for different hold times	53
3-1	Flow cytometry forward vs. side scatter intensity plots of HUVEC room temperature controls	80
3-2	Flow cytometry forward vs. side scatter intensity plots of HUVEC after plunging in liquid nitrogen	81

3-3	SytoEB membrane integrity analysis of HUVEC control samples as measured by flow cytometry	82
3-4	SytoEB membrane integrity analysis of HUVEC plunge samples as measured by flow cytometry	83
3-5	Membrane integrity analysis of events identified as cells	84
3-6	JC-1 mitochondrial polarization analysis of events gated as cells and debris in HUVEC control samples measured with flow cytometry	85
3-7	JC-1 mitochondrial polarization analysis of HUVEC plunge samples measured with flow cytometry	86
3-8	JC-1 mitochondrial polarization analysis of HUVEC red fluorescence measured with flow cytometry	87
4-1	Representation of HUVEC control at room temperature	110
4-2	Contour plots of HUVEC mitochondrial polarization analysis with JC-1	111
4-3	Contour plots of mitochondrial polarization of directly thawed HUVEC from different temperatures when cooled at 0.2 °C/min	112
4-4	Contour plots of mitochondrial polarization of plunge-thawed HUVEC from different temperatures after cooling at 0.2 °C/min	113
4-5	Summary of HUVEC mitochondrial polarization (JC-1) analysis	114
4-6	Comparison of membrane integrity (SytoEB) and mitochondrial polarization (JC-1) analysis of HUVEC	115
A-1	Contour plots of HUVEC membrane integrity analysis with SytoEB	127

List of symbols and abbreviations

Symbols

L_p	hydraulic conductivity	$\mu\text{m}/\text{min}/\text{atm}$
K	Temperature	K

Abbreviations

HUVEC	human umbilical vein endothelial cells
IIF	intracellular ice formation
Me_2SO	dimethyl sulfoxide
EB	ethidium bromide
EBM	endothelial basal media
ANOVA	analysis of variance
CO_2	carbon dioxide
PBS	phosphate buffered saline
JC-1	5',6,6'-tetrachloro-1,1',3,3'-tetraethylbenzimidazolylcarbocyanine Iodide
AU	Arbitrary units

Chapter 1 – Introduction

The success of cryopreservation protocols is dependent on the ability of cells to survive the process of freezing and thawing. Survival is typically assessed by interpreting the state of the cell post-thaw. The integrity of the plasma membrane has become one of the standard methods of determining the viability of cells in cryopreservation procedures. However, the cell is a complex entity and the capability of cells to carry out a diverse number of critical processes within the human body suggests that the cell plasma membrane is only a partial reflection of cell viability. There has been increased interest in testing various aspects of cell function when developing cryopreservation protocols to alleviate damage to various components of frozen-thawed cells. A comparison of freezing injury to two different cell constituents will give insight into the mechanisms of cell damage during cryopreservation, and lead to the development of novel approaches of protecting cryopreserved cells in future protocols.

1.1 Cryobiology and its applications

The field of cryobiology is concerned with the study of life at low temperatures. Cryopreservation is the utilization of low temperatures for the purpose of long term storage of cells and tissues. However, the change of conditions involved with decreasing temperatures and the

phase transition as water solidifies to ice have deleterious effects on cells. This presents cryobiologists with a peculiar dilemma as low temperatures have the ability to preserve cells for long periods of time by slowing metabolic activity and suppressing biochemical reactions, but the progression to these temperatures is potentially harmful. The underlying challenge in cryobiology is to bring cells down to preservation temperatures without damaging them in the process. Cryobiologists continue to pursue this ambitious undertaking and have had much success in the preservation of cells and tissues despite the potentially damaging effects of freezing.

Preservation of cells and tissues benefits through collaboration among a diverse number of scientific fields, including medicine, bio-conservation, agriculture, and food science. The challenges involved in preservation often require a 'mixed bag' of experts from diverse fields including engineers, medical physicians, physicists, chemists, and biologists.

Cryopreservation plays a key role in the long term storage of natural and engineered tissues for medical applications. The availability of smaller components such as valves and vessels for reconstructive surgery help to alleviate the demand for whole organ transplantation. Human umbilical cord cells are a readily available and ethically attainable source of endothelial cells that are being investigated for use in engineered cardiovascular tissues [19]. Endothelial cell loss and degeneration during

cryopreservation [17, 41] poses a particular problem in preservation of engineered tissues. The added complexity of cell-cell and cell-matrix interactions influences the cryobiological responses of cells at low temperatures [43, 56]. This study uses human umbilical endothelial cells (HUVEC) in suspension to investigate the cryobiological responses of these cells throughout slow and rapid interrupted cooling protocols.

1.2 Cryoinjury

There are several excellent reviews on the effects of freezing when subjecting cells to low temperatures [12, 15, 25, 35, and 36]. The cooling of cells in suspension and the initiation of ice nuclei at high subzero temperatures results in ice growth in the extracellular space, and continual cooling to further subzero temperatures leads to continued ice crystal growth that removes pure water from the solution as ice. Removing water as ice leads to the solutes in the remaining unfrozen liquid fraction becoming increasingly concentrated. An imbalance in osmolality occurs as the solute concentration in the interior of the cell is less than in the exterior, resulting in the formation of an osmotic gradient. In order to restore equilibrium, a cooling rate dependent cell response will take place. At low cooling, the cell will efflux water in response to formation of extracellular ice and the cell will be able to remain close to osmotic equilibrium as long as the cooling rate is sufficiently low to allow for dehydration at the same rate that extracellular ice is forming. At cooling

rates too high for the cell to maintain equilibrium by loss of intracellular water, the unfrozen fraction within the cell becomes increasingly supercooled and equilibrium is then achieved by the formation of ice intracellularly. Under both of these circumstances the responses of cells to maintain equilibrium at cooling rates too low or too high have the potential to induce injury.

The “two-factor hypothesis” of freezing injury proposed by Mazur *et al.* includes both of these potentially injurious scenarios [29]. The water lost from dehydrating cells at lower cooling rates leads to increased intracellular and extracellular solutes, causing what has been termed “solution effects” injury [29]. Rapid cooling does not allow enough time for water to sufficiently efflux from the cell as the cytoplasm becomes increasingly supercooled, increasing the probability of intracellular ice formation (IIF) [29]. A cooling rate is considered optimal for a given cell type if it is high enough to minimize solution effects but low enough to decrease the probability of intracellular ice.

There are various theories to explain the occurrence of cell injury when cooling at lower than optimal rates. Lovelock proposed that cell damage was due to high salt concentrations, as water is removed during water efflux and solutes concentrate inside the cell [22]. These high salt concentrations cause the cell membrane to become leaky, leading to higher concentrations of intracellular salt and a greater influx of water upon dilution causing cell lysis [22]. Meryman hypothesized that there is a

critical limit of volume to which a cell can shrink and that a mechanical resistance to further shrinkage occurs when reaching this minimal volume. According to Meryman, this minimum volume leads to the occurrence of a pressure gradient across the cell membrane that allows for influx of solutes into the cell [38]. Returning the cell to isotonic conditions upon thawing significantly increases cell volume, resulting in membrane damage and lysis [38]. Cells may also be adversely affected by temperature changes (thermal shock) and show post-hypertonic damage during thawing (dilution shock) [11]. The damage from slow cooling presents a potentially injurious scenario to cells as solutes concentrate both intracellularly and extracellularly in the presence of ice that can alter the cell membrane and its properties.

The occurrence of cell damage due to high cooling rates has been most commonly linked with the formation of intracellular ice. There is a significant amount of evidence to suggest that the formation of intracellular ice is a lethal event for cells in suspension [14, 25, 26, 39, 40, 42, and 59]. At these high rates of cooling in the presence of extracellular ice the cell cytoplasm can become supercooled. This may be attributed to the plasma membrane acting as a barrier to propagation of extracellular ice [27] and the existence of few ice nucleators in the cytoplasm to initiate ice formation [13, 47]. The response of cells at low temperatures is dictated by the movement of water across the membrane during cooling. When cooling rates are too high for the cell to efflux enough water to maintain an

osmotic equilibrium with the extracellular solution, the potential for IIF occurs. However the mechanism of intracellular ice nucleation is still a matter of debate and may occur through different mechanisms. i) Extracellular ice crystals could induce intracellular ice to form by the tip of the ice crystal growing through pores in the cell plasma membrane [27]. ii) A damaged or leaky membrane may allow for the propagation of extracellular ice crystals intracellularly and initiate IIF [5]. iii) The plasma membrane may act as an ice nucleator, allowing for the formation of intracellular ice as the plasma membrane structure is altered when it interacts with extracellular ice, allowing for surface catalyzed nucleation [59].

The occurrence of damage is not limited to the cooling portion of protocols alone. Small ice crystals that form during rapid cooling may recrystallize during warming. These small ice nuclei grow into larger ice crystals at lower warming rates that can be damaging to the cell [29]. The phenomena of recrystallization is generally avoided at rapid warming rates as there is insufficient time for ice crystals to grow before they reach their melting point [26].

1.3 Methods in cryopreservation

1.3.1 Conventional cryopreservation procedures

Taking into account the aforementioned causes of cell damage at low and high cooling rates, cryoinjury generally results from two things:

elevated solute concentrations [22, 29], and the formation of intracellular ice [24, 28, 59]. Cooling strategies aim to minimize these main causes of cryoinjury as cells progress through the freeze-thaw cycle, and have been implemented into conventional methods of cryopreserving cells.

Conventional cryopreservation protocols use a single constant cooling rate and cryoprotectant concentrations that are empirically optimized in order to minimize freeze related stresses for a particular cell type. These protocols aim to minimize the amount of ice formation during cryopreservation by depressing the freezing point; at low cooling rates reduced extracellular ice will lessen the concentration of solutes and at high cooling rates repression or inhibition of ice will decrease probability of IIF.

In addition to cooling rate, cryoprotectants have played a large role in conventional cryopreservation protocols. Since the discovery of the cryoprotective action of glycerol in 1949 by Smith, Polge and Parkes, [46] cryoprotectants have shaped the manner of cell preservation for decades to follow. Typically these cryoprotectants are divided into two classes of permeating and non-permeating agents based on their ability to traverse the cell membrane [37]. Permeating cryoprotectants are mainly associated with protection from slow cooling injury by reducing ice formation and protecting cells by decreasing the concentration of extracellular solutes and amount of cell dehydration during cooling [37]. The action of non-permeating cryoprotectants is less understood but may allow for loss of

cell water from higher subzero temperatures and protect cells from injury during high rates of cooling [30]. However, osmotic stresses from the addition and removal of cryoprotective agents themselves potentially impose stress on cells in addition to freezing and thawing [16, 49]. Although cryoprotectants have played a large role in past preservation studies they are not the focus of this thesis.

1.3.2 Interrupted cooling protocols

Conventional cooling protocols minimize cell damage by combining cryoprotectants with constant cooling rates to cool cells down to storage temperatures. However, it has been shown that interrupting this cooling process at higher subzero temperatures may improve the outcome of surviving cells after plunging into liquid nitrogen (-196 °C) [9], a strategy that had been previously shown in studies by Luyet and Keane [23], as well as by Taylor [54]. These studies emphasized a step that pre-exposed cells to an intermediate temperature to minimize cell damage when plunging to storage temperature in liquid nitrogen [23, 54].

The interrupted rapid cooling technique, also referred to as two-step cooling, can not only be used to optimize cell recovery but also to investigate cell responses during cryopreservation protocols. Farrant *et al.* subjected lymphocytes directly to various high subzero temperatures by immersing sample tubes into an alcohol bath for various periods of time before either a) directly thawing from that temperature, or b) plunging into liquid nitrogen and subsequently thawing [9]. The beneficial effect of this

cooling strategy over conventional procedures is that cells are initially cooled directly to a particular temperature, and then held at that temperature for a period of time while a protection is conferred before the subsequent plunge. The protective effect may be explained by the removal of intracellular water at the hold temperature, thereby decreasing the probability of IIF during the plunge into liquid nitrogen [34]. This technique has been used in other studies to explore the effects of prolonged hold time at intermediate subzero temperatures [31], as well as to investigate the action of penetrating and non-penetrating cryoprotective agents [34].

Around the time that interrupted cooling techniques were being introduced, there was particular interest in understanding the effects of cooling rate and cryoprotectant for a variety of cell types [8, 10, 20]. McGann used a variation of the two-step freezing procedure to examine the effects of cooling rate on the survival of fibroblasts over a range of subzero temperatures [30]. During interrupted slow cooling, or graded freezing, cells were cooled at relatively low rates to various intermediate subzero temperatures before being a) directly-thawed from that temperature, or b) plunged into liquid nitrogen and subsequently thawed [30].

These techniques allow for separation of damage that occurs when cells are cooled to, held at (two-step), and thawed from the intermediate temperature; from damage to cells that occurs when cooling cells to the

storage temperature (-196 °C). Using two-step cooling McGann and Farrant showed that two different phases of damage occurred to Chinese hamster fibroblasts as directly thawed cells were damaged by lower hold temperatures and long hold times, whereas damage was reduced for plunge-thawed cells at lower hold temperatures and longer hold times [31]. Interrupted cooling can be used to investigate the occurrence of cell damage during cooling protocols in order to further understand how low temperatures affect cells and also to help discern mechanisms of cryoinjury.

1.4 Assessments of cryoinjury

1.4.1 The integrity of the plasma membrane

The success of cryopreservation protocols is evaluated using cell survival or viability. Viability can be described as “the ability of a treated sample to exhibit a specific function or functions, expressed as a proportion of the same function exhibited by the same sample before treatment or an identical fresh untreated sample” [44]. In cryobiological studies, the measurable function for viability is commonly a quantification of the integrity of the plasma membrane.

The plasma membrane plays an important role in the context of cryopreservation, as it is actively involved in the cell osmotic responses and acts as a physical barrier during the formation of extracellular ice. The membrane may also be physically involved in IIF either through its

interaction with extracellular ice [59] or as a result of being damaged [5]. Acker and McGann, using a cryomicroscope, have shown that membrane damage correlated with IIF [2, 3], but could not resolve whether IIF was the cause of, or the result of, membrane damage. The survival of cells post-thaw and the fate of the plasma membrane appear to be two intricately linked phenomena in cryobiology. The membrane has long been considered the primary site of cryoinjury [53], leading to a reliance on membrane integrity as the primary method of assessment in cryobiological studies.

Membrane integrity assays have become a common method of assessment for quantifying the survival of post-thawed cells. The membrane integrity assay gives the upper limit of viability, so that in a sample with a majority of membrane compromised cells, further more detailed observations are unnecessary. However, membrane integrity assessments give little insight in the functional capacity of post-thawed cells. Different components of the cell may be susceptible to varying degrees of damage during freezing, and subcellular injury may be overlooked in studies that rely on membrane integrity assessments alone.

1.4.2 Subcellular alterations

Low temperature conditions have the capability to affect subcellular structures of the cell. It has been shown that subcellular organelles [4, 45, 51, 52], as well as molecular components of the cell [7, 21, 50], are adversely affected by low temperature conditions. McGann *et al.* have

conducted studies demonstrating the extent of cryoinjury to cytoplasmic and metabolic components of granulocytes [4, 33, 60]. Other studies have found disconnects between membrane damage and metabolic activity in split-thickness skin and isolated keratinocytes [61], as well as canine kidney cells [55]. Mitochondria have been of particular interest, as this organelle is involved in a variety of cell processes including cellular metabolism, oxidative phosphorylation and ATP production, the citric acid cycle, cell signaling, and apoptosis. A study in mouse kidneys cells showed “ultrastructural” changes to slowly cooled mitochondria that correlated with reduced respiratory function [51, 52]. Mitochondria are an attractive target for the investigation of a secondary site of cryoinjury in post-thawed cells.

1.4.3 Tools for investigating cryoinjury

Fluorescence microscopy is a common tool used in cellular assessment. The diverse array of fluorescent dyes available allows for assessment of various sites of cell damage during cryopreservation. Fluorescent assays have combined the fluorescent microscope with automatic counting programs in order to quantify healthy and damaged cryopreserved cells [48]. Although the microscope is capable of revealing detailed information of cell morphology and patterns of fluorescence it is limited in the number of cells assessed in a single image.

Flow cytometry is gaining increasing momentum in cell biology. It can be described as a high throughput apparatus that gives quantifiable

values of light scatter and fluorescence properties for each individual cell at a rate of thousands of cells per minute. The flow cytometer has primarily been used in immunofluorescent studies and can be applied in cryopreservation applications [1, 6, 18]. The freezing conditions in cryobiological studies impact the ability of the flow cytometer to properly distinguish osmotically stressed and frozen-thawed cells from debris based on their light scatter properties [32]. The flow cytometer has the potential to be a valuable tool in studies of cryoinjured cells but must be properly adapted for such use. Cells are typically identified from debris in flow cytometry based on their light scattering properties using pre-set thresholds. However, due to the changes in light scatter properties of cryoinjured cells [32], it is difficult to identify and assess these cells separate from debris and extraneous particulate in the cell suspension using conventional methods of light scatter gating. Fluorescence properties have also been considered as a method of cell identification in addition to light scatter [57, 58] and may present a suitable alternative to identify healthy and damaged cryopreserved cells.

1.5 Aim of thesis

To further understand the nature of cryoinjury, it is necessary to observe how different components of the cell respond to changes in temperature during cooling protocols. The aim of this thesis is to probe the occurrence of damage at different sites of cryoinjury when cells are

subjected to a particular cooling strategy. It will involve a comparison of plasma membrane integrity and depolarization of mitochondria during the freeze-thaw cycle of a cryopreservation protocol. The response of human umbilical vein endothelial cells (HUVEC) as a function of subzero temperature will be analyzed during interrupted cooling procedures.

Assessment will be conducted with both the fluorescence microscope and flow cytometry for membrane integrity and mitochondrial polarization as a function of temperature. A direct comparison of these two assays will be used to investigate relationships between these two sites of cryoinjury.

1.6 Hypotheses

- 1) Using flow cytometry under cryobiological conditions, HUVEC are more readily identified using fluorescence intensity rather than light scatter properties of cells
- 2) The mitochondrial membrane potential of HUVEC in suspension show an increased susceptibility to freezing injury when compared to plasma membrane integrity when subjected to identical cooling conditions using interrupted cooling protocols

1.7 Objectives, tools and approach

Current cryopreservation protocols rely primarily on membrane integrity assays as primary methods of assessing cell survival post-thaw. Although membrane integrity is a useful determinant of the upper limit of

viability in cells, it gives little insight into the functional and metabolic capability of cells. The complex morphology and sensitivity of cells to freezing indicates that subcellular changes may take place during cryopreservation protocols that may not be detected by membrane integrity assays. This thesis will use a comparative assessment of membrane integrity and mitochondrial polarization assays to determine if mitochondrial changes correlate with membrane responses during the course of the freeze-thaw cycle.

The objectives of this thesis are:

1. To use a membrane integrity assay to quantify the cryobiological response of human umbilical vein endothelial cells (HUVEC) to rapid and slow interrupted cooling protocols using a membrane integrity assay

In chapter 2, a membrane integrity assay is used to measure the occurrence of cryoinjury when HUVEC are subjected to two different interrupted cooling protocols in the absence of cryoprotectant. A rapid cooling protocol (interrupted rapid cooling with a hold time) with variations in hold time and temperature, and a slow cooling protocol (interrupted slow cooling without a hold time) with variations in cooling rate, are both used to determine cryobiological responses.

2. To demonstrate the ineffectiveness of light scatter based gating strategies in identifying cells in cryobiological studies and propose an alternative strategy of using fluorescence based gates to identify cells from background and debris

In chapter 3, flow cytometry will be used to assess control samples of cells in suspension, including positive control cells at room temperature and negative control cells plunged into liquid nitrogen. Conventional light scatter gating will be used to demonstrate the inadequacies of this method in identifying cryoinjured cells, and an alternative strategy of fluorescence gating will be tested. Two assays: membrane integrity and mitochondrial polarization are examined for their effectiveness in identifying post-thawed cells.

3. To compare membrane integrity and mitochondrial polarization cryobiological responses of HUVEC when subjected to interrupted slow cooling

In chapter 4, an interrupted cooling protocol (interrupted slow cooling without a hold time) is used to quantify and document HUVEC cryoinjury. A mitochondrial polarization assay is used to assess cell survival and the results are compared to previous assessments of membrane integrity under the same cooling conditions.

1.7 References

- [1] J.F. Abrahamsen, A.M. Bakken, Ø. Brusserud, B.T. Gjertsen, Flow cytometric measurement of apoptosis and necrosis in cryopreserved PBPC concentrates from patients with malignant diseases, *Bone Marrow Transplant.* 29 (2002) 165-171.
- [2] J.P. Acker, L.E. McGann, Innocuous intracellular ice improves survival of frozen cells, *Cell Transplant.* 11 (2002) 563-571.
- [3] J.P. Acker, L.E. McGann, Membrane damage occurs during the formation of intracellular ice, *Cryo-Letters* 22 (2001) 241-254.
- [4] F. Arnaud, H. Yang, L.E. McGann, Freezing injury of granulocytes during slow cooling: Role of the granules, *Cryobiology* 33 (1996) 391-403.
- [5] E. Asahina, Frost injury in living cells, *Nature* 196 (1962) 445-446.
- [6] B. Balint, D. Paunovic, D. Vucetic, D. Vojvodic, M. Petakov, M. Trkuljic, N. Stojanovic, Controlled-rate versus uncontrolled-rate freezing as predictors for platelet cryopreservation efficacy, *Transfusion* 46 (2006) 230-235.
- [7] J.M. Baust, R. Van Buskirk, J.G. Baust, Cell viability improves following inhibition of cryopreservation-induced apoptosis, *In Vitro Cell. Dev. Biol.-Anim.* 36 (2000) 262-270.
- [8] L.L. Callow, J. Farrant, Cryopreservation of the promastigote form of *Leishmania tropica* var major at different cooling rates, *Int. J. Parasitol.* 3 (1973) 77-88.
- [9] J. Farrant, S.C. Knight, L.E. McGann, J. O'Brien, Optimal recovery of lymphocytes and tissue culture cells following rapid cooling, *Nature* 249 (1974) 452-453.
- [10] J. Farrant, S.C. Knight, G.J. Morris, Use of different cooling rates during freezing to separate populations of human peripheral blood lymphocytes, *Cryobiology* 9 (1972) 516-525.
- [11] J. Farrant, G. Morris, Thermal shock and dilution shock as causes of freezing injury, *Cryobiology* 10 (1973) 134-140.
- [12] A. Fowler, M. Toner, Cryo-injury and biopreservation. *Ann. N. Y. Acad. Sci.* 1066 (2005) 119-135.

- [13] F. Franks, S. Mathias, P. Galfre, S. Webster, D. Brown, Ice nucleation and freezing in undercooled cells, *Cryobiology* 20 (1983) 298-309.
- [14] S. Fujikawa, Freeze-fracture and etching studies on membrane damage on human erythrocytes caused by formation of intracellular ice, *Cryobiology* 17 (1980) 351-362.
- [15] D. Gao, J.K. Critser, Mechanisms of cryoinjury in living cells, *ILAR J.* 41 (2000) 187-196.
- [16] D.Y. Gao, J. Liu, C. Liu, L.E. McGann, P.F. Watson, F.W. Kleinhans, P. Mazur, E.S. Critser, J.K. Critser, Prevention of osmotic injury to human spermatozoa during addition and removal of glycerol, *Hum. Reprod.* 10 (1995) 1109-1122.
- [17] M.J. Gimeno, G. Pascual, N. Garcia-Honduvilla, B. Dominguez, J. Buján, Arterial damage induced by cryopreservation is irreversible following organ culture, *Eur. J. Vasc. Endovasc. Surg.* 17 (1999) 136-143.
- [18] M. Hagedorn, J. Ricker, M. McCarthy, S.A. Meyers, T.R. Tiersch, Z.M. Varga, F.W. Kleinhans, Biophysics of zebrafish (*Danio rerio*) sperm, *Cryobiology* 58 (2009) 12-19.
- [19] A. Kadner, S.P. Hoerstrup, J. Tracy, C. Breymann, C.F. Maurus, S. Melnitchouk, G. Kadner, G. Zund, M. Turina, Human umbilical cord cells: A new cell source for cardiovascular tissue engineering, *Ann. Thorac. Surg.* 74 (2002) S1422-S1428.
- [20] S.P. Leibo, J. Farrant, P. Mazur, M.G. Hanna Jr., L.H. Smith, Effects of freezing on marrow stem cell suspensions: Interactions of cooling and warming rates in the presence of pvp, sucrose, or glycerol, *Cryobiology* 6 (1970) 315-332.
- [21] J. Levitt, A sulfhydryl-disulfide hypothesis of frost injury and resistance in plants, *J. Theor. Biol.* 3 (1962) 355-391.
- [22] J.E. Lovelock, The haemolysis of human red blood-cells by freezing and thawing, *Biochim. Biophys. Acta* 10 (1953) 414-426.
- [23] B. Luyet, J. Keane Jr., A critical temperature range apparently characterized by sensitivity of bull semen to high freezing velocity. *Biodynamica* 7 (1955) 281-292.
- [24] P. Mazur, Equilibrium, quasi-equilibrium, and nonequilibrium freezing of mammalian embryos, *Cell Biophys.* 17 (1990) 53-92.

- [25] P. Mazur, Freezing of living cells: mechanisms and implications. *Am. J. Physiol.* 247 (1984) C125-142.
- [26] P. Mazur, The role of intracellular freezing in the death of cells cooled at supraoptimal rates, *Cryobiology* 14 (1977) 251-272.
- [27] P. Mazur, The role of cell membranes in the freezing of yeast and other single cells. *Ann. N. Y. Acad. Sci.* 125 (1965) 658-676.
- [28] P. Mazur, Kinetics of water loss from cells at subzero temperatures and the likelihood of intracellular freezing, *J. Gen. Physiol.* 47 (1963) 347-369.
- [29] P. Mazur, S.P. Leibo, E.H.Y. Chu, A two-factor hypothesis of freezing injury. Evidence from Chinese hamster tissue-culture cells, *Exp. Cell Res.* 71 (1972) 345-355.
- [30] L.E. McGann, Optimal temperature ranges for control of cooling rate, *Cryobiology* 16 (1979) 211-216.
- [31] L.E. McGann, J. Farrant, Survival of tissue culture cells frozen by a two step procedure to -196°C . I. Holding temperature and time, *Cryobiology* 13 (1976) 261-268.
- [32] L.E. McGann, M.L. Walterson, L.M. Hogg, Light scattering and cell volumes in osmotically stressed and frozen-thawed cells, *Cytometry* 9 (1988) 33-38.
- [33] L.E. McGann, H. Yang, M. Walterson, Manifestations of cell damage after freezing and thawing, *Cryobiology* 25 (1988) 178-185.
- [34] L.E. McGann, Differing actions of penetrating and nonpenetrating cryoprotective agents, *Cryobiology* 15 (1978) 382-390.
- [35] H.T. Meryman, Cryopreservation of living cells: Principles and practice, *Transfusion* 47 (2007) 935-945.
- [36] H.T. Meryman, Freezing injury and its prevention in living cells. *Annu. Rev. Biophys. Bioeng.* 3 (1974) 341-363.
- [37] H.T. Meryman, Cryoprotective agents, *Cryobiology* 8 (1971) 173-183.
- [38] H. Meryman, Modified model for mechanism of freezing injury in erythrocytes, *Nature* 218 (1968) 333-336.

- [39] K. Muldrew, L.E. McGann, The osmotic rupture hypothesis of intracellular freezing injury, *Biophys. J.* 66 (1994) 532-541.
- [40] K. Muldrew, L.E. McGann, Mechanisms of intracellular ice formation, *Biophys. J.* 57 (1990) 525-532.
- [41] G. Pascual, F. Jurado, M. Rodríguez, C. Corrales, P. López-Hervás, J.M. Bellón, J. Buján, The use of ischaemic vessels as prostheses or tissue engineering scaffolds after cryopreservation, *Eur. J. Vasc. Endovasc. Surg.* 24 (2002) 23-30.
- [42] D.E. Pegg, The relevance of ice crystal formation for the cryopreservation of tissues and organs. *Cryobiology* 60 (2010) S36-44.
- [43] D.E. Pegg, Cryopreservation of vascular endothelial cells as isolated cells and as monolayers, *Cryobiology* 44 (2002) 46-53.
- [44] D.E. Pegg, Viability assays for preserved cells, tissues, and organs, *Cryobiology* 26 (1989) 212-231.
- [45] M.D. Persidsky, Lysosomes as primary targets of cryoinjury, *Cryobiology* 8 (1971) 482-488.
- [46] C. Polge, A.U. Smith, A.S. Parkes, Revival of spermatozoa after vitrification and dehydration at low temperatures, *Nature* 164 (1949) 666.
- [47] D. Rasmussen, M. Macaulay, A. Mackenzie, Supercooling and nucleation of ice in single cells, *Cryobiology* 12 (1975) 328-339.
- [48] L.U. Ross-Rodriguez, J.A.W. Elliott, L.E. McGann, Characterization of cryobiological responses in TF-1 cells using interrupted freezing procedures, *Cryobiology* 60 (2010) 106-116.
- [49] U. Schneider, P. Mazur, Osmotic consequences of cryoprotectant permeability and its relation to the survival of frozen-thawed embryos, *Theriogenology* 21 (1984) 68-79.
- [50] J.G. Shaddock Jr., J.E. Snawder, D.A. Casciano, Cryopreservation and long-term storage of primary rat hepatocytes: effects on substrate-specific cytochrome P450-dependent activities and unscheduled DNA synthesis, *Cell Biol. Toxicol.* 9 (1993) 345-357.
- [51] J.K. Sherman, Comparison of in vitro and in situ ultrastructural cryoinjury and cryoprotection of mitochondria, *Cryobiology* 9 (1972) 112-122.

- [52] J.K. Sherman, correlation in ultrastructural cryoinjury of mitochondria with aspects of their respiratory function, *Exp. Cell Res.* 66 (1971) 378-384.
- [53] P. Steponkus, Role of the plasma membrane in freezing-injury and cold acclimation, *Annu. Rev. Plant Physiol. Plant Mol. Biol.* 35 (1984) 543-584.
- [54] A.C. Taylor, The physical state transition in the freezing of living cells. *Ann. N. Y. Acad. Sci.* 85 (1960) 595-609.
- [55] J. Tchir, J.P. Acker, Mitochondria and membrane cryoinjury in micropatterned cells: Effects of cell-cell interactions, *Cryobiology* 61 (2010) 100-107.
- [56] K.Y. Teo, T.O. DeHoyos, J.C. Dutton, F. Grinnell, B. Han, Effects of freezing-induced cell-fluid-matrix interactions on the cells and extracellular matrix of engineered tissues, *Biomaterials* 32 (2011) 5380-5390.
- [57] L.W.M.M. Terstappen, M.R. Loken, Five-dimensional flow cytometry as a new approach for blood and bone marrow differentials, *Cytometry* 9 (1988) 548-556.
- [58] L.W.M.M. Terstappen, V.O. Shah, M.P. Conrad, D. Recktenwald, M.R. Loken, Discriminating between damaged and intact cells in fixed flow cytometric samples, *Cytometry* 9 (1988) 477-484.
- [59] M. Toner, E.G. Cravalho, M. Karel, Thermodynamics and kinetics of intracellular ice formation during freezing of biological cells, *J. Appl. Phys.* 67 (1990) 1582-1593.
- [60] H. Yang, F. Arnaud, L.E. McGann, Cryoinjury in human granulocytes and cytoplasm, *Cryobiology* 29 (1992) 500-510.
- [61] M.A.J. Zieger, E.E. Tredget, L.E. McGann, Mechanisms of cryoinjury and cryoprotection in split-thickness skin, *Cryobiology* 33 (1996) 376-389.

Chapter 2 - Characterizing HUVEC cryobiological responses using interrupted cooling protocols

2.1 Introduction

Cryopreservation is the use of low temperatures to preserve cells and tissues for extended periods of time. The success of cryopreservation protocols is dependent on minimizing the stresses that are associated with low temperature conditions. Mazur *et al.* proposed the two-factor hypothesis of freezing injury, stating that there are two independent mechanisms of freezing damage that impose stress on cells, [19], mechanisms that are cell type specific and dependent on plasma membrane hydraulic conductivity: the first mechanism involves cooling at relatively slow rates that prolong exposure time to increasing concentrations of solutes during the presence of extracellular ice [13, 19]; the second mechanism involves cooling at relatively rapid rates that do not allow sufficient time for loss of intracellular water for cells to maintain equilibrium with their surroundings [16, 19]; as the cells become increasingly supercooled the probability of forming intracellular ice (IIF) increases. The low temperature conditions that induce either of these mechanisms have been found to be inherently lethal to cells. Cryopreservation protocols aim to use cooling rates that are sufficiently rapid to avoid prolonged exposure to elevated concentrations of solutes

and sufficiently slow to reduce the probability of IIF [12, 19]. However for most cells, cooling rates that cause slow and rapid cooling injury tend to overlap.

In conventional cryopreservation experiments cells are typically assessed post-thaw, after completion of the freeze-thaw cycle and storage in liquid nitrogen. It has been shown that cell damage primarily occurs as cells traverse an intermediate zone of subzero temperatures (-15 to -60 °C) [18]. Conducting assessments post-thaw after storage in liquid nitrogen does not give insight into the cryobiological response of cells within this intermediate zone during a cooling protocol. In addition, it has been shown that cell recovery can be improved by interrupting the cooling process within this intermediate range of subzero temperatures [14].

There are currently two methods of interrupted cooling that are used to explore cryoinjury by separating the damage that occurs upon cooling to (and possibly holding at) the intermediate temperature range and the damage that occurs after plunging to the storage temperature (liquid nitrogen, -196 °C). These methods are interrupted slow cooling without a hold time [20], and interrupted rapid cooling with a hold time [8].

Interrupted slow cooling without use of a hold time is more simply referred to as “interrupted slow cooling” or “graded freezing”. In this procedure cells are cooled at relatively slow rates to intermediate temperatures before being either a) directly thawed, or b) plunged to the storage temperature in liquid nitrogen (-196 °C) before subsequent

warming. Relative slow cooling of cells allows them to remain in equilibrium with their surroundings during the presence of extracellular ice. The advantage of this technique is the ability to conduct separate analyses of damage during initial slow cooling to the experimental temperature and damage after rapid cooling to the storage temperature (plunge into liquid nitrogen). At the time this method was established there was particular interest in the effect of cooling rate on various cell types [6, 9, 11]. McGann used interrupted slow cooling to examine the impact of manipulating cooling rate on cell survival over a range of subzero temperatures [20]. It was observed that the maximum recovery of cells (hamster fibroblasts) was obtained when slow cooling cells to higher subzero temperatures (-5 and -20 °C) before plunging them into liquid nitrogen [20]. More recently Ross-Rodriguez *et al.* used a combination of simulations and experiments to investigate cell responses to interrupted slow cooling conditions using intracellular supercooling and intracellular osmolality as indicators of cell injury [31]. It was found that directly thawed TF-1 hematopoietic stem cells were damaged by solution effects alone, whereas plunged cells were observed to be damaged by IIF when rapidly cooled from high subzero temperatures (-3 to -6 °C) and by a combination of both solution effects and IIF when plunged from lower intermediate temperatures [31].

The second method of interrupted cooling is interrupted rapid cooling with a hold time, also referred to as “two-step freezing”. The

two-step technique involves an initial rapid uncontrolled cooling to a hold temperature, where the cells are held for a pre-designated time before being either a) directly thawed or b) plunged to the storage temperature (-196 °C) before subsequent warming. Interrupted rapid cooling has been described in earlier studies that involved a pre-freezing or stepwise cooling from intermediate temperatures prior to exposure to the storage temperature [5, 14, 35]. Farrant *et al.* showed that there are two stages of the cell response during two-step cooling: the initial occurrence of damage when cells are first subjected to the hold temperature and an incurred protection from further damage when cells are held at the intermediate hold temperature prior to plunging to the storage temperature [8]. This protection has been correlated with cell shrinkage during the hold time at the experimental temperature [10], and this decrease in cell volume is attributed to the osmotic removal of intracellular water that decreases the probability of IIF during the subsequent plunge [24]. The versatility of the two-step freezing method has been demonstrated in other studies exploring the effects of prolonged hold times [21], slower warming rates [22] and the differing actions of penetrating and non-penetrating cryoprotectants [24]. Recent work used simulations and practical experiments to investigate cryobiological responses of TF-1 hematopoietic stem cells to two-step cooling in the absence of cryoprotectant [29]. It was found that two-step freezing of cells without cryoprotectant gave a similar result for cell survival to traditional preservation methods with dimethyl

sulfoxide (Me_2SO) [29]. Although two-step cooling was shown to be beneficial, cooling at more rapid than optimal rates led to a decrease in cell survival when plunging into liquid nitrogen from higher subzero temperatures (-3 to -6 °C), and this decrease in survival was found to be linked to IIF [30]

TF-1 hematopoietic stem cells also showed a high incidence of cell survival after interrupted rapid cooling protocols (two-step freezing) in comparison with slower ones (graded freezing) [29]. The objective of the present work was to determine if this trend of cooling strategy and cell survival hold true for a different cell type. To determine this, the cryobiological responses of human umbilical vein endothelial cells (HUVEC) in suspension to both rapid and slow interrupted cooling protocols in the absence of cryoprotectant were investigated. For rapid interrupted cooling, the HUVEC response was assessed for a range of decreasing subzero temperatures (-3 to -40 °C) and various hold times (3, 5, and 10 minutes). For interrupted slow cooling the HUVEC response was assessed over the same range of temperatures (-3 to -40 °C) at various cooling rates (0.1, 0.2, and 1.0 °C/min).

The HUVEC response was measured with a membrane integrity assay. Membrane integrity has become a standard method of assessment for indicating cell viability in cryobiology. This is attributed to the current notion that the plasma membrane is the primary site of cell damage during freeze-thaw stress [17, 34]. Though there are limitations to membrane

integrity assays, such as not revealing any functional or subcellular indications of damage during freeze-thaw stress, they do provide an upper limit of cellular viability when assessing the cryobiological responses of cells.

2.2 Materials and methods

2.2.1 Cell cultures

Human umbilical vein endothelial cells ((Lot# 0000120825) HUVEC; Lonza®, Walkersville, MD, USA) were cultured at 37 °C and 5 % CO₂ in endothelial basal media (EBM-2) supplemented with a bullet kit (LONZA®) containing human fibroblast growth factor B, hydrocortisone, vascular endothelial growth factor, ascorbic acid, heparin, human endothelial growth factor, and fetal bovine serum. For continued passage of healthy cells, cultures were incubated to approximately 70-80 % confluency according to LONZA guidelines. For experiments requiring higher numbers of cells, cultures were left incubated until a higher confluency was observed (approximately 80-90 %). These cultures were continually monitored to ensure healthy cells with normal morphology (figure 2-1). Cells were harvested by exposure to trypsin-EDTA (Lonza®) for 2 minutes at 37 °C. Cell suspensions were centrifuged at 201 g for 5 min in an Eppendorf 5810R tabletop centrifuge, and resuspended in endothelial growth media at a concentration of 1.0×10^6 cells/mL. Cells from multiple passages were used for each 1 mL aliquot contained in a

12x75 mm round bottom plastic tube (VWR, Edmonton Canada) for experimentation.

2.2.2 Interrupted cooling protocols

Interrupted slow cooling without hold time (graded freezing procedure)

The interrupted slow cooling procedure [20] was conducted as described in Ross-Rodriguez *et al.* [29]. A schematic representation of the interrupted slow cooling procedure is depicted in figure 2-2. Aliquots (0.2mL) of HUVEC cell suspension in endothelial growth media were transferred to 6x50 mm glass culture tubes (VWR, Edmonton, AB, Canada) and allowed to equilibrate at room temperature for 5 minutes. Positive controls were assessed at room temperature. Negative controls were plunged from room temperature directly into liquid nitrogen and assessed post-thaw. Experimental samples were transferred to a stirring methanol bath preset at -3 °C and allowed to equilibrate for 2 minutes before ice was nucleated with cold forceps. Immediately post-nucleation the samples were then cooled, setting the methanol bath to 1.0 °C/min where the temperature was monitored using a T-type thermocouple and Personal Daq View software. At each experimental temperature (-3, -6, -9, -12, -15, -20, -30 and -40 °C) one sample was directly thawed in a 37 °C water bath (warming rate: 121 ± 14 °C/min) while the other was plunged into liquid nitrogen (cooling rate: 574 ± 104 °C/min). The rate of cooling (e.g., plunging cells to -196 °C (liquid nitrogen) from -12 °C) and the rate of warming (e.g., placing cells in a 37 °C from -12 °C) were calculated by

dividing the change in temperature (ΔT in $^{\circ}\text{C}$) over the time taken to reach that temperature (Δt in minutes). The plunged samples were kept in liquid nitrogen for a minimum of 1 hour before being thawed in a 37°C water bath (warming rate: $616 \pm 16^{\circ}\text{C}/\text{min}$). Additional experiments were conducted using cooling rates of 0.1 and $0.2^{\circ}\text{C}/\text{min}$. Duplicates of each sample were used for each experiment and were repeated at least in triplicate using cells from different passages.

Two-step freezing procedure (interrupted rapid cooling with a hold time)

The interrupted rapid cooling procedure [8] was conducted as described in Ross-Rodriguez *et al.* [29]. A schematic representation is depicted in figure 2-3. Aliquots (0.2mL) of HUVEC cell suspension in endothelial growth media were transferred to 6×50 mm glass culture tubes (VWR, Edmonton, AB, Canada) and allowed to equilibrate at room temperature for 5 minutes. Positive controls were left at room temperature. Negative controls were plunged from room temperature directly into liquid nitrogen. The experimental samples were transferred individually into a stirred methanol bath (FTS Systems inc., Stone Ridge NY, USA) that was preset to -3 , -6 , -9 , -12 , -15 , -20 , -30 , or -40°C and equilibrated at that temperature for 2 minutes before ice was nucleated with cold forceps. After nucleation the samples were held at the experimental temperature for 3 minutes before either being thawed in a 37°C water bath (VWR, Edmonton, AB, Canada) (warming rate: $122 \pm 14^{\circ}\text{C}/\text{min}$) or plunged into liquid nitrogen (cooling rate: $574 \pm 104^{\circ}\text{C}/\text{min}$). The plunged samples

were kept in liquid nitrogen for a minimum of 1 hour before being thawed in a 37 °C water bath (warming rate: 616 ± 16 °C/min). Additional experiments were conducted at these same temperatures for hold times of 5 and 10 minutes.

Additional samples were cooled to experimental hold temperatures of -9, and -12 °C, nucleated with cold forceps and held for 1, 2, 3, 4, 5, 7.5, 10, and 15 minutes. The samples were monitored using a type T thermocouple acquiring the data with Personal Daq View software (version 1.9; Omega Laval, QC, Canada). Samples below -15 °C were prone to spontaneous nucleation prior to reaching the hold temperature; time zero was determined to be at completion of the 2 minute equilibration period. For warming, samples were held in the 37 °C water bath until no ice was present. Duplicates of each sample were used for each experiment and were repeated at least in triplicate using cells from different passages.

2.2.3 Assessment of cell recovery

Membrane integrity

A dual fluorescent assay (SytoEB) using a combination of two fluorescent dyes, Syto13® (Molecular Probes, Eugene, OR, USA) and ethidium bromide (EB) (Sigma-Aldrich, Mississauga, ON, Canada) was used to assess the membrane integrity. The SytoEB assay was prepared using 1x phosphate buffered saline (PBS) and aliquots of Syto and EB diluted from stock solutions. The final dye solution was comprised of 25

μM of EB and $12.5 \mu\text{M}$ of Syto13®, and $20 \mu\text{L}$ were added to a $200 \mu\text{L}$ aliquot of HUVEC in suspension, mixed and incubated for 2 minutes at room temperature. Images of fluorescent cells were captured using a Pixera viewfinder digital camera (Pixera Corporation, Los Gatos, CA, USA) fitted onto a Leitz Dialux 22 fluorescence (440–480 nm) microscope (Leitz, Germany).

Fluorescent cells were observed with a Leitz Dialux 22 fluorescence (440–480 nm) microscope (Leitz, Germany) with a dual band red/green filter set to detect emission of Syto13 (509 nm) and ethidium bromide (600 nm) and images were captured using a fitted Pixera viewfinder digital camera (Pixera Corporation, Los Gatos, CA, USA). An in-house custom counting program, Viability 3.2 (Locksley McGann, Edmonton AB, Canada) was used to assess cell membrane integrity from captured digital images. For each experimental sample the relative cell recovery was calculated by dividing the number of intact (green) cells by the total number of cells present including both compromised (red) and intact (green) cells.

2.2.4 Statistical Analysis

Statistical analysis comparisons were conducted using a one-way analysis of variance (ANOVA) ($P = 0.05$ level of significance). This analysis was used to evaluate statistical differences in membrane integrity between intermediate temperatures and the highest subzero temperature ($-3 \text{ }^\circ\text{C}$). A one-way ANOVA was also used to evaluate statistical

differences between the values for membrane integrity of directly-thawed and plunge-thawed samples ($P = 0.05$ level of significance). The mean values and standard error of the mean was also calculated and included in the result (mean \pm sem).

2.3 Results and discussion

Figure 2-4 shows a fluorescent microscope image illustrating the SytoEB membrane integrity assay. The combination of these two dyes makes a binary assay that identifies membrane intact cells with green fluorescence and membrane compromised cells with red fluorescence (figure 2-4). When assessed, positive control samples at room temperature (figure 2-4A) show a majority of membrane intact cells; a HUVEC sample directly thawed from -9°C during interrupted rapid cooling shows a mixed population of membrane intact and membrane compromised cells (figure 2-4B) and negative control samples plunged into liquid nitrogen (figure 2-4C) show primarily membrane compromised cells.

2.3.1 Investigating the impact of cooling rate on the HUVEC response to interrupted slow cooling

The cryobiological response of cells during cryopreservation varies based on the type of cooling strategy they are subjected to. One of the characteristics of cells that may affect their response is hydraulic conductivity, a measured value of the cells' water permeability. A

difference in the water permeability of two cell types may influence their cryobiological response. Measurements of TF-1 hematopoietic stem cells showed that these cells have a higher value of hydraulic conductivity in comparison with HUVEC over a range of temperatures [28, 29] (figures 2-5 and 2-6).

The membrane integrity of HUVEC during interrupted slow cooling is shown in figure 2-7 as a function of temperature at different cooling rates. Data were normalized to positive control samples (HUVEC at room temperature; 86.7 ± 2.1 %), and summarized in table 2-1. For directly thawed cells, a similar pattern of membrane integrity was observed at all cooling rates (0.1, 0.2, and 1.0 °C/min). High values (90-100 %) of normalized membrane integrity was observed at higher subzero temperatures (-3 to -12 °C), and membrane integrity significantly decreased with exposure to lower intermediate temperatures (-20 to -40 °C) ($P < 0.05$). Plunge-thaw samples also show a similar pattern of membrane integrity at all cooling rates (0.1, 0.2, and 1.0 °C/min), but unlike directly thawed cells, plunged cells from higher experimental temperatures initially increase in membrane integrity with temperature (-3 to -15 °C) and then remain unchanged with further decreasing temperatures (-20 to -40 °C). At a cooling rate of 0.1 °C/min cells, a significant increase in membrane intact cells was observed from -15 to -30 °C ($P > 0.05$).

It is generally recognized that slower cooling rates are associated with a reduction in cell volume as well as prolonged exposure to hypertonic conditions during cooling [19]. These hypertonic conditions have been found to cause solution effects injury and result in lowered integrity of the plasma membrane. Cell damage due to solution effects explains the decrease in membrane integrity with temperature that was observed in slowly cooled directly thawed cells. In contrast to directly thawed samples, plunge-thawed cells from high subzero temperatures did experience membrane damage, as they were subjected to much more rapid cooling upon plunging into liquid nitrogen. It has been shown that rapid cooling rates are associated with IIF, and that the occurrence of IIF correlates with cell lethality [7, 16, 26]. IIF is the most likely explanation for the prominent decrease in membrane integrity of plunged cells from high subzero temperatures (-3 to -12 °C), whereas there was a lesser degree of membrane damage when cells were plunged from lower subzero temperatures (-15 to -40 °C).

In both directly thawed and plunge-thawed cells, a dependence of membrane integrity on cooling rate was observed during interrupted slow cooling (figure 2-7). The membrane integrity of cells thawed from higher subzero temperatures (-3 to -15 °C) was not strongly dependent on cooling rate ($P > 0.05$); however the membrane integrity of cells thawed from lower subzero temperatures (-20 to -40 °C) did show a dependence on cooling rate ($P < 0.05$). Slowly cooled HUVEC plunged into liquid

nitrogen from experimental temperatures showed a more pronounced dependence on cooling rate than directly thawed cells. It was observed that plunged samples cooled at a rate of 1.0 °C/min showed additional damage when plunged into liquid nitrogen from -30 °C; compared to cells cooled at a relatively slower rate (0.1 °C/min) that showed no additional damage between directly thawed and plunge-thaw samples. At -30 °C cells cooled slowly (0.1 °C/min) had more time to equilibrate to these conditions (270 minutes) than the time provided (27 minutes) when cooled at a higher rate (1.0 °C/min) (figure 2-7). As the temperature lowers, water is removed from the extracellular solution in the form of ice, increasing the concentration of solutes in the remaining unfrozen fraction. At slow cooling rates cells had sufficient time for water to efflux from the cell, allowing these cells to remain closer to osmotic equilibrium [16].

Slower cooling rates generally resulted in higher values of membrane integrity for HUVEC plunged into liquid nitrogen from decreasing subzero temperatures (figure 2-7). The membrane integrity of directly thawed cells was found to progressively decrease with temperature, in contrast to plunged cells where membrane integrity was observed to increase with exposure to progressively lower experimental temperatures. The increased membrane integrity that was observed during slow cooling (0.1 °C/min), as compared with 1.0 °C/min suggests HUVEC show some resistance to solution effects injury with respect to membrane integrity. The considerable decreased membrane integrity that

was observed when these cells were rapidly cooled by plunging into liquid nitrogen from high subzero temperatures suggests that they may be susceptible to IIF.

2.3.2 A detailed investigation of HUVEC responses to changes in hold time at -9 °C and -12 °C for interrupted rapid cooling

Figure 2-8 shows the membrane integrity of HUVEC during rapid cooling as a function of hold time (1-15 minutes) at hold temperatures of -9 and -12 °C. The data for experimental samples were normalized to positive controls (HUVEC room temperature controls; 86.3 ± 2.2 % and 88.4 ± 1.5 % for -9 and -12 °C).

Directly thawed cells from both hold temperatures (-9 and -12 °C) showed a decrease in membrane integrity with increasing hold time. At -9 °C, a decrease in membrane integrity was observed for longer hold times of 7.5 and 15 minutes ($P < 0.05$), whereas at -12 °C membrane integrity decreased for all hold times longer than 2 minutes ($P < 0.05$). The steepest decline in membrane integrity was observed at the shortest hold times from 1 to 2 minutes, where membrane integrity decreased approximately 14 and 20 % at -9 and -12 °C respectively. The correlation between decreased membrane integrity and increased hold time suggests that these cells were being damaged by solution effects. However, when these cells were slow cooled to -12 °C (90 minutes) the resultant normalized membrane integrity was approximately 90 % (figure 2-7) compared to the less than 50 % (normalized) membrane intact cells that

were observed during rapid cooling (time 2 minutes) (figure 2-8). The prolonged exposure to increased solute concentrations during slow cooling (figure 2-7) showed that these cells were able to withstand conditions that are associated with solution effects injury. The observed decrease in membrane integrity under rapid cooling conditions (figure 2-8) was more likely attributed to IIF upon cooling to the hold temperature after ice nucleation.

Membrane damage was more pronounced in cells plunged into liquid nitrogen compared to cells directly thawed from both hold temperatures (-9 and -12 °C) (figure 2-8). Plunge-thawed samples showed low recovery of membrane intact cells, with a slight increase (to a maximum of 11.8 ± 0.7 %) with shorter hold times (from 1-5 minutes), this was followed by a plateau of membrane integrity with longer hold times (5 to 15 minutes) when held -12 °C ($P < 0.05$) prior to plunging. The slight increase in membrane integrity with shorter hold times showed that lengthening the hold time (from 1-5 minutes) allowed cells to lose intracellular water and decreased the probability of IIF during the plunge, whereas longer hold times (from 5 to 15 minutes) did not allow these cells any further loss of intracellular water and the probability of IIF remained the same. Though it has been documented that the occurrence of intracellular ice correlates with membrane damage for cells in suspension [1, 2, 36] it is uncertain as to whether this damage is the cause of, or the result of, IIF. Acker and McGann were able to link membrane damage to

IIF but could not establish a time course to separate the occurrence of membrane rupture from IIF [2, 3]. Regardless of the mechanism, intracellular ice is most likely occurring as HUVEC are plunged into liquid nitrogen from -9 and -12 °C resulting in a low number of membrane intact cells.

A more distinct decrease in membrane integrity with hold time was observed in directly thawed cells from lower hold temperatures (-12 °C compared to -9 °C), whereas plunged samples showed no differences in membrane integrity between these hold temperatures. A possible explanation for this occurrence is the existence of a subset of freeze resistant cells that may, for example, be attributed to cell volume as smaller cells contained less intracellular water and were less likely to undergo IIF [16, 25]. Another explanation may be the cells' present phase of the growth cycle, which may influence cell survival when subjected to decreasing temperatures, as McGann showed that fibroblasts in the M phase were more susceptible to freezing damage compared to other phases of the cell cycle [23].

Rapidly cooling HUVECs to -12 °C and subjecting them to an increasing hold time showed a significant increase in membrane integrity with longer hold times (3 - 15 minutes, Figure 2-8) ($P < 0.05$). These results reinforce our conclusions from interrupted slow cooling (figure 2-7), that HUVEC show a resiliency to damage when exposed to hypertonic

conditions that result in solution effects injury, and a susceptibility to damage from rapid cooling and IIF.

2.3.3 Investigating the HUVEC response to decreasing hold temperatures during interrupted rapid cooling

Figure 2-9 shows the experimental results for HUVEC cooled rapidly to an experimental subzero temperature, held for 3, 5 or 10 minutes, before being directly thawed or plunged into liquid nitrogen and subsequently thawed. Experimental results were normalized to HUVEC positive controls ($86.3 \pm 2.2 \%$); a summary of the data is present in table 2-2.

Directly thawed samples of HUVEC showed a trend of decreasing membrane integrity with decreasing experimental temperatures, where a significant decrease in membrane integrity was observed at $-9 \text{ }^{\circ}\text{C}$ and below ($P < 0.05$), including a particularly sharp decrease from -6 to $-15 \text{ }^{\circ}\text{C}$ for all hold times (figure 2-9) followed by a gradual decline at $-15 \text{ }^{\circ}\text{C}$ ($19.7 \pm 2.8 \%$) that continued at lower temperatures until there were no membrane intact cells left at a hold temperature of $-40 \text{ }^{\circ}\text{C}$. Increasing the hold time to 5 and 10 minutes showed no further change, indicating that damage most likely occurred during the initial equilibration period, from ice nucleation prior to the start of, or early in, the hold time (figure 2-3: i). At hold temperatures below $-15 \text{ }^{\circ}\text{C}$ samples were prone to spontaneous ice nucleation prior to completion of the 2 min equilibration period, where this

event may have contributed to a loss of HUVEC membrane integrity prior to the hold time.

A comparison of HUVEC membrane integrity from rapid cooling protocols to that of slow cooling protocols showed that a greater number directly thawed cells were damaged during rapid cooling: as cooling to hold temperatures of -15 °C and below resulted in more than 80 % membrane damaged cells (figure 2-9), whereas no more than 50 % of cells were damaged when slow cooled (0.1 °C/min) to the same temperature (figure 2-7). The high rate of cooling associated with rapid cooling methods leads to the cytoplasm becoming increasingly supercooled and increases the probability of IIF [15].

Aliquots of HUVEC (0.2 mL) plunged into liquid nitrogen showed a slight increase in membrane integrity with decreasing hold temperature (-3 to -12 °C), and the membrane integrity then decreased with further decreasing temperatures (-15 to -40 °C) (figure 2-9). This indicated that some protection was conferred to these cells by being held for 3 minutes at high subzero temperatures (-3 to -12 °C) before plunging into liquid nitrogen. Further increasing the hold time to 10 minutes slightly but significantly increased the number of membrane intact cells to a maximum at -12 °C (15 ± 1.2 %) ($P < 0.05$). Plunging HUVEC from room temperature directly into liquid nitrogen resulted in no membrane intact cells (figure 2-4: C) and showed that the absence of a holding period at an

intermediate subzero temperature results in complete loss of HUVEC membrane integrity upon plunging.

At hold temperatures lower than $-20\text{ }^{\circ}\text{C}$ there was little to no difference in the membrane integrity of directly thawed and plunge-thawed cells, as no additional damage was observed when these cells were plunged into liquid nitrogen from experimental hold temperatures (-15 to $-40\text{ }^{\circ}\text{C}$). This suggests that the majority of cells at hold temperatures below $-15\text{ }^{\circ}\text{C}$ already have frozen intracellular water and that no additional intracellular freezing occurred upon plunging. The inability of these cells to efflux water may be explained by the hydraulic conductivity, since this measured value of water permeability for HUVEC has been found to be relatively low [28]. This low value of hydraulic conductivity may partly explain the susceptibility of HUVEC to IIF when subjected to rapid cooling procedures.

In this study, HUVEC sustained less injury when cells were cooled with slow cooling protocols (graded freezing) compared to more rapid cooling protocols (two-step freezing), showing similar results to other interrupted cooling studies involving rapid [24] and slowly [20] cooled fibroblasts. However, results for both of these cell types are in contrast to results of cooling TF-1 hematopoietic stem cells that sustained less injury during two-step freezing [30] compared to slower cooling methods [31]. Our data indicated that HUVEC show a resistance to solution effects injury during slow cooling conditions but may be susceptible to IIF during rapid

cooling, as the highest survival of HUVEC was achieved at the slowest cooling rate used (0.1 °C/min). The low hydraulic conductivity of HUVEC [28] may explain why membrane integrity is higher at slower cooling rates, in contrast to TF-1 hematopoietic stem cells that have a higher value for hydraulic conductivity [28] (figures 1 and 2) and benefit from more rapid cooling methods such as two-step freezing.

2.4 Conclusions

This study investigated the HUVEC cryobiological response to two different interrupted cooling protocols. Interrupted slow cooling keeps the cells in equilibrium with their surroundings as the temperature decreases in the presence of extracellular ice and solutes become increasingly concentrated. The long exposure to concentrated solutes during slow cooling may be damaging to cells in the form of solution effects. Interrupted rapid or two-step cooling has been found to confer a protection to cells when they are held at a designated experimental hold temperature for a period of time prior to plunging into liquid nitrogen. However, these high rates of cooling also leave cells susceptible to IIF, an inherently lethal event. For HUVEC, slower cooling methods (graded freezing) were shown to improve cell survival, in contrast to rapid cooling protocols (two-step freezing) that showed drastic decreases in membrane integrity. These results indicated that HUVEC had an observed resistance to solution effects injury under slow cooling conditions, but may be susceptible to IIF.

In cryopreservation of cells in suspension the cooling strategy used in the cryopreservation protocol must be catered to the appropriate cell type. TF-1 hematopoietic stem cells sustained less injury when subjected to rapid cooling protocols [29] compared with slow cooling protocols [31], unlike the observed cell survival of HUVEC that benefitted from slower cooling rates. The characteristics of individual cell types such as the hydraulic conductivity (figures 2-5 and 2-6) influence their response to various cooling strategies.

This study used membrane integrity as the primary method of assessment of HUVEC under cryobiological conditions and is the traditional assay of choice for cryobiologists. However, freezing has been shown to affect other components of cells [4, 27, 32, 33] in addition to the plasma membrane. The assessment results in this chapter using membrane integrity can now be used as a basis for comparison to additional assays that examine other aspects of cells that may be affected by cryobiological conditions.

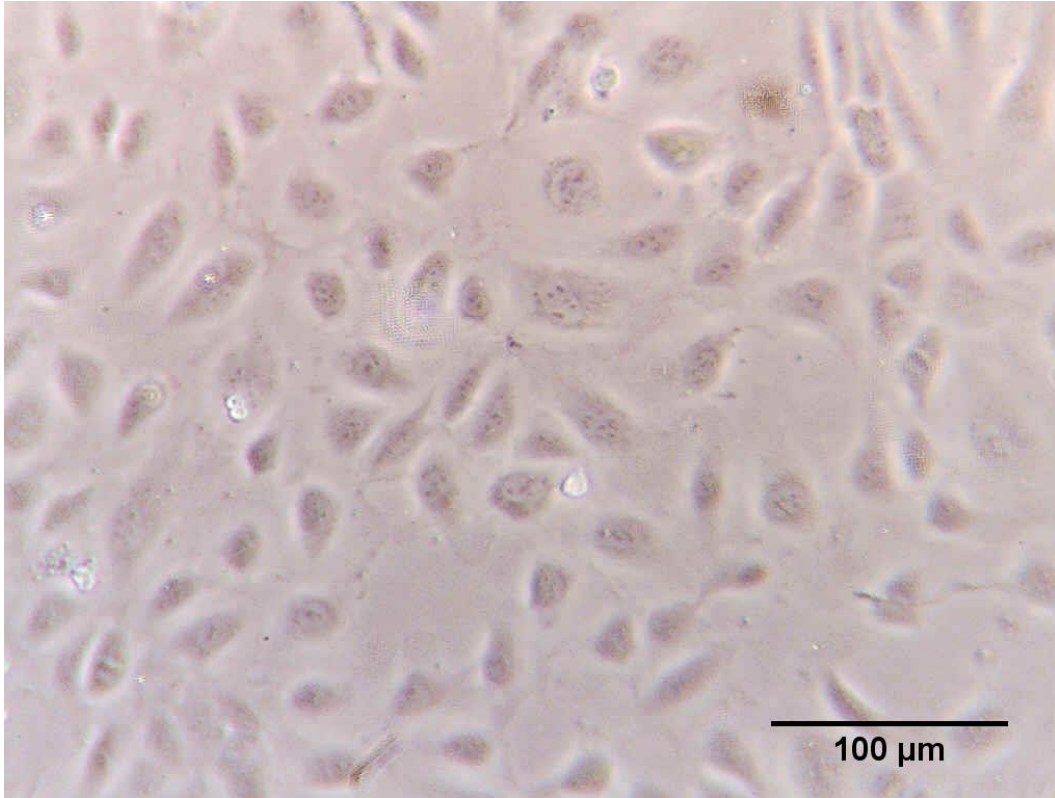


Figure 2-1. Representative light microscopy photograph depicting appearance of adhered HUVEC culture prior to trypsinization for experimentation.

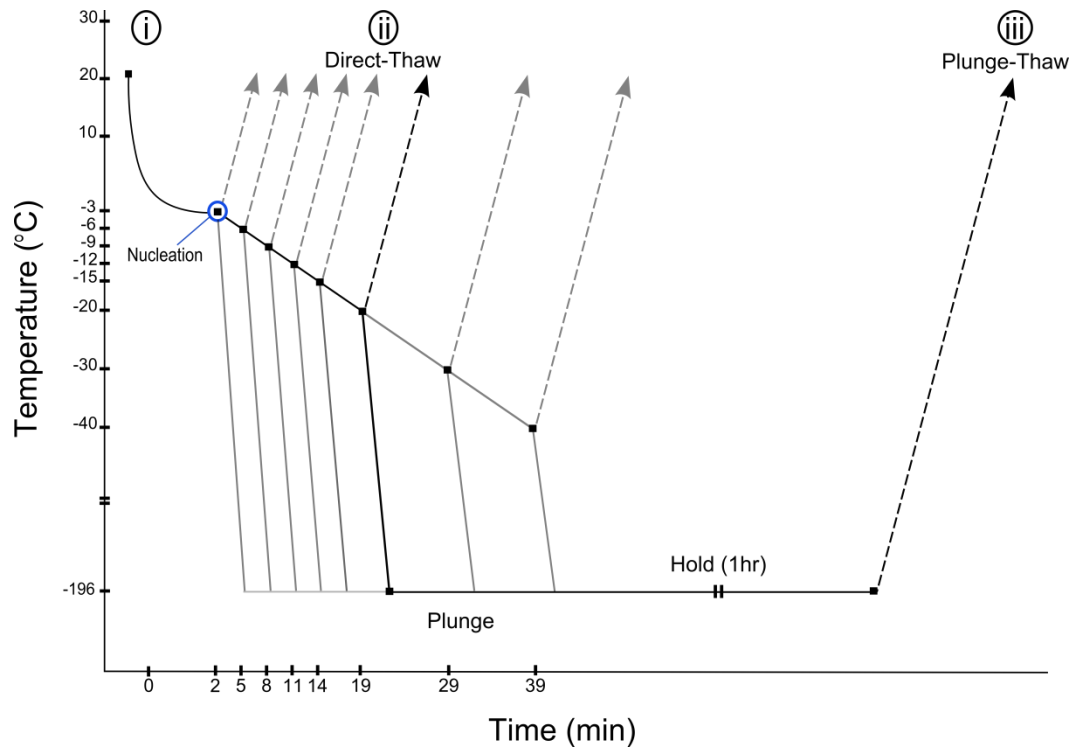


Figure 2-2. Schematic of interrupted slow cooling at a rate of 1.0 °C/min.

- i. Pre-cooling of samples to -3 °C from room temperature and controlled ice nucleation
- ii. Linear slow cooling (post-nucleation) to experimental temperatures and either directly thawing or plunging into liquid nitrogen (-196 °C)
- iii. Subsequent thawing after storage time (>1 hour)

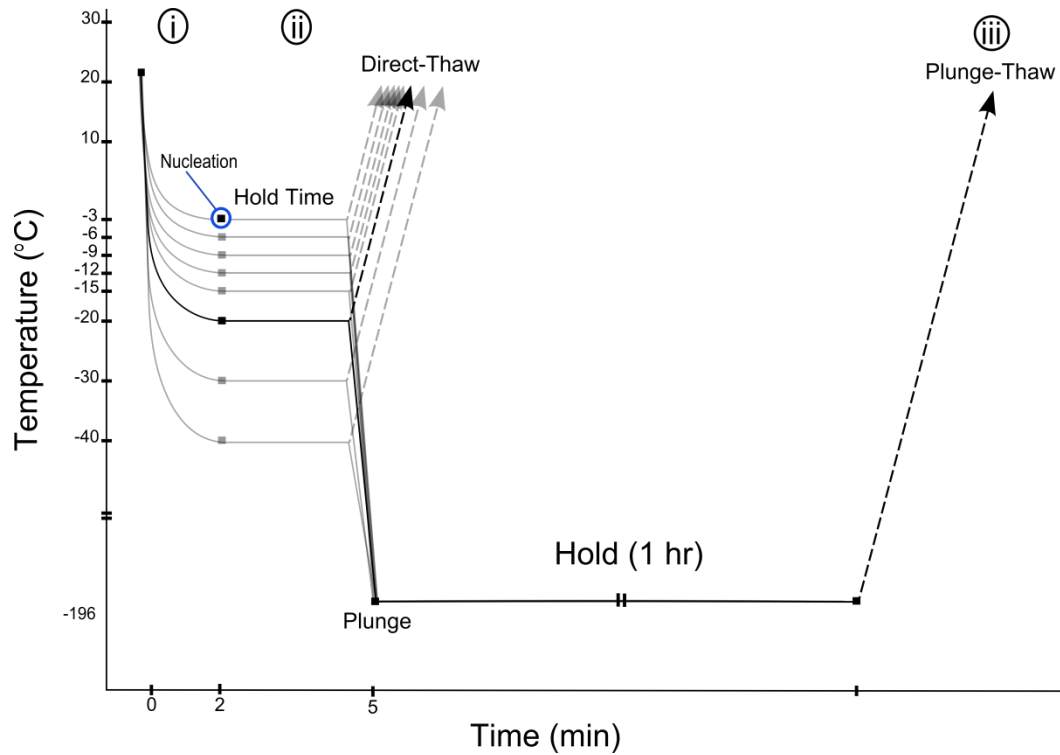


Figure 2-3. Schematic of interrupted rapid cooling with a 3 minute hold time.

- i. Pre-cooling of samples to -3 °C from room temperature and controlled ice nucleation
- ii. Hold time, followed by either direct thaw or plunge into liquid nitrogen (-196 °C)
- iii. Subsequent thawing after storage time (>1 hour)

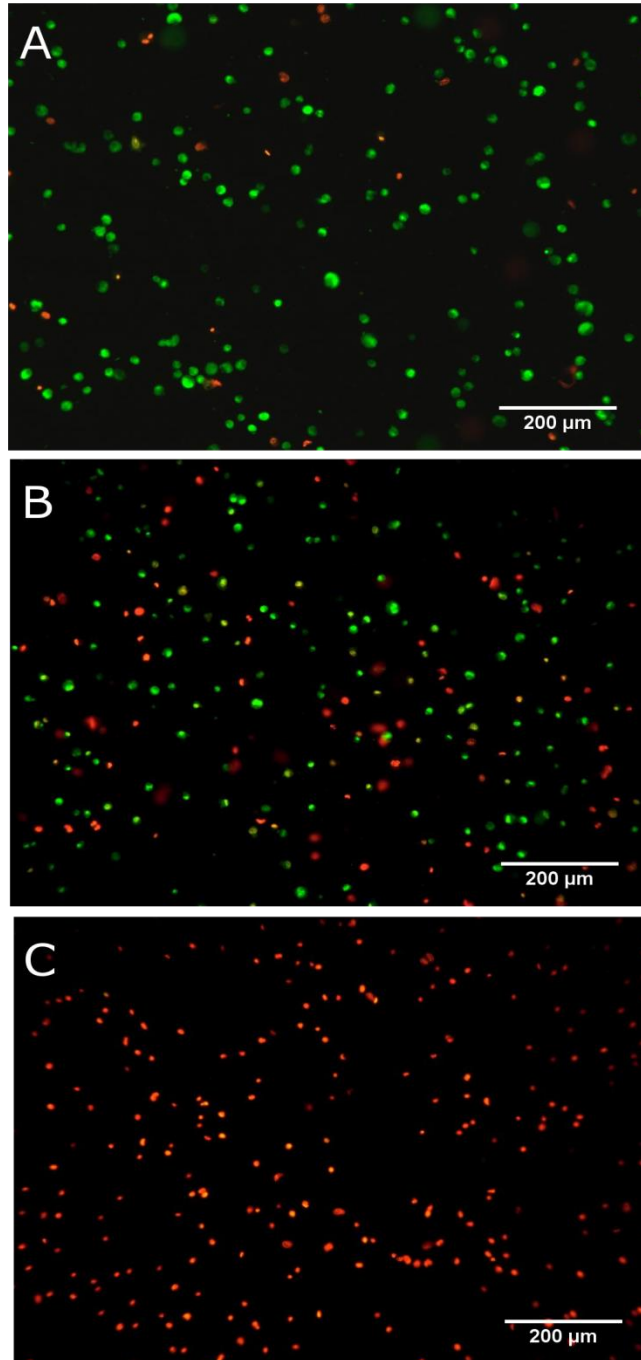


Figure 2-4. Fluorescent microscope images of HUVEC stained with SytoEB

- A. Room temperature control sample
- B. Directly-thawed cells from -9 °C during interrupted rapid cooling
- C. Sample plunged into liquid nitrogen

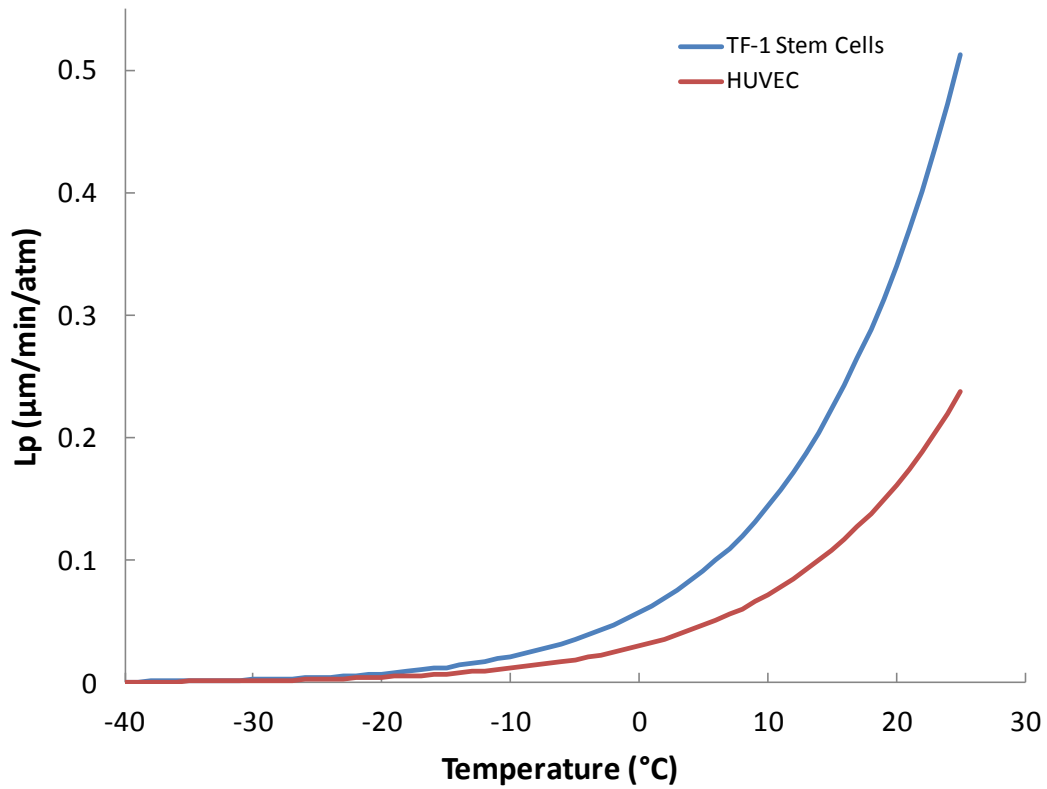


Figure 2-5. Plot of hydraulic conductivity (L_p) as a function of temperature

for HUVEC and TF-1 cells. Extrapolated using equation: $L_p = k \exp\left(\frac{-E_a^{Lp}}{RT}\right)$

and parameters from Ross-Rodriguez *et al.* [28, 29] for:

TF-1 cells ($k = 1.33 \times 10^{10} \mu\text{m}/\text{min}/\text{atm}$ and $E_a^{Lp} = 14.2 \pm 1.1 \text{ kcal}/\text{mol}$) and

HUVEC ($k = 1.59 \times 10^9 \mu\text{m}/\text{min}/\text{atm}$ and $E_a^{Lp} = 13.4 \pm 0.3 \text{ kcal}/\text{mol}$)

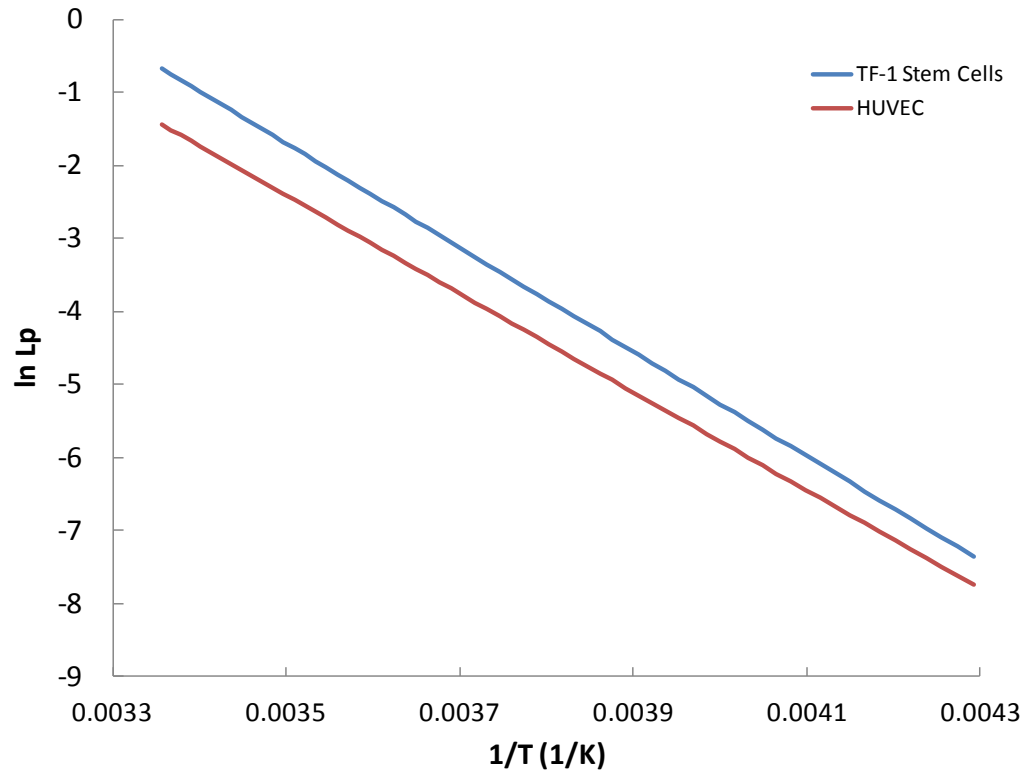


Figure 2-6. Arrhenius plot of natural logarithm of L_p ($\mu\text{m}/\text{min}/\text{atm}$) for HUVEC and TF-1 cells as a function of inverse temperature (K^{-1}).

Extrapolated using equation: $\ln L_p = \ln k \left(-\frac{E_a^{Lp}}{RT} \right)$ and parameters from

Ross-Rodriguez *et al.* [28, 29] for:

TF-1 cells ($k = 1.33 \times 10^{10} \mu\text{m}/\text{min}/\text{atm}$ and $E_a^{Lp} = 14.2 \pm 1.1 \text{ kcal/mol}$) and

HUVEC ($k = 1.59 \times 10^9 \mu\text{m}/\text{min}/\text{atm}$ and $E_a^{Lp} = 13.4 \pm 0.3 \text{ kcal/mol}$)

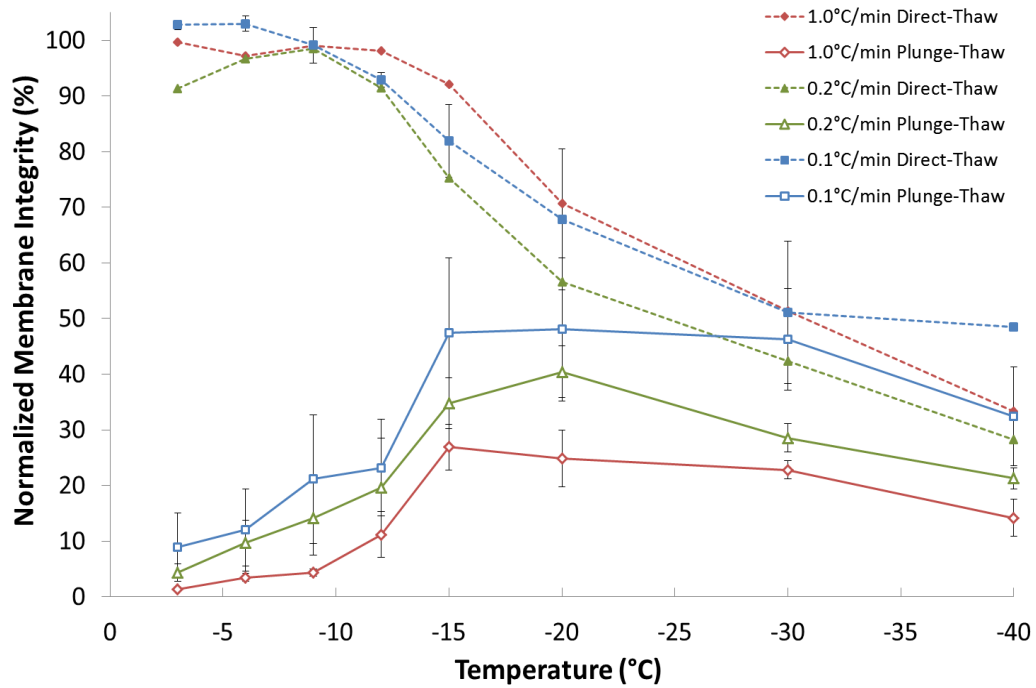


Figure 2-7. Response of HUVEC to interrupted slow cooling at different cooling rates. Membrane integrity of HUVEC (mean \pm sem; normalized to control; n = 3) cooled at rates of 0.1, 0.2, and 1.0 °C/min to various subzero temperatures, then either thawed directly (dashed) or plunged into liquid nitrogen (solid) and subsequently thawed.

Table 2-1. Membrane integrity response of HUVEC to interrupted slow cooling at different cooling rates (mean \pm sem; n=3).

Temp (°C)	Normalized Membrane Integrity (%)					
	Cooled at 1.0 °C/min		Cooled at 0.2 °C/min		Cooled at 0.1 °C/min	
	Direct- thaw	Plunge- thaw	Direct- thaw	Plunge- thaw	Direct- thaw	Plunge- thaw
- 3	99.6 \pm 2.8	1.3 \pm 0.1 ^c	91.3 \pm 5.9	4.3 \pm 1.6 ^c	102.8 \pm 2.0	8.9 \pm 6.1 ^c
- 6	97.2 \pm 4.8	3.5 \pm 0.7 ^c	96.6 \pm 2.2	9.6 \pm 4.1 ^c	103.0 \pm 0.9	12.0 \pm 7.4 ^c
- 9	99.1 \pm 2.6	4.3 \pm 0.6 ^c	98.5 \pm 1.5	14.2 \pm 6.8 ^c	99.1 \pm 1.3	21.2 \pm 11.6 ^c
- 12	98.2 \pm 2.1	11.2 \pm 4.1 ^c	91.4 \pm 2.5	19.7 \pm 8.8 ^c	92.9 \pm 3.2	23.2 \pm 8.7 ^c
- 15	92.2 \pm 2.6	26.9 \pm 4.1 ^c	75.2 \pm 2.2	34.8 \pm 4.6 ^c	81.9 \pm 1.3	47.5 \pm 13.4 ^{*c}
- 20	70.7 \pm 6.2 [*]	24.9 \pm 5.1 ^c	56.6 \pm 6.7 [*]	40.4 \pm 4.6	67.8 \pm 6.6 [*]	48.1 \pm 12.8 [*]
- 30	51.4 \pm 6.4 [*]	22.8 \pm 1.7	42.3 \pm 6.2 [*]	28.6 \pm 2.5	51.2 \pm 12.7 [*]	46.3 \pm 9.1 [*]
- 40	33.4 \pm 10.3 [*]	14.2 \pm 3.3	28.3 \pm 4.3 [*]	21.3 \pm 1.9	48.4 \pm 12.8 [*]	32.4 \pm 8.8

* Signifies statistically significant difference in membrane integrity at the measured temperature from the initial temperature (-3 °C) of the same curve (P < 0.05)

^c Signifies statistically significant difference in membrane integrity of plunge-thaw samples from respective direct-thaw sample (P < 0.05)

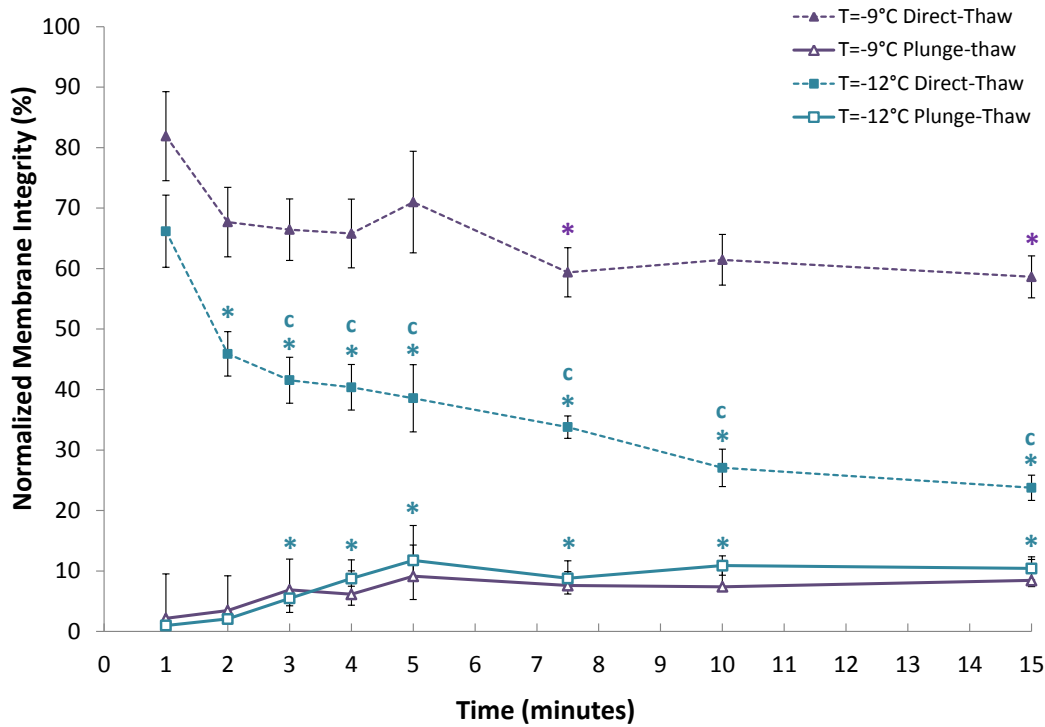


Figure 2-8. Response of HUVEC to interrupted rapid cooling as a function of hold time for two different hold temperatures. Membrane integrity of HUVEC (mean \pm sem; normalized to controls; n = 6) as a function of hold time for cells cooled rapidly to -9, and -12 °C before either being directly thawed from the experimental temperature (dashed) or plunged into liquid nitrogen before subsequent thaw (solid).

* Signifies statistically significant difference in membrane integrity at the measured hold time from the initial hold time (1 min) of the same curve (P < 0.05)

° Signifies statistically significant difference in membrane integrity of -12 °C samples from respective -9 °C samples under the same conditions (P < 0.05)

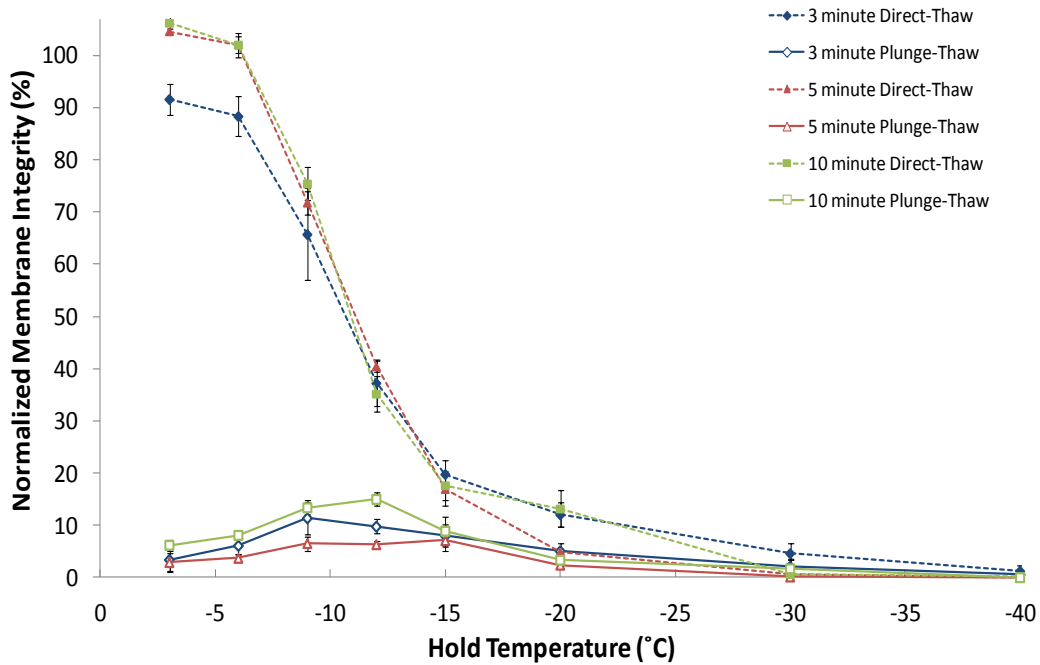


Figure 2-9. Response of HUVEC to interrupted rapid cooling as a function of hold temperature for different hold times. Membrane integrity of HUVEC (mean \pm sem; normalized to controls; n = 6) as a function of hold temperature for cells with hold times of 3, 5, and 10 minutes before either being directly thawed from the experimental temperature or plunged into liquid nitrogen before subsequent thaw.

Spontaneous ice nucleation occurred during the equilibration period at hold temperatures of -15 °C and below.

Table 2-2. Membrane integrity response of HUVEC to interrupted rapid cooling as a function of hold temperature for different hold times.

(mean \pm sem; n=3).

	Normalized membrane integrity (%)					
	Holding time 3 minutes		Holding time 5 minutes		Holding time 10 minutes	
Temp (°C)	Direct- thaw	Plunge- thaw	Direct- thaw	Plunge- thaw	Direct- thaw	Plunge- thaw
- 3	91.6 \pm 2.9	3.4 \pm 2.4 ^c	104.5 \pm 0.5	2.9 \pm 1.7	106.2 \pm 1.6	6.2 \pm 1.1 ^c
- 6	88.3 \pm 3.8	6.1 \pm 1.6 ^c	101.9 \pm 2.3	3.7 \pm 0.8 ^c	102.0 \pm 1.6	8.1 \pm 0.8 ^c
- 9	65.7 \pm 8.8*	11.4 \pm 3.1*	71.7 \pm 2.2*	6.6 \pm 1.4 ^c	75.4 \pm 3.2*	13.4 \pm 1.4* ^c
- 12	37.2 \pm 4.4*	9.8 \pm 1.3 ^c	40.4 \pm 1.1*	6.3 \pm 0.6 ^c	35.2 \pm 3.4*	15 \pm 1.2* ^c
- 15	19.8 \pm 2.8*	7.9 \pm 2.1	16.9 \pm 3.2*	7.1 \pm 1.9* ^c	17.6 \pm 2.7*	8.9 \pm 2.7 ^c
- 20	12.0 \pm 2.3*	5.1 \pm 1.5	4.8 \pm 0.3*	2.4 \pm 0.6	13.2 \pm 3.5*	3.4 \pm 1.0 ^c
- 30	4.6 \pm 1.9*	2.1 \pm 1.6	0.6 \pm 0.2*	0.2 \pm 0.1	0.6 \pm 0.2*	1.7 \pm 1.6
- 40	1.2 \pm 1.0*	0.6 \pm 0.5	0.1 \pm 0.1*	0.1 \pm 0.0	0.2 \pm 0.1*	0.0 \pm 0.0* ^c

* Signifies statistically significant difference in membrane integrity at the measured temperature from the initial temperature (-3 °C) of the same group (P < 0.05)

^c Signifies statistically significant difference in membrane integrity of plunge-thaw samples from respective direct-thaw sample (P < 0.05)

2.5 References

- [1] J.P. Acker, L.E. McGann, Innocuous intracellular ice improves survival of frozen cells, *Cell Transplant.* 11 (2002) 563-571.
- [2] J.P. Acker, L.E. McGann, Membrane damage occurs during the formation of intracellular ice, *Cryo-Letters* 22 (2001) 241-254.
- [3] J.P. Acker, L.E. McGann, Cell-cell contact affects membrane integrity after intracellular freezing, *Cryobiology* 40 (2000) 54-63.
- [4] F. Arnaud, H. Yang, L.E. McGann, Freezing injury of granulocytes during slow cooling: Role of the granules, *Cryobiology* 33 (1996) 391-403.
- [5] E. Asahina, Prefreezing as a method enabling animals to survive freezing at an extremely low temperature, *Nature* 184 (1959) 1003-1004.
- [6] L.L. Callow, J. Farrant, Cryopreservation of the promastigote form of *Leishmania tropica* var major at different cooling rates, *Int. J. Parasitol.* 3 (1973) 77-88.
- [7] K.R. Diller, E.G. Cravalho, C.E. Huggins, Intracellular freezing in biomaterials, *Cryobiology* 9 (1972) 429-440.
- [8] J. Farrant, S.C. Knight, L.E. McGann, J. O'Brien, Optimal recovery of lymphocytes and tissue culture cells following rapid cooling, *Nature* 249 (1974) 452-453.
- [9] J. Farrant, S.C. Knight, G.J. Morris, Use of different cooling rates during freezing to separate populations of human peripheral blood lymphocytes, *Cryobiology* 9 (1972) 516-525.
- [10] J. Farrant, C.A. Walter, H. Lee, L.E. McGann, Use of two-step cooling procedures to examine factors influencing cell survival following freezing and thawing, *Cryobiology* 14 (1977) 273-286.
- [11] S.P. Leibo, J. Farrant, P. Mazur, M.G. Hanna Jr., L.H. Smith, Effects of freezing on marrow stem cell suspensions: Interactions of cooling and warming rates in the presence of pvp, sucrose, or glycerol, *Cryobiology* 6 (1970) 315-332.
- [12] S.P. Leibo, P. Mazur, The role of cooling rates in low-temperature preservation, *Cryobiology* 8 (1971) 447-452.

- [13] J.E. Lovelock, The haemolysis of human red blood-cells by freezing and thawing, *Biochim. Biophys. Acta* 10 (1953) 414-426.
- [14] B. Luyet, J. Keane Jr., A critical temperature range apparently characterized by sensitivity of bull semen to high freezing velocity. *Biodynamica* 7 (1955) 281-292.
- [15] P. Mazur, Freezing of living cells: mechanisms and implications. *Am. J. Physiol.* 247 (1984) C125-142.
- [16] P. Mazur, The role of intracellular freezing in the death of cells cooled at supraoptimal rates, *Cryobiology* 14 (1977) 251-272.
- [17] P. Mazur, The role of cell membranes in the freezing of yeast and other single cells. *Ann. N. Y. Acad. Sci.* 125 (1965) 658-676.
- [18] P. Mazur, Kinetics of water loss from cells at subzero temperatures and the likelihood of intracellular freezing, *J. Gen. Physiol.* 47 (1963) 347-369.
- [19] P. Mazur, S.P. Leibo, E.H.Y. Chu, A two-factor hypothesis of freezing injury. Evidence from Chinese hamster tissue-culture cells, *Exp. Cell Res.* 71 (1972) 345-355.
- [20] L.E. McGann, Optimal temperature ranges for control of cooling rate, *Cryobiology* 16 (1979) 211-216.
- [21] L.E. McGann, J. Farrant, Survival of tissue culture cells frozen by a two step procedure to -196°C . I. Holding temperature and time, *Cryobiology* 13 (1976) 261-268.
- [22] L.E. McGann, J. Farrant, Survival of tissue culture cells frozen by a two step procedure to -196°C . II. Warming rate and concentration of dimethyl sulphoxide, *Cryobiology* 13 (1976) 269-273.
- [23] L. McGann, J. Kruuv, H. Frey, Effect of Hypertonicity and Freezing on Survival of Unprotected Synchronized Mammalian-Cells, *Cryobiology* 9 (1972) 107-111.
- [24] L.E. McGann, Differing actions of penetrating and nonpenetrating cryoprotective agents, *Cryobiology* 15 (1978) 382-390.
- [25] K. Muldrew, L.E. McGann, The osmotic rupture hypothesis of intracellular freezing injury, *Biophys. J.* 66 (1994) 532-541.

- [26] K. Muldrew, L.E. McGann, Mechanisms of intracellular ice formation, *Biophys. J.* 57 (1990) 525-532.
- [27] M.D. Persidsky, Lysosomes as primary targets of cryoinjury, *Cryobiology* 8 (1971) 482-488.
- [28] L.U. Ross-Rodriguez, Cellular osmotic properties and cellular responses to cooling, PhD Thesis, Laboratory Medicine Pathology, University of Alberta, Edmonton (2009) 239.
- [29] L.U. Ross-Rodriguez, J.A.W. Elliott, L.E. McGann, Characterization of cryobiological responses in TF-1 cells using interrupted freezing procedures, *Cryobiology* 60 (2010) 106-116.
- [30] L.U. Ross-Rodriguez, J.A.W. Elliott, L.E. McGann, Investigating cryoinjury using simulations and experiments. 1: TF-1 cells during two-step freezing (rapid cooling interrupted with a hold time), *Cryobiology* 61 (2010) 38-45.
- [31] L.U. Ross-Rodriguez, J.A.W. Elliott, L.E. McGann, Investigating cryoinjury using simulations and experiments: 2. TF-1 cells during graded freezing (interrupted slow cooling without hold time), *Cryobiology* 61 (2010) 46-51.
- [32] J.K. Sherman, Comparison of in vitro and in situ ultrastructural cryoinjury and cryoprotection of mitochondria, *Cryobiology* 9 (1972) 112-122.
- [33] J.K. Sherman, correlation in ultrastructural cryoinjury of mitochondria with aspects of their respiratory function, *Exp. Cell Res.* 66 (1971) 378-384.
- [34] P. Steponkus, Role of the plasma membrane in freezing-injury and cold acclimation, *Annu. Rev. Plant Physiol. Plant Mol. Biol.* 35 (1984) 543-584.
- [35] A.C. Taylor, The physical state transition in the freezing of living cells. *Ann. N. Y. Acad. Sci.* 85 (1960) 595-609.
- [36] M. Zhurova, E.J. Woods, J.P. Acker, Intracellular ice formation in confluent monolayers of human dental stem cells and membrane damage, *Cryobiology* 61 (2010) 133-141.

Chapter 3 - Fluorescence as an alternative to light scatter gating strategies to identify frozen-thawed cells with flow cytometry

3.1 Introduction

Flow cytometry has been shown to be a valuable tool for assessing viability of individual cells in suspension. The principle of flow cytometry is to gather light scattered by individual cells in a laser beam, and to use the light scatter properties from cells to distinguish cell populations. In addition, specific wavelengths are analyzed to probe fluorescent emission from surface markers on cells [10] after specific labeling. Different characteristics of cells can influence the pattern of detected scattered light at forward and side angles. Forward light scatter has widely been used as an indicator of cell size as it has been shown that under specific conditions forward light scatter changes in relation to cell volume [13, 24, 25, 41], whereas side scattered light is influenced by nuclear morphology and cytoplasmic granulation reflecting the complexity of the internal structure of cells [5, 26]. In analysis of flow cytometry data the combination of forward and side scatter has been used to identify specific cell types and subpopulations [26, 37, 46].

Common practice in flow cytometry is to identify and separate cells from background and debris using a trigger, also referred to as the discriminator, that is traditionally based on a forward scatter threshold [6,

18, 27]. This method of identification is based on the assumption that forward scattered light directly correlates with cell or particle volume. However, a study of cell osmotic stress in hamster fibroblasts, granulocytes, and lymphocytes showed that forward light scatter was inversely proportional to cell volume in anisotonic solutions [21], contradicting previous theoretical predictions [14]. The complexity of the cell and its properties suggests that size is not the only factor that affects forward scattered light [11]. There are additional factors that may also affect the forward light scatter properties of cells such as the wavelength used to generate light scatter signals [16, 28], the angle of detection of scattered signals [17, 36], differences in the refractive index [38, 39], as well as the properties of the plasma membrane and the presence of internal cell structures [23].

Light scatter is not the only option when utilizing a trigger for distinguishing cells; there have also been applications of fluorescence as a method of cell identification in flow cytometry. The fluorescence of nucleic stains and monoclonal antibodies has been combined with light scatter to identify damaged and intact cells in fixed flow cytometric samples [48], and also as a variable to separate components of heterogeneous whole blood [47]. A study by Loken *et al.* showed that in a light scatter distribution, the position of a peak of two attached cells was not double that of the peak for single cells, and this non additive property was an indication that light scatter was not directly proportional to cell

volume [15]. However, in this same study, a fluorescence profile of these same cells showed cell doublets emitting twice the fluorescent intensity of single cells [15]. A more recent study by Lu *et al.* showed that light scatter measurements gave inaccurate counts when determining cells from other particles in sperm cell concentrates; further analysis by Petrunkina and Harrison provided a mathematical basis for these misestimations [19, 31]. Although light scatter is an important parameter in flow cytometry, there are situations where fluorescence may be a more reliable indicator to identify cells. The concept of using fluorescence as a threshold has been used for sorting minor subpopulations of cells [20] and for detection of rare events [33] in flow cytometry, but it can also be applied to studies of cell responses to low temperatures.

There is increasing interest in using flow cytometry as a quantitative method of cellular assessment in cryobiological studies [1, 3, 9].

Cryobiology is the study of biological responses to low temperatures and cryopreservation provides a means of preserving viability and function of cells and tissues for long periods. The term viability has been defined as “the ability of a treated sample to exhibit a specific function, or functions expressed as a proportion of the same function exhibited by the same sample before treatment” [30]. Assessment of cellular viability is used in cryobiology to measure the quality of individual samples, and optimize protocols to improve cryopreservation outcomes [4].

The plasma membrane is considered a primary site of cryoinjury, so in cryobiology membrane integrity assessment is one of the most common methods for determining viability. Membrane integrity assays are simple, rapid assessments of plasma membrane integrity measured using dye exclusion methods, or combinations of fluorescence [2, 7, 21, 44]. Cryopreservation studies have also used membrane integrity assays in conjunction with other, more detailed assessments of cellular function to outline understanding of the cellular response, including changes in metabolic function [4, 29], DNA fragmentation [8], and mitochondrial polarization [45].

However, cryobiological conditions induce significant alterations in cellular light scattering properties. A study by McGann *et al.* exposing cells to cryobiological conditions showed that cooling to low temperatures resulted in low membrane integrity and decreased forward light scatter properties of cells, accompanied by only a slight reduction in cell volume [21]. These observations disagreed with the assumption that the forward light scatter properties of cells are proportional to cell volume as previously predicted [14], and it was suggested that other components of the cell surface and the cytoplasm may also contribute to the cell light scatter properties [21].

The objective of the present study was to demonstrate that gating strategies based on forward light scattering may introduce inaccuracies in experiments that require the identification of total cell populations,

including not only live, but also dead and damaged cells. In addition, this study will also investigate the use of fluorescence based gating as an alternative strategy of identifying these cells. The complicating factors that are involved in a cryobiological study present a situation where using light scatter as a trigger may be ineffective and fluorescence could alternatively be used to discriminate and assess cells in suspension.

3.2 Materials and methods

3.2.1 Cell cultures

Human umbilical vein endothelial cells ((Lot#0000120825) HUVEC; Lonza®, Walkersville, MD, USA) were cultured at 37 °C and 5 % CO₂ in endothelial basal media (EBM-2) supplemented with a bullet kit (Lonza®) containing human fibroblast growth factor B, hydrocortisone, vascular endothelial growth factor, ascorbic acid, heparin, human endothelial growth factor, and fetal bovine serum. For continued passage of healthy cells, cultures were incubated to approximately 70-80 % confluency according to LONZA guidelines. For experiments requiring higher numbers of cells, cultures were left incubated until a higher confluency was observed (approximately 80-90 %) and then harvested by exposure to trypsin-EDTA (Lonza®) for 2 minutes at 37 °C. Cell suspensions were centrifuged at 201 g for 5 minutes in an Eppendorf 5810R tabletop centrifuge, and resuspended in endothelial growth media at a concentration of 1.0×10^6 cells/mL. Cells from multiple passages were used

for each 1 mL aliquot contained in a 12x75 mm round bottom plastic tube (VWR, Edmonton Canada) for experimentation.

3.2.2 Assessment of cell recovery

Membrane integrity

The dual fluorescent assay (SytoEB) uses a combination of two fluorescent dyes, Syto13 (Molecular Probes, Eugene, OR, USA) and ethidium bromide (EB; Sigma-Aldrich, Mississauga, ON, Canada) to assess cell membrane integrity. Syto13 is a DNA/RNA binding stain that permeates all cells and fluoresces green upon excitation by UV wavelengths. Ethidium bromide permeates cells with damaged plasma membranes, exhibiting red fluorescence upon UV exposure. The combination of these two dyes makes a binary assay with membrane intact cells exhibiting green fluorescence and membrane compromised cells exhibiting red fluorescence. The SytoEB stain was prepared using a 1x phosphate buffered saline (PBS), and aliquots of Syto and EB diluted from the stock solution. The final dye was comprised of 25 μ M EB and 12.5 μ M Syto13, and 10 μ L of the prepared dye were added to a 1 mL aliquot of HUVEC in suspension and incubated for 2 minutes at room temperature before analysis.

Mitochondrial membrane potential

The ratiometric dye 5',6,6'-tetrachloro-1,1',3,3'-tetraethylbenzimidazolylcarbocyanine-iodide (JC-1) (Molecular Probes,

Eugene, OR, USA) was used to assess the mitochondrial membrane potential of HUVEC in suspension. The fluorescence shifts from green (~525 nm) in low polarization states (non-functional mitochondria) to red (~590 nm) in high polarization states (functioning mitochondria). This change in color of fluorescence is based on a concentration-dependent shift from monomers of the dye which fluoresce green to aggregates which fluoresce red. Initially the dye is present as cationic monomers (green) that permeate into cells, drawn by a negative intracellular potential. In healthy cells these monomers then permeate into the mitochondrial matrix, drawn by the electronegative interior of mitochondria where these monomers form J-aggregates (red) [12]. Therefore cells with depolarized mitochondria predominately emit green fluorescence from monomers present in the cytoplasm, and cells with polarized mitochondria predominantly emit red fluorescence from J-aggregates of the dye.

The JC-1 assay was prepared starting with the stock solution by combining 5 mg of the JC-1 reagent with 5 mL of Me₂SO (Sigma-Aldrich) to a concentration of 1 mg/mL. 0.8 µL of JC-1 reagent/ Me₂SO solution was added to 0.4 mL aliquots of HUVEC (final concentration of 2 µg/mL) and incubated for 30 minutes in the incubator at 37 °C and 5 % CO₂.

3.2.3 Flow cytometry analysis

Aliquots of HUVEC (1 mL) were subjected to one of two experimental conditions. The first group (the positive control) was left for 5 min at room temperature after treatment prior to analysis with the flow

cytometer. Sample tubes from the second group (the negative control) were plunged directly into liquid nitrogen for 2 min, and then subsequently thawed in a 37 °C water bath until no visible ice was present, prior to analysis with the flow cytometer.

The above described parameters were assessed with an unmodified Coulter® EPICS® XL-MCL™ flow cytometer (Beckman-Coulter) equipped with a 488 nm argon laser. Emission of Syto13 and JC-1 monomers were detected using the FL1 (505-545 nm) bandpass filter; that of JC-1 aggregates was detected using the FL2 (560-590 nm) bandpass filter and that of ethidium bromide was detected using the FL3 (605 to 635 nm) bandpass filter. Aliquots of HUVEC (0.4 mL) were loaded and run for a time interval of 2 minutes in Isoflow™ sheath fluid (Beckman-Coulter).

Fluorescence compensation and data acquisition was performed using System II™ software (Beckman-Coulter). Fluorescence compensation of membrane integrity assay (SytoEB) was achieved by subtracting 27.5 % of FL1 (Syto13) from FL2 (EB), whereas compensation of mitochondrial membrane potential was achieved by subtracting 43 % FL1 (JC-1 green) from FL2 (JC-1 red). The corresponding compensated data was analyzed with the Kaluza® flow cytometry analysis software v1.2 from Beckman Coulter, producing one and two parameter histograms of both the light scatter and fluorescent properties for each sample.

3.3.4 Statistical Analysis

Statistical analysis comparisons were conducted using a one-way analysis of variance (ANOVA) ($P = 0.05$ level of significance). This analysis was used to evaluate statistical differences between the number of cells gated on the basis of fluorescence intensity and light scatter properties. The mean values and standard error of the mean was also calculated and included in the result (mean \pm sem).

3.3 Results

3.3.1 Effectiveness of forward light scatter gating

A typical light scatterplot of the forward scatter (y-axis) and side scatter (x-axis) measurements of untreated HUVEC control cells in suspension is shown in figure 3-1. Each dot on this plot represents a single event through the flow cytometer. Figure 3-1A shows the raw unprocessed data of all events, and depicts three distinct populations, grouped into regions: R1 with high forward and high side scatter events (22 %), R2 with low forward and high side scatter events (5 %), and R3 with low forward and low side scatter events (73 %). Commonly, a threshold is established on the forward scatter channel under the assumption that this threshold allows for the discrimination of cells from debris, where only events greater than the value of this threshold will be registered by the flow cytometer. Figure 3-1B shows the same data as figure 3-1A after application of a threshold on the forward scatter intensity,

where events with forward scatter intensity below the threshold have been removed. Though it may be true that debris makes up the majority of events in R3, this is not necessarily true for the events in R2, leaving the possibility that cells along with debris have been removed by the forward scatter threshold. Figure 3-2 shows a plot of forward vs. side scatter for HUVEC directly plunged into liquid nitrogen without cryoprotectant to induce cryoinjury. Figure 3-2A shows the raw unprocessed data of all events, where two populations R2 (32 %) and R3 (68 %) consist of the majority of events, with a few events present in R1. Figure 3-2B shows the data after application of the forward scatter threshold, where the applied threshold now excludes the majority of events.

A comparison of figure 3-1A (control) and figure 3-2A (plunged) shows that the number of events in R1 has decreased and the number in R2 has increased, indicating that the events of R1 have moved to R2 after plunging these cells into liquid nitrogen. This indicates that events from R1 represent healthy cells, whereas events from R2 represent damaged cells. In the untreated control (figure 3-1A) there are some events present in R2 (5 % of total events). Identifying these events as damaged cells indicates that they make up approximately 20 % of total cells present; this is similar to our observations using fluorescence microscopy, as approximately 20 % of cells were found to be membrane damaged in control cell populations of freshly trypsinized HUVEC in suspension (data not shown).

Applying the typical forward scatter threshold to figure 3-2B (plunged) removes these damaged cells, excluding them from further analysis.

3.3.2 Effectiveness of fluorescence gating with a membrane integrity assay – SytoEB

Figure 3-3 shows a membrane integrity analysis performed using flow cytometry of HUVEC control samples stained with fluorescent dyes Syto13 and EB. Figure 3-3A shows a histogram of events according to their green fluorescence of Syto13, a dye that enters all cells, and figure 3-3B shows a histogram of red fluorescence of ethidium bromide, a dye that permeates membrane damaged cells. Both histograms show a peak of low fluorescence events separated from a peak of highly fluorescent events. Because Syto13 and EB have a high yield of fluorescence when bound to nucleic acids [43, 49], it is reasonable to conclude that the low intensity peaks represent debris and high intensity peaks represent cells.

A threshold was placed at the base between the peaks of events to separate the low green from high green regions as well as low red from high red regions. For both dyes this threshold was placed to identify events as either cells (high green and high red, figure 3-3) or debris (low green and low red, figure 3-3) and with the dyes identifying the membrane integrity of those cells as membrane intact (high green, figure 3-3A) or membrane damaged (high red, figure 3-3B). Figure 3-3C shows the raw forward vs. side scatter data of HUVEC control samples, with high intensity Syto13 events (green), high intensity EB (red), and the remaining

events in grey, indicating that membrane intact cells (green) and membrane compromised cells (red) could be distinguished from debris (grey). The membrane intact cells make up approximately 82 % of total cells and also matches the cell population in R1 (figure 3-1), whereas membrane compromised cells make up approximately 18 % of the total cells and matches the cell population in R2 (figure 3-1), further indicating that R1 and R2 are comprised of healthy and damaged cells respectively. It is noted that there is a proportion of cells (high red, figure 3-3) that are present in region R3 (figure 3-1). These red fluorescent events is an indication that damaged cells with low light scatter properties may be present in R3, or may be due to the presence of portions of cells or microparticles containing nucleic content present in the cell suspension.

Figure 3-4 shows a membrane integrity analysis of HUVEC plunged into liquid nitrogen. The same green and red fluorescence thresholds that were established in figure 3-3 were used for plunge samples to separate debris (low green and low red in figures 3-4A and B) from cells (high green and high red in figures 3-4A and B). Figure 3-4A shows a histogram of the green fluorescence raw data with a peak present in the low green region, but no peak in the high green region, indicating that there are almost no membrane intact cells after plunging cells in liquid nitrogen. Figure 3-4B shows a histogram of the red fluorescence raw data with a low intensity peak in the low red region, and a high intensity peak in the high red region. Figure 3-4C shows the raw forward vs. side scatter data

of membrane intact (green), and membrane compromised cells (red) separated from debris (grey) using fluorescence thresholds. It would be difficult to distinguish cells from debris within intermixed populations of damaged cells and debris without the addition of these fluorescence thresholds.

Comparing figure 3-3A (control) and figure 3-4A (plunge) shows the number of healthy cells that become damaged when plunged into liquid nitrogen, represented here by a shift from green to red fluorescence. The thresholds based on membrane integrity fluorescent dyes are able to distinguish both healthy control cells and cells damaged by cryoinjury from debris, which is impossible using a traditional forward scatter threshold.

Figure 3-5 shows the events registered by the flow cytometer that have been identified as cells when using either a light scatter, or a fluorescence threshold. The multiparameter capability of the flow cytometer allows for direct comparison of the light scatter and fluorescence properties of each recorded event. A comparison of these thresholds with HUVEC controls shows a similar number of healthy cells gated by either light scatter or fluorescence. Using fluorescence gates, a significant increase was observed in the number of damaged cells (EB) in plunged samples compared to controls ($P < 0.05$). However, the light scatter threshold excludes damaged cells from control samples as there was no difference between the number of damaged cells (EB) in control and plunged samples using light scatter gates ($P > 0.05$).

A drastic decrease was also observed in the total number of cells identified by light scatter thresholds compared with fluorescence gating, indicating that light scatter thresholds are ineffective at detecting damaged cells in both control and plunged samples whereas fluorescence gating allows for detection of most cells in the suspension.

3.3.3 Effectiveness of fluorescence gating with a mitochondrial polarization assay – JC-1

JC-1 was used as an indicator of mitochondrial polarization to identify healthy and cryoinjured cells from debris. Figure 3-6 shows JC-1 green fluorescence in HUVEC control samples. Figure 3-6A shows a fluorescence histogram separating low intensity events (low green, figure 3-6A) from high intensity events (high green, figure 3-6A). Since the JC-1 assay is membrane potential dependent and requires a negatively charged intracellular environment in order for the molecules to concentrate, cells can be associated with the higher intensity events (high green) and debris can be associated with lower intensity events (low green). A threshold was established based on the fluorescent intensity of JC-1 monomers to identify cells from debris for further analysis.

Within the high green region (figure 3-6A), two peaks are present: a lower intensity peak with a high percentage of events (peak 1: 75.8 ± 2.0 %), and a higher intensity peak with a low percentage of events (peak 2: 24.6 ± 2.0 %). Since the green fluorescent intensity of JC-1 depends on the concentration of its monomers, lower intensity events (peak 1, figure

3-6A) will correspond with cells that contain predominantly J-aggregates of the dye that results in lower green fluorescent intensity and suggests that these events represent cells with polarized mitochondria. Higher intensity JC-1 green events (peak 2, figure 3-6A) contain predominantly monomers of the dye that results in higher green fluorescent intensity and suggests that these events represent cells with depolarized mitochondria.

Figure 3-6B shows the raw forward vs. side scatter data of HUVEC control samples after the application of this fluorescence threshold with cells containing polarized (light green) and depolarized mitochondria (orange) clearly distinguished from debris (grey). Cells with polarized mitochondria (green, figure 3-6B) show similar light scatter properties to membrane intact cells (green, figure 3-3C). Correspondingly, cells with depolarized mitochondria (orange, figure 3-6B) show similar light scatter properties to membrane compromised cells (red, figure 3-3C). This provides further evidence of the accuracy of fluorescence thresholds, as two separate assays were capable of not only discriminating cells from debris but also identifying healthy from damaged cells.

Figure 3-7 shows the JC-1 green fluorescence of HUVEC plunge samples. Figure 3-7A shows a fluorescence histogram separating low intensity debris (low green, figure 3-7A) from high intensity cells (high green, figure 3-7A). A comparison of fluorescent intensity (expressed in units of intensity from the flow cytometer, au) showed that cells (high

green) had increased fluorescence in plunged samples (66.3 ± 1.0 au, figure 3-7A) compared to controls (34.6 ± 2.3 au, figure 3-6A). The lower intensity of green fluorescence in controls (high green, figure 3-6A) is due to the lack of JC-1 monomers present in cells, as under control conditions monomers form aggregates in mitochondria and fluoresce red, lowering the overall intensity of green fluorescence. As such, monomers of the JC-1 dye aggregate to emit red fluorescence from polarized mitochondria indicating healthy cells, where depolarization reflects damaged cells [40]. The higher peak of fluorescent intensity (high green, figure 3-7A) shows damaged cells with depolarized mitochondria. In figures 3-6B, and 3-7B, healthy and damaged cells are accurately distinguished from debris with a fluorescence threshold.

The mitochondrial membrane potential of events identified as cells (from figures 3-6 and 3-7) was assessed using one parameter histograms of the intensity of red fluorescence. The red fluorescence intensity of J-aggregates from the mitochondrial polarization assay JC-1 and the corresponding light scatter properties of HUVEC are presented in figure 3-8. The forward and side light scatter properties of control (figure 3-8A), and plunged (figure 3-8B) samples are presented with a corresponding histogram of JC-1 red fluorescence (figure 3-8C).

The high red fluorescence in control cells (red peak, figure 3-8C) is from the formation of J-aggregates present in cells with polarized mitochondria, whereas the low red fluorescence of plunged cells (blue

peak, figure 3-8C) occurs when mitochondrial membrane potential is not present, therefore the dye cannot form J-aggregates and the dye remains as a monomer. Cells with high red fluorescence and corresponding high forward and high side scatter properties indicate healthy cells (red) and cells with low red fluorescence and low forward scatter properties indicate damaged cells (blue). JC-1 not only discriminates cells from debris but also reflects the functional capacity of HUVEC based on the polarized state of their mitochondria indicated by the presence of red fluorescent J-aggregates.

3.4 Discussion

Light scatter is used as a key parameter in flow cytometry to reveal information about cell size and morphological characteristics that can aid in the identification of cell types and subpopulations; however the relationship between particle properties and scattered light is complex. Since Mullaney *et al.* demonstrated a relationship between forward light scatter and cell volume under the assumption that cells were homogenous spheres with a uniform refractive index [25], a common generalization has emerged that light scatter in the forward direction gives an estimation of cell size. Though volume does play a major role, there are limitations to this generalization, and it has been shown that even for microspheres, forward scattered light increases with diameter in a non-linear manner [35], indicating that other factors are also involved. It is obvious that cells

are not merely spheres with set diameters and refractive indices whose behavior is unaltered by a changing environment. It must be recognized that there are limitations to using forward scattered light as a trigger to discriminate cells from background and debris.

The non-specific binding of antibodies in immunofluorescence studies to dead and damaged cells was problematic when trying to distinguish intact cells of interest [22], especially in samples containing different cell types; using a forward scatter threshold to distinguish cells was the simplest means of reducing artifacts from this non-specific binding. The application of this threshold to HUVEC room temperature controls shows how easily intact cells are identified from debris (figure 3-1B).

In cryobiological studies that require numeration of both damaged and healthy cells during assessments, traditional use of a light scatter threshold would lead to the exclusion of damaged cells of interest. These investigations often use the ratio of healthy to total cells (healthy and damaged) to determine the effectiveness of cryopreservation protocols. Plunging HUVEC directly into liquid nitrogen shows the extent of damage that can occur to cells in a cryopreservation procedure and the ineffectiveness of the forward scatter threshold to discriminate between debris, damaged cells and healthy cells (figure 3-2). For cryobiological studies that need to include damaged cells in the final assessment an alternative strategy of gating and discriminating cells is required.

The plasma membrane which has been shown to be a contributing factor to light scatter characteristics of cells is also an important determinant of cell viability. Under cryobiological conditions the membrane acts as a barrier to ice propagation during freezing, and is believed to be one of the primary sites of cryoinjury during exposure to freeze-thaw stress [32, 42]. The plasma membrane is an ideal candidate to test the effectiveness of light scatter and fluorescence gating strategies to discriminate healthy and damaged cells from debris. A fluorescent membrane integrity assay (SytoEB) was used to assess the state of the cell membrane in HUVEC room temperature controls (figure 3-3), and HUVEC plunged into liquid nitrogen (figure 3-4).

The nucleic acid staining dyes of the membrane integrity assay (SytoEB) demonstrate the versatility of fluorescence measurements as healthy cells have high forward scatter and high green fluorescence, whereas damaged cells have low forward scatter and high red fluorescence. Due to the similarities in forward light scatter of damaged cells and debris it is difficult to accurately distinguish damaged cells from debris using forward light scatter alone. In cryobiological studies where the proportion of damaged to total (healthy and damaged) cells is to be used; discarding damaged cells from final assessment would introduce bias in the final result (figure 3-5). The use of fluorescence intensity gives a more accurate depiction of a measure for viability and a comparison of control and plunged HUVEC samples shows the advantage of using fluorescence

over light scatter based thresholds in cryobiological applications (figure 3-5).

Fluorescent assays are not limited to assessments of the plasma membrane; there is the capability of probing the cell in depth with assays reflecting their function. The JC-1 fluorescent dye is an indicator of mitochondrial membrane polarization from its formation of red-orange fluorescent J-aggregates [40]. In control samples the high green region (high green, figure 3-6A) shows cells with a higher intensity of green fluorescence than the extraneous events in suspension (low green, figure 3-6A) indicating that not all monomers of the dye form J-aggregates in healthy cells and that a number of green fluorescent monomers remain in the cell cytoplasm. A closer observation of control JC-1 green fluorescence actually shows two peaks, a first peak correlating cells with high forward scatter properties, and a second peak that correlates with low forward scatter, further confirming our results of using fluorescence to discriminate between healthy and damaged cells (figure 3-6). As expected, events with low forward light scatter were primarily found in the plunged sample depicting cryoinjured cells (figure 3-7). Despite the differences in the fluorescent mechanism of a mitochondrial polarization assay compared to a membrane integrity assay, the same result was attained, further reinforcing the versatility of fluorescence based cell discrimination.

In addition to discriminating cells, JC-1 also gives an indication of the functional state of mitochondria based on the intensity of red fluorescent JC-1 aggregates. The polarized state of mitochondria in control samples gave off significantly higher intensity of fluorescence when compared to plunged cells (figure 3-8). JC-1 has been found useful as a ratiometric assay as healthy cells primarily give off high red and low green fluorescence, whereas damaged cells give off low red and high green fluorescence, this ratio may be used to determine the polarization state of mitochondria in cells [34].

3.5 Conclusions

In this study the effectiveness of using light scatter and fluorescence gating strategies in flow cytometry were compared. These strategies were used to identify HUVEC from debris in samples at room temperature and in samples that had been plunged directly into liquid nitrogen. The traditional method of using forward scattered light as a trigger signal to discriminate cells excluded the majority of cryoinjured cells from assessment along with debris. Though this is not a concern when conducting studies with immunofluorescence, it is problematic for studies that need to take into account the proportion of viable to total (viable and non-viable) cells such as in cryobiology. An alternative to forward light scatter is to use the fluorescence signal intensity to discriminate both healthy and damaged cells from debris.

In this study HUVEC healthy and cryoinjured cells were effectively identified under control and plunged conditions using fluorescence assessments of membrane integrity, a commonly used assessment of cell viability, and mitochondrial polarization an effective indicator of the functional capability of cellular mitochondria. A common nucleic acid based membrane integrity assay such as the combination of Syto13 and ethidium bromide easily identifies as cells those events giving off strong fluorescent signals. The JC-1 dye not only discriminated cells from background and debris based on the intensity of green JC-1 monomers but in addition also indicated the functional capability of cellular mitochondria. These assays demonstrate that fluorescent stains of very different mechanisms can be equally effective at identifying healthy and damaged cells with the flow cytometer under conditions where light scatter has shown to be unreliable. Flow cytometry can be a valuable tool in studies involving cryo-damage as long as the limitations of traditional gating methods are taken into account, and the alternatives are considered.

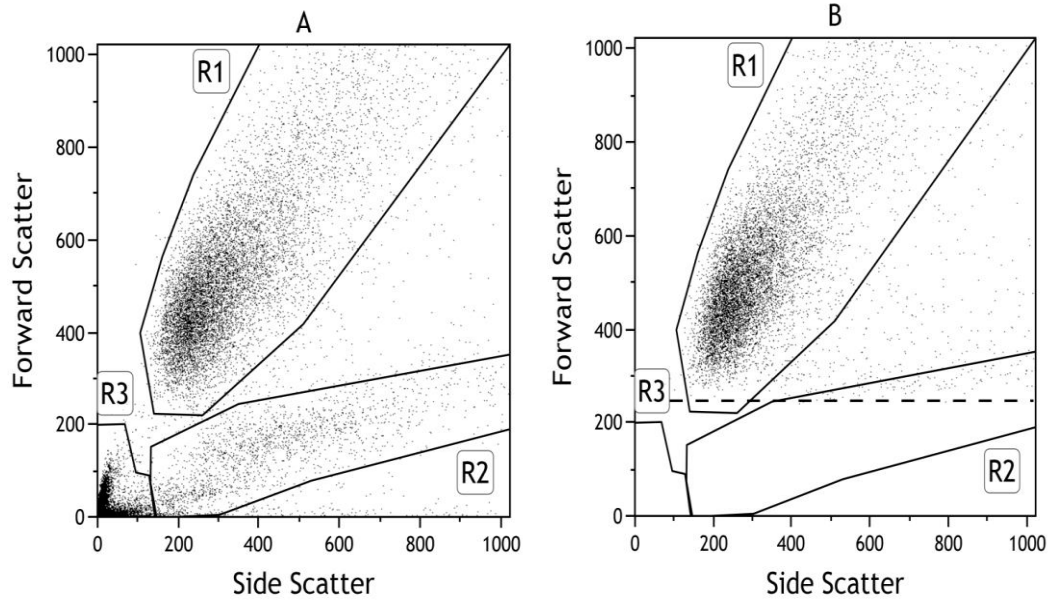


Figure 3-1. Flow cytometry forward vs. side scatter intensity plots of

HUVEC room temperature controls:

- A) Raw data showing all events
- B) Data after application of a threshold on the forward scatter intensity

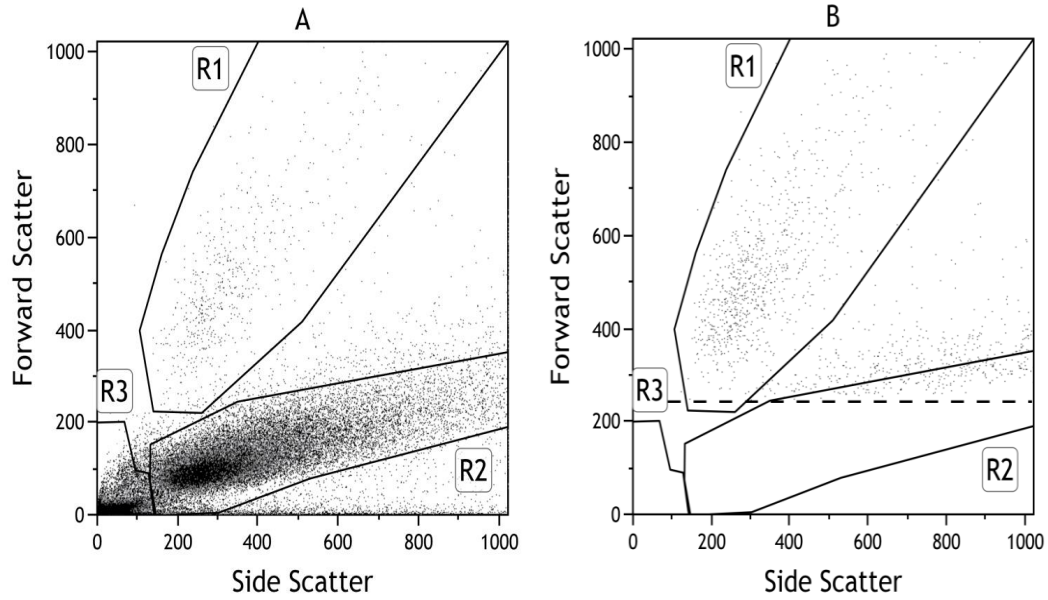


Figure 3-2. Flow cytometry forward vs. side scatter intensity plots of HUVEC after plunging in liquid nitrogen:

- A) Raw data showing all events
- B) Data after application of a threshold on the forward scatter intensity

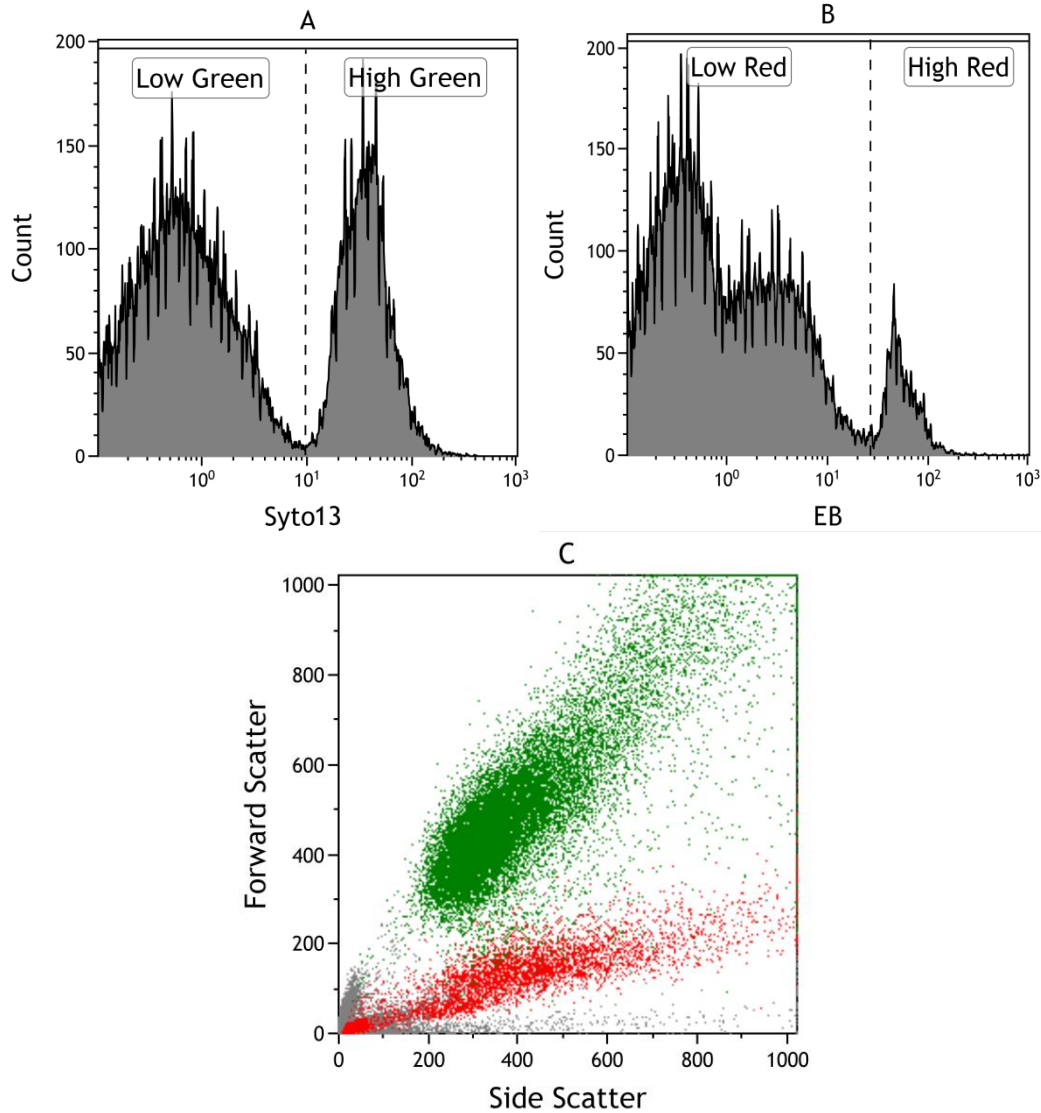


Figure 3-3. SytoEB membrane integrity analysis of HUVEC control samples as measured by flow cytometry.

- A) Histogram of Syto13 fluorescence intensity
- B) Histogram of ethidium bromide fluorescence intensity
- C) Forward vs. side scatter showing segregation of membrane intact cells (green), membrane compromised cells (red), and debris (grey)

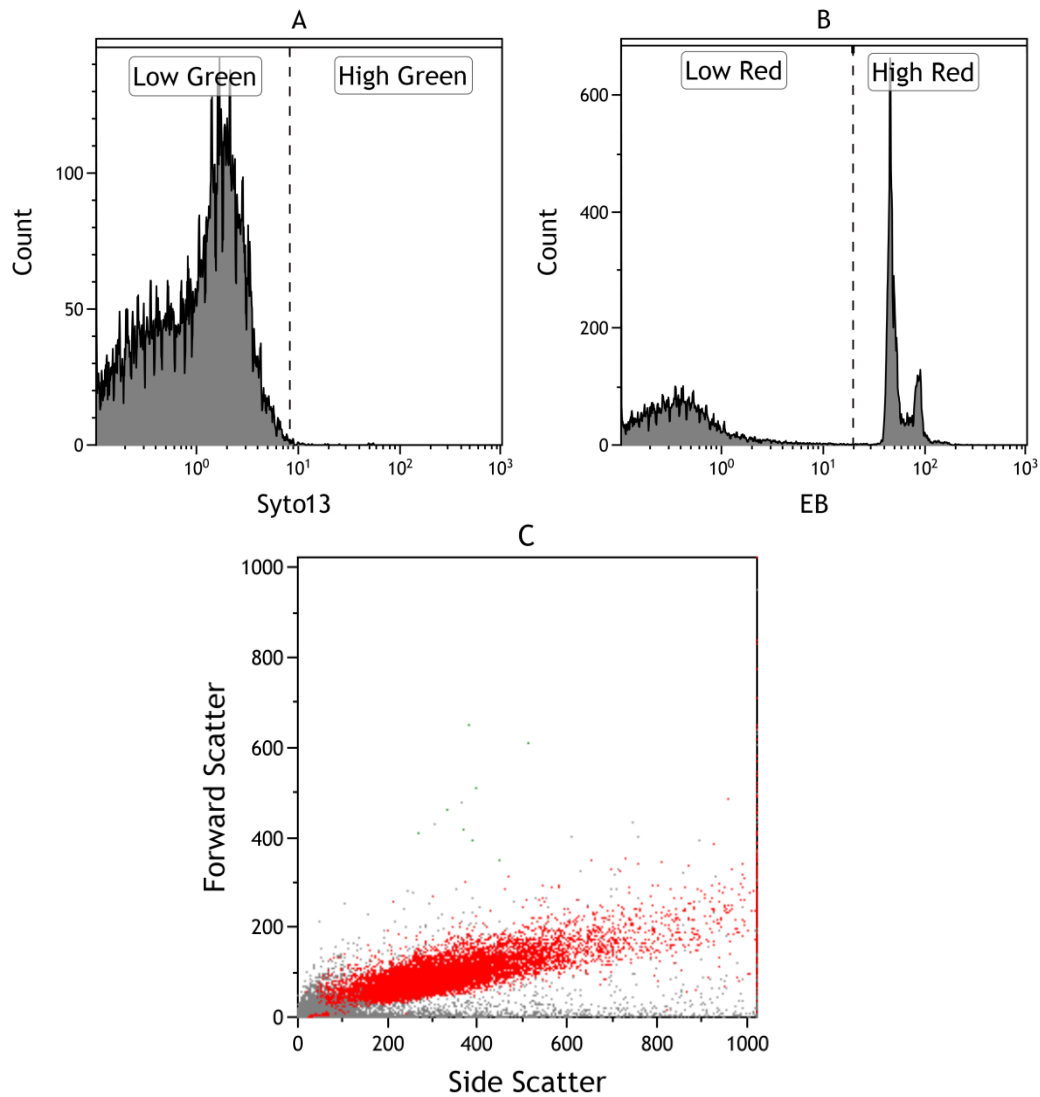


Figure 3-4. SytoEB membrane integrity analysis of HUVEC plunge samples as measured by flow cytometry.

- A) Histogram of Syto13 fluorescence intensity
- B) Histogram of ethidium bromide fluorescence intensity
- C) Forward vs. side scatter showing segregation of membrane intact cells (green), membrane compromised cells (red), and debris (grey)

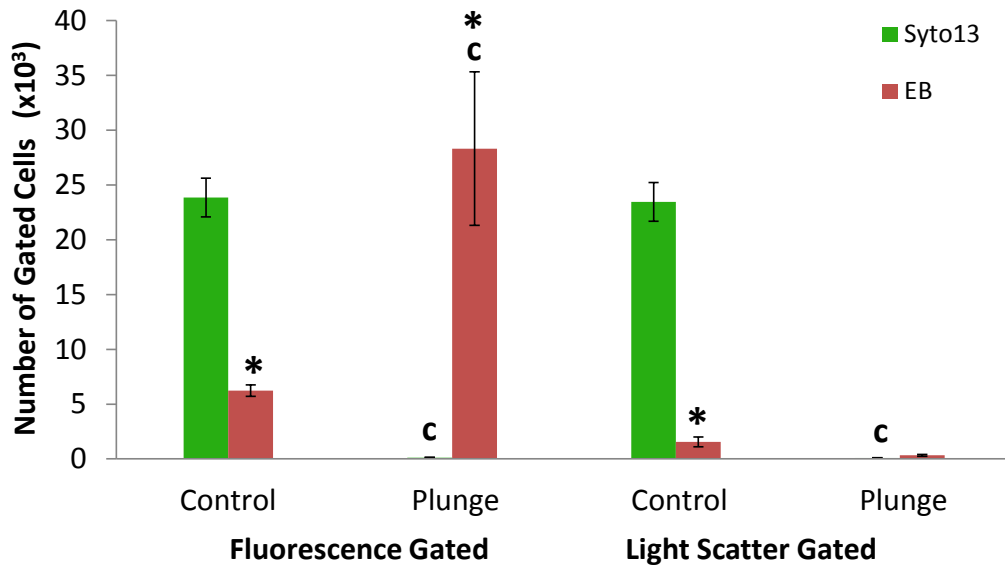


Figure 3-5. Membrane integrity analysis of events identified as cells.

Membrane integrity of HUVEC observed with Syto13 (green) and ethidium bromide (red) in control and plunge samples gated with either light scatter or fluorescence (mean \pm sem; n = 3).

* Signifies statistically significant difference in the number of EB gated cells from Syto13 of the same group (P < 0.05)

^c Signifies statistically significant difference in membrane integrity of plunge-thaw sample from the respective control sample (P < 0.05)

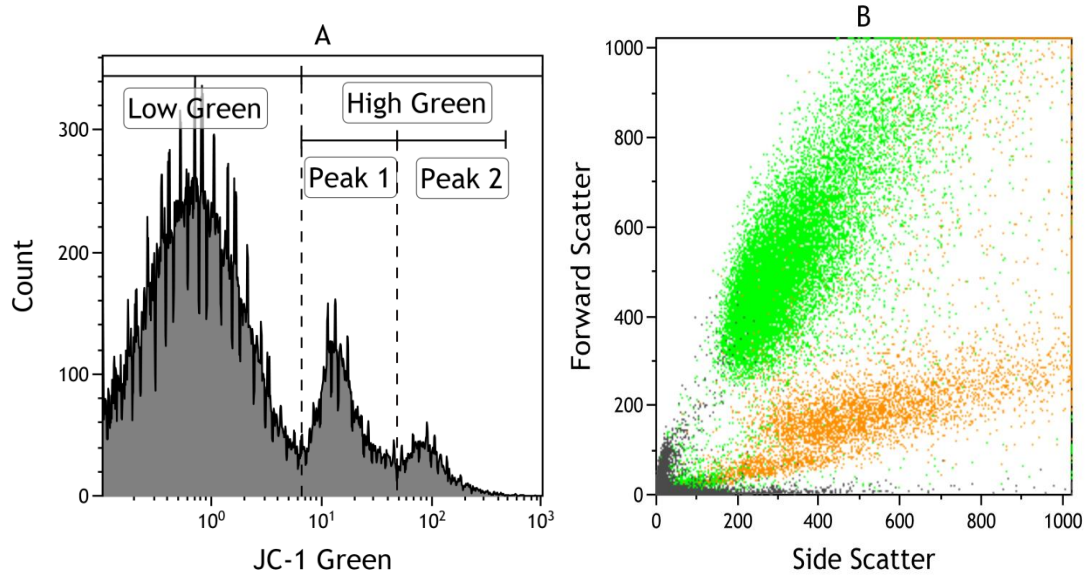


Figure 3-6. JC-1 mitochondrial polarization analysis of events gated as cells and debris in HUVEC control samples measured with flow cytometry

- A) Histogram of JC-1 green fluorescence intensity showing cells (high green) with polarized (peak 1) and depolarized (peak 2) mitochondria separate from debris (low green)
- B) Forward vs. side scatterplot showing segregation of cells with polarized (light green) and depolarized (orange) mitochondria from debris (grey)

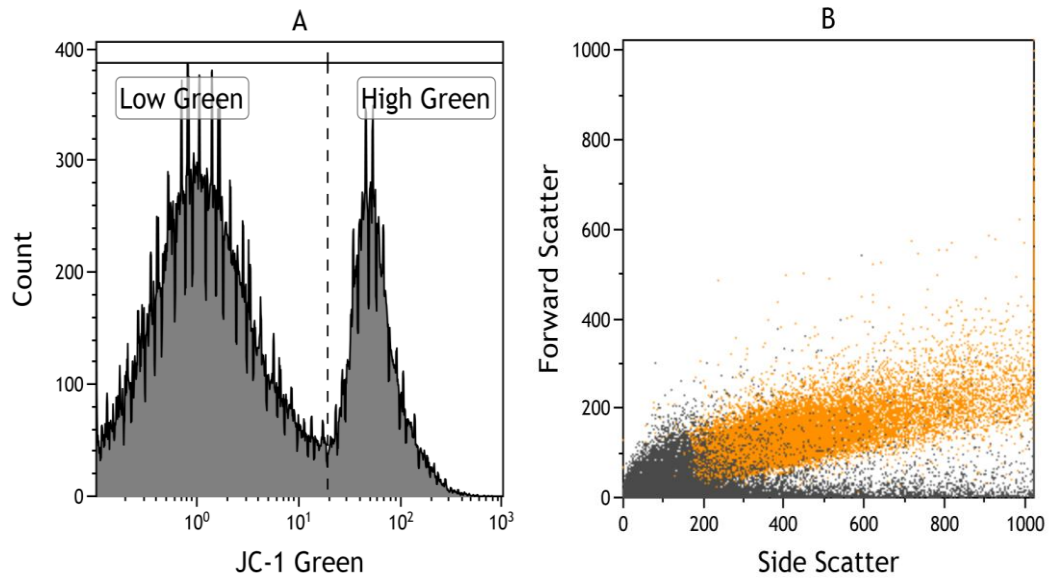


Figure 3-7. JC-1 mitochondrial polarization analysis of HUVEC plunge samples measured with flow cytometry

- A) Histogram of JC-1 green fluorescence intensity
- B) Forward vs. side scatter plot showing segregation of damaged cells (orange) from debris (grey)

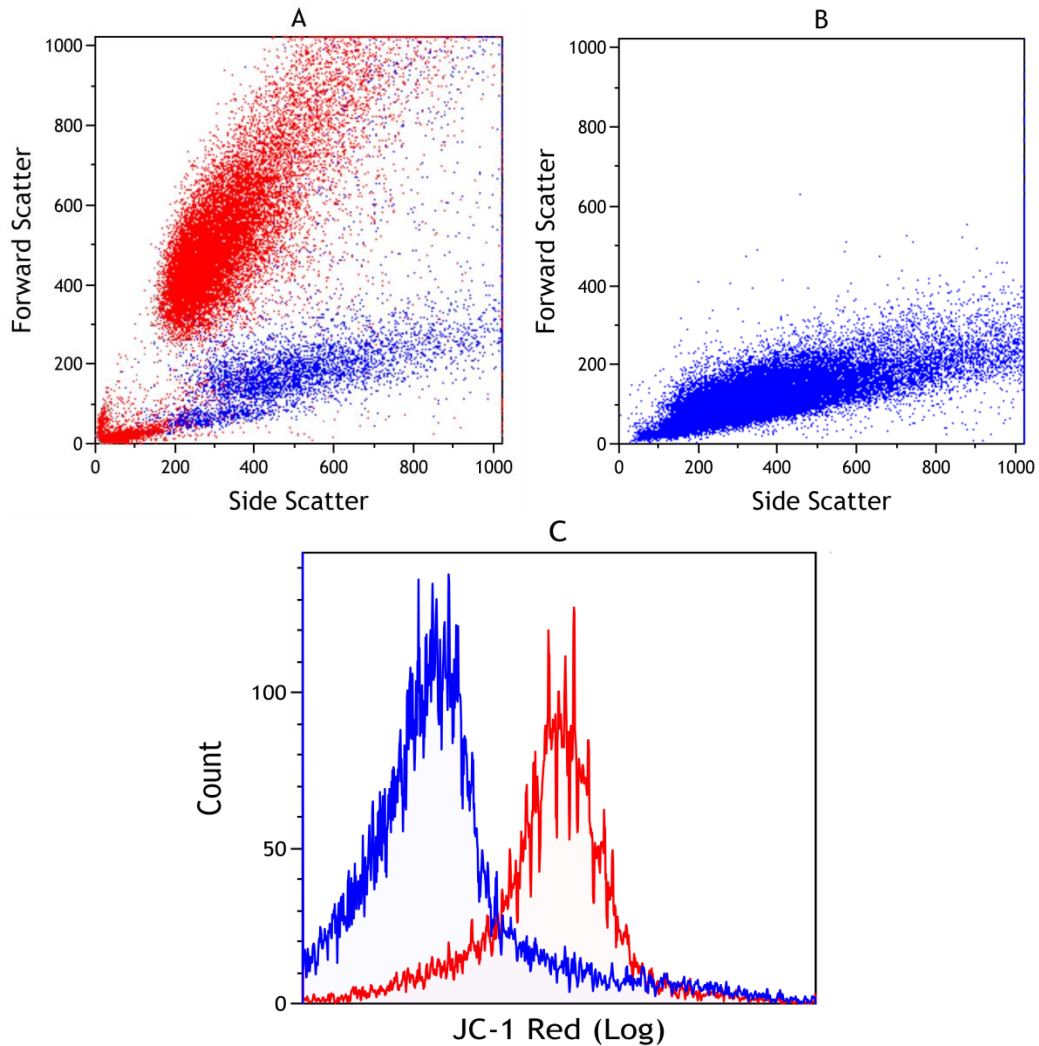


Figure 3-8. JC-1 mitochondrial polarization analysis of HUVEC red fluorescence measured with flow cytometry

- A) Forward vs. side scatter plot of control cells at room temperature showing cells with polarized (red) and depolarized (blue) mitochondria
- B) Forward vs. side scatter plot of plunged cells directly into liquid nitrogen showing only cells with depolarized mitochondria (blue)
- C) Histogram comparing the intensity of red fluorescence of control (red) and plunged (blue) cells

3.6 References

- [1] J.F. Abrahamsen, A.M. Bakken, Ø. Brusserud, B.T. Gjertsen, Flow cytometric measurement of apoptosis and necrosis in cryopreserved PBPC concentrates from patients with malignant diseases, *Bone Marrow Transplant.* 29 (2002) 165-171.
- [2] J.P. Acker, L.E. McGann, Cell-cell contact affects membrane integrity after intracellular freezing, *Cryobiology* 40 (2000) 54-63.
- [3] B. Balint, D. Paunovic, D. Vucetic, D. Vojvodic, M. Petakov, M. Trkuljic, N. Stojanovic, Controlled-rate versus uncontrolled-rate freezing as predictors for platelet cryopreservation efficacy, *Transfusion* 46 (2006) 230-235.
- [4] J. Baust, R. Van Buskirk, J. Baust, Cell viability improves following inhibition of cryopreservation-induced apoptosis, *In Vitro Cell. Dev. Biol. - Anim.* 36 (2000) 262-270.
- [5] M.C. Benson, D.C. McDougal, D.S. Coffey, The application of perpendicular and forward light scatter to assess nuclear and cellular morphology, *Cytometry* 5 (1984) 515-522.
- [6] G. Boeck, Current status of flow cytometry in cell and molecular biology, *Int. Rev. Cytol.* 204 (2001) 239-298.
- [7] F. Dankberg, M.C. Persidsky, A test of granulocyte membrane integrity and phagocytic function, *Cryobiology* 13 (1976) 430-432.
- [8] T.M. Gliozzi, L. Zaniboni, S. Cerolini, DNA fragmentation in chicken spermatozoa during cryopreservation, *Theriogenology* 75 (2011) 1613-1622.
- [9] M. Hagedorn, J. Ricker, M. McCarthy, S.A. Meyers, T.R. Tiersch, Z.M. Varga, F.W. Kleinhans, Biophysics of zebrafish (*Danio rerio*) sperm, *Cryobiology* 58 (2009) 12-19.
- [10] M. Jaroszeski, G. Radcliff, Fundamentals of flow cytometry, *Mol. Biotechnol.* 11 (1999) 37-53.
- [11] M. Kerker, Elastic and inelastic light scattering in flow cytometry. *Cytometry* 4 (1983) 1-10.

- [12] G. Kroemer, N. Zamzami, S. Susin, Mitochondrial control of apoptosis, *Immunol. Today* 18 (1997) 44-51.
- [13] P. Latimer, Light scattering vs. microscopy for measuring average cell size and shape, *Biophys. J.* 27 (1979) 117-126.
- [14] P. Latimer, B.E. Pyle, Light scattering at various angles. Theoretical predictions of the effects of particle volume changes. *Biophys. J.* 12 (1972) 764-773.
- [15] M.R. Loken, L.A. Herzenberg, Analysis of cell populations with a fluorescence activated cell sorter, *Ann. N. Y. Acad. Sci.* Vol 254 (1975) 163-171.
- [16] M.R. Loken, D.W. Houck, Light scattered at two wavelengths can discriminate viable lymphoid cell populations on a fluorescence-activated cell sorter, *J. Histochem. Cytochem.* 29 (1981) 609-615.
- [17] M.R. Loken, R.G. Sweet, L.A. Herzenberg, Cell discrimination by multiangle light scattering, *J. of Histochem. Cytochem.* 24 (1976) 284-291.
- [18] A. Longobardi-Givan, *Flow Cytometry: First Principles*, second ed., Wiley-Liss inc., New York, NY, USA, 2001. 34.
- [19] J.C. Lu, F. Chen, H.R. Xu, Y.M. Wu, X.Y. Xia, Y.F. Huang, N.Q. Lu, Is flow cytometry really adapted to the determination of sperm concentration? *Scand. J. Clin. Inves.* 67 (2007) 394-401.
- [20] J.P. McCoy Jr., W.H. Chambers, R. Lakomy, J.A. Campbell, C.C. Stewart, Sorting minor subpopulations of cells: Use of fluorescence as the triggering signal, *Cytometry* 12 (1991) 268-274.
- [21] L.E. McGann, M.L. Walterson, L.M. Hogg, Light scattering and cell volumes in osmotically stressed and frozen-thawed cells, *Cytometry* 9 (1988) 33-38.
- [22] M.R. Melamed, T. Lindmo, M.L. Mendelsohn (Eds.) *Flow Cytometry and Sorting*, second ed., Wiley-Liss, New York, 1990, chapter 5.
- [23] R.A. Meyer, A. Brunsting, Light scattering from nucleated biological cells, *Biophys. J.* 15 (1975) 191-203.
- [24] P.F. Mullaney, M.A. Van Dilla, J.R. Coulter, P.N. Dean, Cell sizing: A light scattering photometer for rapid volume determination, *Rev. Sci. Instrum.* 40 (1969) 1029-1032.

- [25] P. Mullaney, P. Dean, Small angle light scattering of biological cells - theoretical considerations, *Biophys. J.* 10 (1970) 764-772.
- [26] O. Nielsen, J.K. Larsen, I.J. Christensen, A. Lernmark, Flow sorting of mouse pancreatic B cells by forward and orthogonal light scattering, *Cytometry* 3 (1982) 177-181.
- [27] M.G. Ormerod, *Flow Cytometry : A Practical Approach*, third ed., Oxford University Press, New-York, 2000, p.47.
- [28] G.R. Otten, M.R. Loken, Two color light scattering identifies physical differences between lymphocyte subpopulations, *Cytometry* 3 (1982) 182-187.
- [29] J. Pasch, A. Schiefer, I. Heschel, N. Dimoudis, G. Rau, Variation of the HES concentration for the cryopreservation of keratinocytes in suspensions and in monolayers, *Cryobiology* 41 (2000) 89-96.
- [30] D.E. Pegg, Viability assays for preserved cells, tissues, and organs, *Cryobiology* 26 (1989) 212-231.
- [31] A.M. Petrunkina, R.A.P. Harrison, Systematic misestimation of cell subpopulations by flow cytometry: A mathematical analysis, *Theriogenology* 73 (2010) 839-847.
- [32] V. Ragoonanan, A. Hubel, A. Aksan, Response of the cell membrane-cytoskeleton complex to osmotic and freeze/thaw stresses, *Cryobiology* 61 (2010) 335-344.
- [33] M.A. Rehse, S. Corpuz, S. Heimfeld, M. Minie, D. Yachimiak, Use of fluorescence threshold triggering and high-speed flow cytometry for rare event detection, *Communications in Clinical Cytometry* 22 (1995) 317-322.
- [34] S. Salvioli, A. Ardizzoni, C. Franceschi, A. Cossarizza, JC-1, but not DiOC6(3) or rhodamine 123, is a reliable fluorescent probe to assess $\Delta\Psi$ changes in intact cells: Implications for studies on mitochondrial functionality during apoptosis, *FEBS Lett.* 411 (1997) 77-82.
- [35] G.C. Salzman, Light scatter: detection and usage. *Current protocols in cytometry / editorial board, J.P. Robinson, managing editor...[et al.] Chapter 1* (2001).
- [36] G.C. Salzman, J.M. Crowell, C.A. Goad, A flow system multiangle light scattering instrument for cell characterization, *Clin. Chem.* 21 (1975) 1297-1304.

- [37] G.C. Salzman, J.M. Crowell, J.C. Martin, Cell classification by laser light scattering: identification and separation of unstained leukocytes, *Acta Cytol.* 19 (1975) 374-377.
- [38] G.C. Salzman, M.E. Wilder, J.H. Jett, Light scattering with stream-in-air flow systems, *J. Histochem. Cytochem.* 27 (1979) 264-267.
- [39] T.K. Sharpless, M. Bartholdi, M.R. Melamed, Size and refractive index dependence of simple forward angle scattering measurements in a flow system using sharply-focused illumination, *J. Histochem Cytochem* 25 (1977) 845-856.
- [40] S. Smiley, M. Reers, C. Mottolahartshorn, M. Lin, A. Chen, T. Smith, G. Steele, L. Chen, Intracellular heterogeneity in mitochondrial membrane potentials revealed by a J-aggregate-forming lipophilic cation JC-1, *Proc. Natl. Acad. Sci.* 88 (1991) 3671-3675.
- [41] S.P. Srinivas, J.A. Bonanno, E. Larivière, D. Jans, W. Van Driessche, Measurement of rapid changes in cell volume by forward light scattering, *Pflugers Arch.* 447 (2003) 97-108.
- [42] P. Steponkus, Role of the plasma membrane in freezing-injury and cold acclimation, *Annu. Rev. Plant Physiol. Plant Mol. Biol.* 35 (1984) 543-584.
- [43] A. Tárnok, SYTO dyes and histoproteins - Myriad of applications, *Cytometry Part A* 73 (2008) 477-479.
- [44] M.J. Taylor, H.L. Bank, M.J. Benton, Selective killing of leucocytes by freezing: Potential for reducing the immunogenicity of pancreatic islets, *Diabetes Res.* 5 (1987) 99-103.
- [45] J. Tchir, J.P. Acker, Mitochondria and membrane cryoinjury in micropatterned cells: Effects of cell-cell interactions, *Cryobiology* 61 (2010) 100-107.
- [46] L.W.M.M. Terstappen, B.G. De Groot, G.M.J. Nolten, Physical discrimination between human T-lymphocyte subpopulations by means of light scattering, revealing two populations of T8-positive cells, *Cytometry* 7 (1986) 178-183.
- [47] L.W.M.M. Terstappen, M.R. Loken, Five-dimensional flow cytometry as a new approach for blood and bone marrow differentials, *Cytometry* 9 (1988) 548-556.

[48] L.W.M.M. Terstappen, V.O. Shah, M.P. Conrad, D. Recktenwald, M.R. Loken, Discriminating between damaged and intact cells in fixed flow cytometric samples, *Cytometry* 9 (1988) 477-484.

[49] A.J. Ullal, D.S. Pisetsky, C.F. Reich III, Use of SYTO 13, a fluorescent dye binding nucleic acids, for the detection of microparticles in in vitro systems, *Cytometry Part A* 77 (2010) 294-301.

Chapter 4. Interrupted slow cooling of HUVEC: a comparative analysis of mitochondrial and membrane cryoinjury

4.1 Introduction

Investigations of damage to single cells in suspension have led to a general understanding of the mechanisms of damage that occurs to cells as a result of slow and rapid cooling rates [6]. Cryobiologists have proposed mechanisms to explain the occurrence of cryoinjury, including: the formation of intracellular ice [9, 11, 28], prolonged exposure to elevated solute concentrations [7, 12], and osmotic stresses from the addition and removal of cryoprotective agents [4, 22]. The “two-factor hypothesis” suggests that damage during rapid cooling is associated with the formation of intracellular ice; and that damage during slow cooling is associated with solution effects injury as intra- and extracellular water is converted to ice [10]. Further investigation into the occurrence of cryoinjury will lead to novel advances in alleviation of cryoinjury in cryopreservation protocols.

There are routine protocols that have been developed to alleviate the injurious effects of freezing; however there are few protocols that focus on cell damage during progression through the freeze-thaw cycle. Farrant *et al.* showed that interrupting the cooling process at high subzero temperatures conferred a protection from damage during rapid cooling to

-196 °C in a variety of cell types [2]. Interrupted cooling protocols could be used not only to alleviate injury but also to investigate the response of cells throughout the cooling process. With fibroblasts as a cell model McGann used interrupted cooling to investigate cell damage at low temperatures during low rates of cooling [13]. More recently, Ross-Rodriguez *et al.* used interrupted cooling techniques to characterize the cryobiological responses of TF-1 hematopoietic stem cells [19-21].

Interrupted slow cooling, also known as graded freezing has been used to investigate cell responses at slower cooling rates. In terms of cell damage, slow cooling minimizes the probability of intracellular ice but leaves the cell susceptible to solution effects injury. The relatively long exposure to a high concentration of solutes associated with slower cooling rates may damage the membrane, increasing susceptibility of the cell to mechanical and osmotic stress [3]. The plasma membrane has been considered one of the primary sites of cryoinjury [26], and the importance of the plasma membrane to protect cells during freeze-thaw stress has led to membrane integrity becoming a standard method of cell assessment. Though membrane integrity assays have played an integral part as an upper limit in assessment of cellular viability, they do not provide insight into other important aspects of cell function that may also be susceptible to cryoinjury.

There has been a growing emphasis on studies investigating other sites of cryoinjury in addition to the plasma membrane. Cellular

components such as lysosomes [18], mitochondria [23, 24] and cytoplasmic granules [1] are adversely affected by freeze thaw-stress, causing structural and metabolic changes in cells. McGann *et al.* have conducted some extensive studies demonstrating cryoinjury to cytoplasmic and metabolic components of granulocytes [1, 14, 29], suggesting a second mechanism of damage may be occurring when cooling these cells. Other studies have found a disconnect between membrane damage and metabolic activity in split-thickness skin, and isolated keratinocytes [30] as well as canine kidney cells [27]. Mitochondria have been a particular point of interest as they are an important part of the functional capability of mammalian cells, involved in cellular metabolism, oxidative phosphorylation and ATP production, the citric acid cycle, cell signaling, and apoptosis. Findings by Sherman had noted “ultrastructural” changes to slowly cooled mitochondria [23], and correlated this damage with reduced respiratory function in mouse kidney tissue [24]. The involvement of mitochondria in such cell processes makes this organelle an attractive target for investigating a secondary site of cryoinjury.

In this study the relationship between mitochondrial and plasma membrane damage throughout the duration of a cryopreservation protocol was investigated. Human umbilical vein endothelial cells (HUVEC) were subjected to a slow cooling protocol (0.2 °C/min) and assessed with a mitochondrial polarization assay, and the results of this assay were

compared to previously obtained results of membrane integrity under the same conditions (chapter 2). The extent of cryoinjury was determined by quantifying membrane intact cells and cells that contained functional (polarized) mitochondria.

The flow cytometer has primarily been used in medical applications and immunofluorescent studies, but has also been an effective tool in cryopreservation studies. Flow cytometry was used to quantify the mitochondrial membrane polarization of slow cooled cells at decreasing experimental temperatures. The exposure of cells to cryobiological conditions and resultant changes in forward scattered light has made it difficult to identify frozen-thawed cells with traditional light scatter gating strategies, but we have shown that fluorescence gating can be used as a method of identifying cells from background (chapter 3). Fluorescent flow cytometric assessments enable high throughput observation of the membrane integrity and mitochondrial polarization of thousands of individual cells, allowing for a more comprehensive look at comparing sites of cryoinjury for cells in suspension.

4.2 Materials and methods

4.2.1 Cell cultures

Human umbilical vein endothelial cells ((Lot#0000120825) HUVEC; Lonza®, Walkersville, MD, USA) were cultured at 37 °C and 5 % CO₂ in endothelial basal media (EBM-2) supplemented with a bullet kit (Lonza®)

containing human fibroblast growth factor B, hydrocortisone, vascular endothelial growth factor, ascorbic acid, heparin, human endothelial growth factor, and fetal bovine serum (FBS). For continued passage of healthy cells, cultures were incubated to approximately 70-80 % confluency according to LONZA guidelines. For experiments requiring higher numbers of cells, cultures were left incubated until a higher confluency was observed (approximately 80-90 %) and then harvested by exposure to trypsin-EDTA (Lonza®) for 2 minutes at 37 °C. Cell suspensions were centrifuged at 201 g for 5 min in an Eppendorf 5810R tabletop centrifuge, and resuspended in endothelial growth media at a concentration of 1.0×10^6 cells/mL. Cells from multiple passages were used for each 1 mL aliquot contained in a 12x75 mm round bottom plastic tube (VWR, Edmonton Canada) for experimentation.

4.2.2 Interrupted cooling protocol

Graded freezing procedure (interrupted slow cooling without hold time)

The interrupted slow cooling procedure [13] was conducted as described in Ross-Rodriguez *et al.* [19]. A schematic representation of the graded freezing procedure is depicted in figure 2-2. Aliquots (0.2mL) of HUVEC cell suspension in endothelial growth media were transferred to 6x50 mm glass culture tubes (VWR, Edmonton, AB, Canada) and allowed to equilibrate at room temperature for 5 minutes. Positive controls were assessed at room temperature. Negative controls were plunged from room temperature directly into liquid nitrogen and assessed post-thaw.

Experimental samples were transferred to a stirred methanol bath preset at -3 °C and allowed to equilibrate for 5 minutes before ice was nucleated with cold forceps. Immediately post-nucleation the samples were then cooled, setting the methanol bath to cool at 0.2 °C/min where the temperature was monitored using a T-type thermocouple and Personal Daq View software. At each experimental temperature (-3, -6, -9, -12, -15, -20, -30 and -40 °C) one sample was directly thawed in a 37 °C water bath (thawing rate: 121 ± 14 °C/min) while the other was plunged into liquid nitrogen (cooling rate: 574 ± 104 °C/min). The plunged samples were kept in liquid nitrogen for a minimum of 1 hour before being thawed at 37 °C (thawing rate: 616 ± 16 °C/min) in the water bath. Duplicates of each sample were used for each experiment and repeated at least in triplicate using cells from different passages.

4.2.3 Assessment of cell recovery

Mitochondrial membrane potential assay

The 5',6,6'-tetrachloro-1,1',3,3'-tetraethylbenzimidazolylcarbocyanine iodide (JC-1) dye (Molecular Probes, Eugene, OR, USA) was used to assess the mitochondrial membrane potential of HUVEC in suspension. This cationic dye shows the extent of mitochondrial transmembrane potential. It shifts from green fluorescence (~525 nm) in low polarization states (non-functional mitochondria) to red fluorescence (~590 nm) in high polarization states (functioning mitochondria). This change in colour is based on a

concentration-dependent shift from monomers of the dye which fluoresce green to aggregates that fluoresce red. Initially the dye is present as membrane permeable, cationic monomers (green) that congregate in cells due to negative intracellular potential. In healthy cells these monomers then accumulate in the mitochondrial matrix, drawn by the negative charge of the inner mitochondrial membrane and form aggregates (red), as a function of the mitochondrial transmembrane potential [5]. Therefore cells with depolarized mitochondria emit green fluorescence from monomers present in the cytoplasm, and cells with polarized mitochondria predominantly emit red fluorescence from aggregates.

The JC-1 assay was prepared starting with the stock solution by combining 5 mg of the JC-1 reagent with 5 mL of Me₂SO (Sigma-Aldrich) to a concentration of 1 mg/mL. 0.8 µL of JC-1 reagent/Me₂SO solution was added to 0.4 mL aliquots of HUVEC (final concentration: 2 µg/mL) and incubated for 30 minutes in the incubator at 37 °C and 5 % CO₂.

4.2.4 Flow cytometry assessment

Assessment of mitochondrial polarization was conducted with an unmodified Coulter[®] EPICS[®] XL-MCL[™] flow cytometer (Beckman-Coulter) equipped with a 488 nm argon laser. Emission of JC-1 monomers was detected using the FL1 (505-545 nm) bandpass filter and that of JC-1 aggregates was detected using the FL2 (560-590 nm) bandpass filter. Aliquots of HUVEC (0.4 mL) were loaded and run for a time interval of 2 minutes in Isoflow[™] sheath fluid (Beckman-Coulter).

The corresponding plots were analyzed with flow cytometry analysis software (Kaluza™ v1.2 from Beckman-Coulter) as two parameter histograms were produced of the fluorescent properties of each sample. HUVEC were identified and isolated using one parameter histograms of the intensity of green fluorescence on a log scale; a threshold was established to separate high fluorescent (HUVEC) from low fluorescent (sub-cellular debris) events (chapter 3). The mitochondrial membrane potential of events identified as cells was assessed using two parameter histograms of the intensity of red and green fluorescence on a log scale. Cells with functional mitochondria were determined by identifying events with a high red/green ratio of fluorescence intensity and the number of functional cells was compared to the total number of cells in suspension.

4.2.5 Statistical Analysis

Statistical analysis comparisons were conducted using a one-way analysis of variance (ANOVA) ($P = 0.05$ level of significance). This analysis was used to evaluate statistical differences between temperatures for membrane integrity and mitochondrial membrane potential. A one-way ANOVA was also used to evaluate statistical differences between the values of directly-thawed and plunge-thawed samples for membrane integrity and mitochondrial membrane potential ($P = 0.05$ level of significance). The mean values and standard error of the mean was also calculated and included in the result (mean \pm sem).

4.3 Results and discussion

4.3.1 Controls and contour plots: measurements of mitochondrial membrane potential with flow cytometry

The mitochondrial membrane potential assay JC-1 used to assess HUVEC control samples at room temperature is presented in figure 4-1. A flow cytometry scatterplot (figure 4-1A) shows each cell represented as a dot with a distinct measure of green (x-axis) and red (y-axis) fluorescence from the JC-1 dye. Events were identified as cells from debris using a previously established fluorescent gating strategy (chapter 3). A previous investigation of HUVEC controls (chapter 3) had shown that there are two populations present in the control sample: a large population representing the majority of cells, the viable cells, and a smaller population with fewer cells, the non-viable cells. Assessment with JC-1 also shows the presence of two populations: a large group of cells with polarized mitochondria, and a smaller group of cells with depolarized mitochondria. However, it is difficult to visually discriminate between these two populations within the scatterplot (figure 4-1A) due to the high number of registered cells.

A contour plot is another visual representation of the flow cytometry data that identifies regions in the two-parameter histogram with the same density of events (figure 4-1B). The contours outline a region that contains a number of densely packed cell events, where the colour of each contour indicates the density of events contained within it; high, moderate, and low density regions are denoted by red, green and blue contours respectively.

Contour plots allow for ease of visualization in discriminating populations of cells assessed with JC-1, and distinguishing the population of cells with polarized mitochondria from the population with depolarized mitochondria.

An assessment of HUVEC controls conducted with the JC-1 mitochondrial polarization assay is shown in figure 4-2. Contour plots were used to assess both positive control cells at room temperature (figure 4-2A) and negative control cells plunged directly into liquid nitrogen and subsequently thawed (figure 4-2B). Using these plots, gates were established to separate cells with polarized mitochondria (R1) that have a high red/green fluorescence ratio from cells with depolarized mitochondria (R2) that have a low red/green fluorescence ratio. Control samples showed a large population of cells with polarized mitochondria (83.3 ± 0.8 %) and a smaller population of cells with depolarized mitochondria (16.7 ± 0.8 %). Cells plunged into liquid nitrogen showed a majority of cells with depolarized mitochondria (88.4 ± 0.4 %) with a smaller number of cells with polarized mitochondria (11.6 ± 0.3 %). The plunging of cells from room temperature into liquid nitrogen causes a decrease in the number of high red/green fluorescent cells (R1) and an increase in the number low red/green fluorescent cells (R2). This was an indication that this change in condition caused the mitochondria of the majority of cells in suspension to become depolarized, shifting them from R1 to R2. Based on the results of these controls, (and the mechanism of JC-1, and the way that JC-1 has been used in the literature [25]) regions R1 and R2 were

used to assess the mitochondrial polarization of HUVEC during interrupted slow cooling.

4.3.2 Investigating the effect of decreasing temperature on the polarization state of HUVEC mitochondria during interrupted slow cooling

A series of contour plots shows the progression of HUVEC mitochondrial membrane potential with decreasing temperature showing directly thawed (figure 4-3) and plunge-thawed (figure 4-4) cells.

The mitochondrial polarization of directly-thawed cells from decreasing experimental temperatures (-3 to -40 °C) during a single experiment is shown in figure 4-3. Directly-thawing cells from the highest experimental temperature (-3 °C, top left panel of figure 4-3) resulted in the majority of cells containing polarized mitochondria; this population is shown as a large contour with high red/green fluorescence (R1). Cooling HUVEC at a relatively slow rate (0.2 °C/min) progressively decreased the size of the contour in R1 and simultaneously increased the size of the contour in R2 as cells were thawed from decreasing experimental temperatures (progressive panels in figure 4-3). This was an indication that when cooled slowly, as the temperature decreased, increasing numbers of HUVEC had depolarized mitochondria, shown as a shift in the number of cells from R1 to R2. Cooling these cells to temperatures lower than -20 °C resulted in a very few cells with polarized mitochondria (<10 %) (last 3 panels of Figure 4-3).

The mitochondrial polarization of cells plunged into liquid nitrogen from decreasing experimental temperatures (-3 to -40 °C) during a single experiment is shown in figure 4-4. Plunging cells from the highest experimental temperature (-3 °C, top left panel of figure 4-4) resulted in the majority of cells having depolarized mitochondria (R2). Post-thaw assessment of plunge-thaw cells from further decreased temperatures (-6 to -40 °C) showed that these temperatures had no further effect on the polarization state of cellular mitochondria.

Figure 4-5 shows the compiled data from mitochondrial assessments comparing results for directly thawed and plunge-thawed HUVEC. The data was normalized to room temperature controls (83.3 ± 0.8 %). The number of directly thawed cells with polarized mitochondria was shown to significantly decrease with decreasing temperature (-12 to -40 °C) ($P < 0.05$), whereas the majority of plunged cells were depolarized at all experimental temperatures.

Interrupted cooling protocols allow for separate observation and assessment of cryoinjury that occurs when cooling to the experimental temperature and when further cooling to the storage temperature. The progressive decrease in mitochondrial polarization that was observed in directly thawed cells may be attributed to slow cooling injury from the relatively slow cooling rate (0.2 °C/min). After extracellular ice nucleation, slower cooling increases the amount of extracellular ice with decreasing temperature, resulting in increased extracellular solutes; to maintain

equilibrium cells efflux water, causing cells to shrink and lose volume; the culmination of these events increases intracellular solutes, and solution effects injury [8, 17]. The plasma membrane has been the main focus around current theories of cell damage due to solution effects [3, 8, 16] but other sites within the cell such as mitochondria may also be affected. Few cells contained polarized mitochondria when these cells were plunged from any of the experimental temperatures (-3 to -40 °C). Rapid cooling rates do not give the cell enough time to lose intracellular water making them susceptible to the formation of intracellular ice [12].

4.3.3 Mitochondria and the membrane: a comparison of HUVEC mitochondrial polarization and membrane integrity during interrupted slow cooling

A comparison of HUVEC cryobiological responses during interrupted slow cooling is shown in figure 4-6 where the mitochondrial membrane potential (JC-1) results are plotted together with the membrane integrity (SytoEB) results from Chapter 2 conducted under the same conditions. A verification for the comparison of membrane integrity with fluorescence microscopy and mitochondrial polarization with flow cytometry is present in appendix A. Data were normalized to positive control samples at room temperature for membrane integrity (86.7 ± 2.1 %) and mitochondrial membrane potential (83.3 ± 0.8 %).

Directly-thawed HUVEC showed a significant decrease with decreasing temperature in both membrane integrity (-20 to -40 °C,

$P < 0.05$) and mitochondrial polarization (-12 to -40 °C, $P < 0.05$) (figure 4-6). At higher experimental temperatures (-3 to -15 °C) there was no change in membrane integrity, whereas mitochondrial polarization decreased at -12 °C and below. A greater number of cells exhibited depolarized mitochondria than exhibited loss of membrane integrity under these conditions, demonstrated by a 50 % loss of mitochondrial polarization at -15 °C, and a 50 % loss of membrane integrity at -30 °C. Progressive slow cooling had a more profound effect on mitochondrial membrane potential than on membrane integrity for directly thawed HUVEC.

HUVEC plunged samples showed a significant increase in the number of membrane intact cells with decreasing temperature from -15 to -30 °C ($P < 0.05$), where mitochondrial polarization of identically-treated samples showed a low percentage of cells with polarized mitochondria (<10 %) throughout the full range of experimental temperatures (-3 to -40 °C).

A comparison of mitochondrial and membrane responses to the same interrupted cooling protocol showed that cells were damaged to a different extent based on the site of injury that was assessed, with mitochondria more greatly affected compared to the plasma membrane of plunge-thawed cells. After normalization to controls, HUVEC slow cooled (0.2 °C/min) to -20 °C and plunged into liquid nitrogen showed approximately 40 % of cells with an intact plasma membrane; but few

(<8 %) of those cells contained polarized mitochondria. Previous studies have suggested that freezing and thawing have an indirect deleterious effect on cellular mitochondria and that these organelles may exhibit differential sensitivities to freezing conditions [23, 24].

The difference between the cryobiological response of mitochondria and the plasma membrane may be explained by two separate mechanisms of damage affecting these sites of injury. McGann *et al.* proposed a general model of slow cooling injury in which lysosomes are initially adversely affected causing a release of hydrolytic enzymes that subsequently damage mitochondria and the plasma membrane [14]. Lysosomes had been identified as primary targets of cryoinjury [18], and the release of hydrolytic enzymes has the capacity to uncouple oxidative phosphorylation in mitochondria [15]. This model provides an explanation for indirect damage to mitochondria that manifested from slow cooling hypertonic conditions causing decreased mitochondrial polarization in cells that had maintained membrane integrity.

This model has been generalized into the occurrence of two types of cell damage during slow cooling: a direct damage to the plasma membrane from solution effects injury, and an indirect damage that adversely affects components of the cytoplasm. Our results indicate that two types of damage are taking place (figure 4-6), that are affecting mitochondria and the plasma membrane differently during interrupted slow cooling. Other evidence of indirect slow cooling damage has been

demonstrated in granulocytes [1, 29], fibroblasts [14], split-thickness skin and isolated keratinocytes [30].

4.4 Conclusions

This study focused on damage to HUVEC at two different sites of cryoinjury during an interrupted slow cooling protocol (graded freezing). Flow cytometry was used to identify and assess the mitochondrial polarization state of HUVEC. Assessment of mitochondrial polarization showed that progressively more cells had depolarized mitochondria with decreasing temperatures, and that few cells showed polarized mitochondria when plunged into liquid nitrogen, regardless of prior exposure to an experimental temperature. When mitochondrial polarization was compared to membrane integrity (chapter 2), assessment of these two different sites of cryoinjury showed that mitochondria were depolarized under cooling conditions where the plasma membrane was still intact. The differential cryobiological response between mitochondrial polarization and membrane integrity may be attributed to different types of damage at each of these sites. Direct damage to the plasma membrane may be attributed to solution effects injury, and indirect damage may be affecting the cytosolic components of cells such as HUVEC mitochondria.

Although the occurrence of indirect damage is well documented, there is only speculation on the mechanism of how this damage occurs. Further studies on the details of damage to other organelles, cell

processes and pathways during slow cooling would provide further insight into the mechanism of how slow cooling injury occurs and whether or not this injury is reversible or results in cell death. Investigation of the details of cryoinjury may lead to novel approaches and breakthroughs in future cryopreservation of cells and tissues.

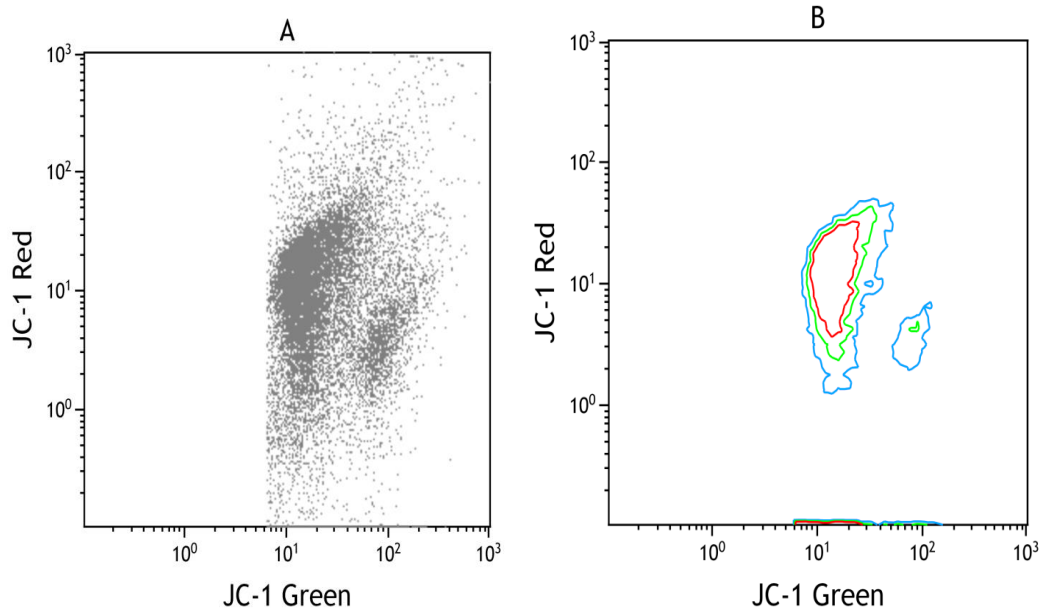


Figure 4-1. Representation of HUVEC control at room temperature, after incorporation of a fluorescent threshold (Chapter 3).

- A) Scatterplot of all cells recorded by the flow cytometer
- B) Scatterplot converted to a contour plot of cells showing regions of high (red contour line), moderate (green contour), and low (blue contour), number of cells measured by flow cytometry

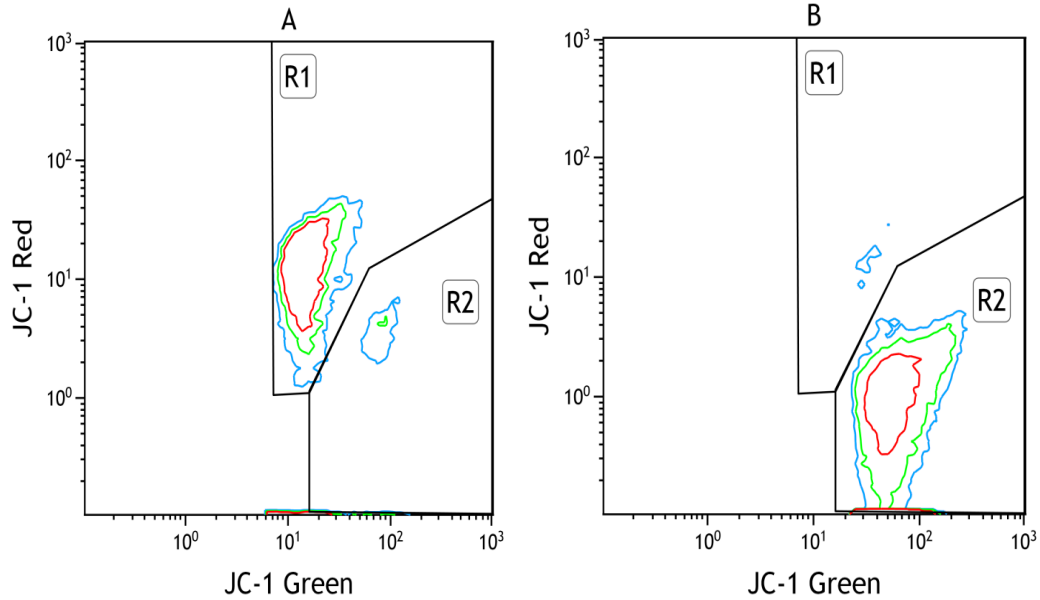


Figure 4-2. Contour plots of HUVEC membrane integrity analysis with JC-1. Showing cells containing polarized (R1) and depolarized (R2) mitochondria, as well as areas with a high (red contour), moderate (green contour), and low (blue contour) number of cells measured by flow cytometry

A) Control samples

B) Samples plunged in liquid nitrogen (-196°C) and thawed rapidly

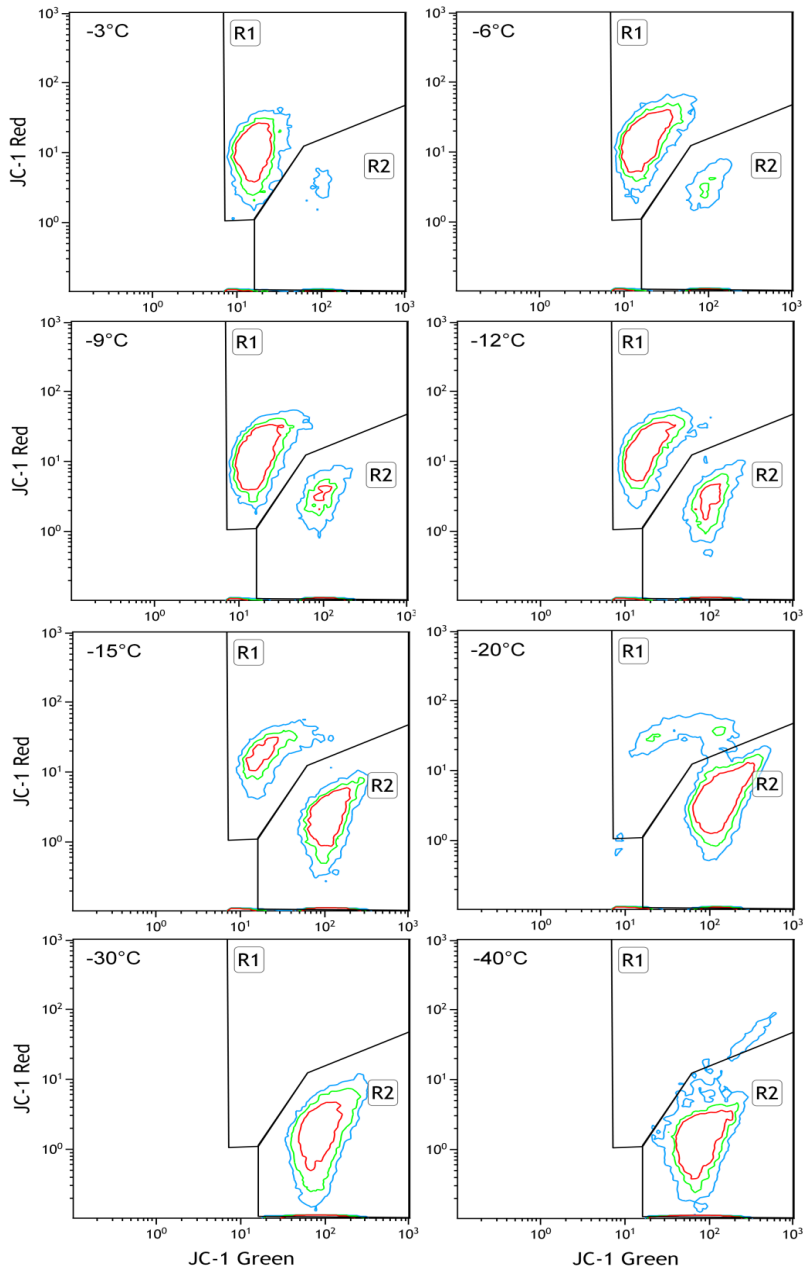


Figure 4-3. Contour plots of mitochondrial polarization of direct-thaw

HUVEC from intermediate temperatures when cooled at 0.2 °C/min.

Showing cells containing polarized (R1) and depolarized (R2)

mitochondria, as well as areas with a high (red contour), moderate (green

contour), and low (blue contour) number of cells measured by flow

cytometry

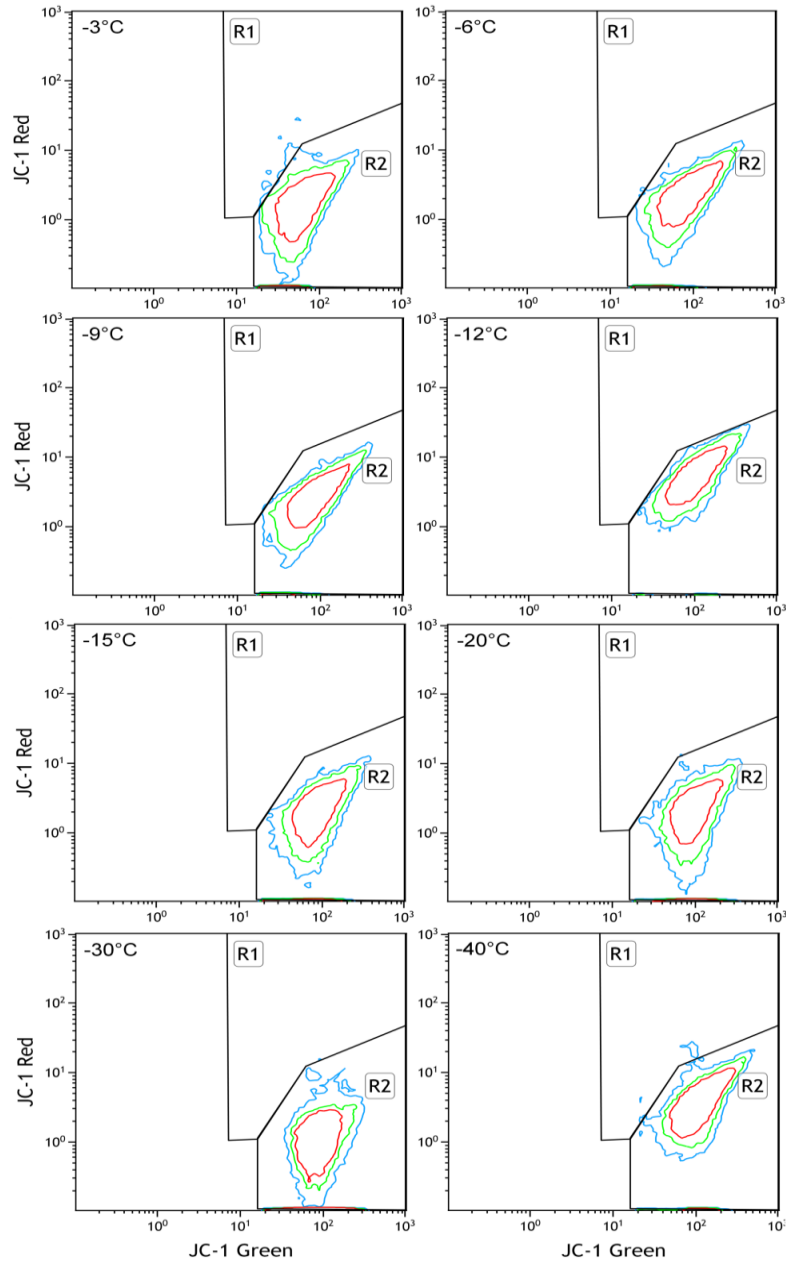


Figure 4-4. Contour plots of mitochondrial polarization of plunge-thawed HUVEC plunged from different temperatures after cooling at 0.2 °C/min. Showing cells containing polarized (R1) and depolarized (R2) mitochondria, as well as areas with a high (red contour), moderate (green contour), and low (blue contour) number of cells measured by flow cytometry

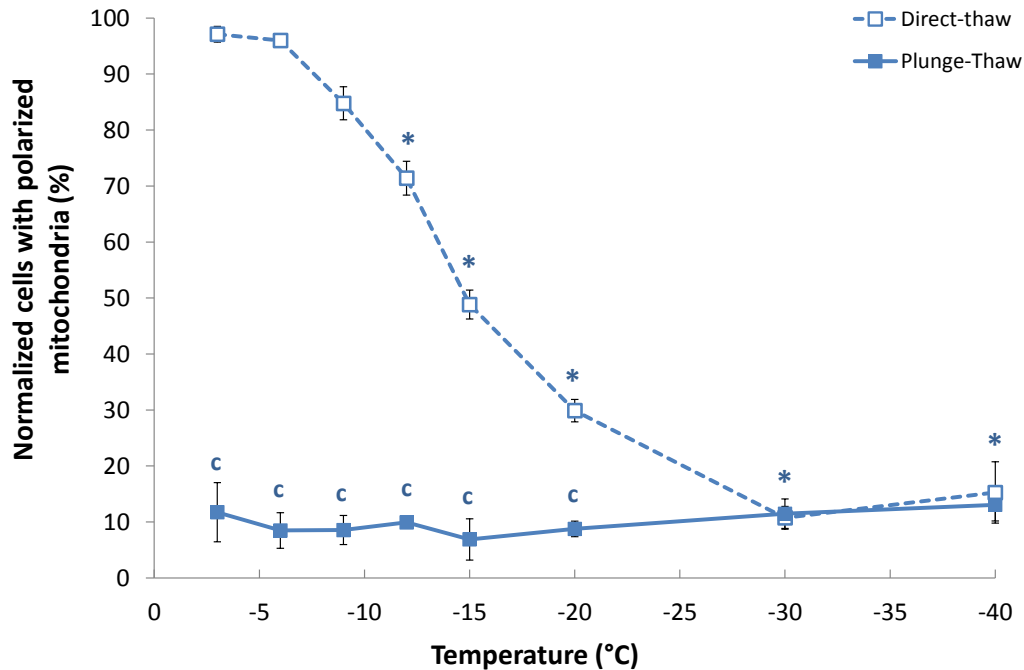


Figure 4-5. Summary of HUVEC mitochondrial polarization (JC-1)

analysis. Cells were cooled to various subzero temperatures at a rate of 0.2 °C/min (mean ± sem; normalized to control; n = 3) and then either thawed directly (dashed) or plunged into liquid nitrogen (solid) before being thawed.

* Signifies statistically significant difference in membrane integrity at the measured temperature from the initial temperature (-3 °C) of the same curve (P < 0.05)

° Signifies statistically significant difference in membrane integrity of plunge-thaw samples from the respective direct-thaw sample (P < 0.05)

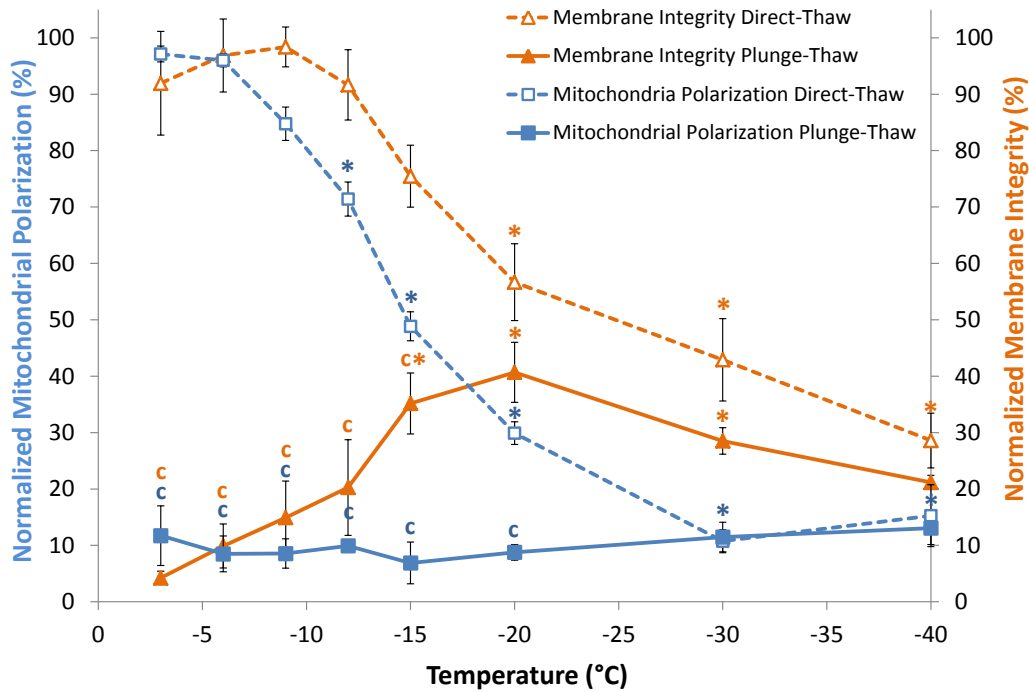


Figure 4-6. Comparison of membrane integrity (SytoEB) and mitochondrial polarization (JC-1) analysis of HUVEC. Cells were cooled to various subzero temperatures at a rate of 0.2 °C/min (mean ± sem; normalized); then either thawed directly (dashed) or plunged into liquid nitrogen (solid) before being thawed.

* Signifies statistically significant difference in membrane integrity at the measured temperature from the initial temperature (-3 °C) of the same curve (P < 0.05)

° Signifies statistically significant difference in membrane integrity of plunge-thaw samples from the respective direct-thaw sample (P < 0.05)

4.5 References

- [1] F. Arnaud, H. Yang, L.E. McGann, Freezing injury of granulocytes during slow cooling: Role of the granules, *Cryobiology* 33 (1996) 391-403.
- [2] J. Farrant, S.C. Knight, L.E. McGann, J. O'Brien, Optimal recovery of lymphocytes and tissue culture cells following rapid cooling, *Nature* 249 (1974) 452-453.
- [3] J. Farrant, G. Morris, Thermal shock and dilution shock as causes of freezing injury, *Cryobiology* 10 (1973) 134-140.
- [4] D.Y. Gao, J. Liu, C. Liu, L.E. McGann, P.F. Watson, F.W. Kleinhans, P. Mazur, E.S. Critser, J.K. Critser, Prevention of osmotic injury to human spermatozoa during addition and removal of glycerol, *Hum. Reprod.* 10 (1995) 1109-1122.
- [5] G. Kroemer, N. Zamzami, S. Susin, Mitochondrial control of apoptosis, *Immunol. Today* 18 (1997) 44-51.
- [6] S.P. Leibo, P. Mazur, The role of cooling rates in low-temperature preservation, *Cryobiology* 8 (1971) 447-452.
- [7] J.E. Lovelock, The denaturation of lipid-protein complexes as a cause of damage by freezing. *Proc. R. Soc. Lond. B. Biol. Sci.* 147 (1957) 427-433.
- [8] J.E. Lovelock, The haemolysis of human red blood-cells by freezing and thawing, *Biochim. Biophys. Acta* 10 (1953) 414-426.
- [9] P. Mazur, Equilibrium, quasi-equilibrium, and nonequilibrium freezing of mammalian embryos, *Cell Biophys.* 17 (1990) 53-92.
- [10] P. Mazur, The role of intracellular freezing in the death of cells cooled at supraoptimal rates, *Cryobiology* 14 (1977) 251-272.
- [11] P. Mazur, Kinetics of water loss from cells at subzero temperatures and the likelihood of intracellular freezing, *J. Gen. Physiol.* 47 (1963) 347-369.
- [12] P. Mazur, S.P. Leibo, E.H.Y. Chu, A two-factor hypothesis of freezing injury. Evidence from Chinese hamster tissue-culture cells, *Exp. Cell Res.* 71 (1972) 345-355.

- [13] L.E. McGann, Optimal temperature ranges for control of cooling rate, *Cryobiology* 16 (1979) 211-216.
- [14] L.E. McGann, H. Yang, M. Walterson, Manifestations of cell damage after freezing and thawing, *Cryobiology* 25 (1988) 178-185.
- [15] A. Mellors, A.L. Tappel, P.L. Sawant, I.D. Desai, Mitochondrial swelling and uncoupling of oxidative phosphorylation by lysosomes, *BBA - Bioenergetics* 143 (1967) 299-309.
- [16] H.T. Meryman, Freezing injury and its prevention in living cells. *Annu. Rev. Biophys. Bioeng.* 3 (1974) 341-363.
- [17] H.T. Meryman, Physical limitations of the rapid freezing method. *Proc. R. Soc. Lond. B. Biol. Sci.* 147 (1957) 452-459.
- [18] M.D. Persidsky, Lysosomes as primary targets of cryoinjury, *Cryobiology* 8 (1971) 482-488.
- [19] L.U. Ross-Rodriguez, J.A.W. Elliott, L.E. McGann, Characterization of cryobiological responses in TF-1 cells using interrupted freezing procedures, *Cryobiology* 60 (2010) 106-116.
- [20] L.U. Ross-Rodriguez, J.A.W. Elliott, L.E. McGann, Investigating cryoinjury using simulations and experiments. 1: TF-1 cells during two-step freezing (rapid cooling interrupted with a hold time), *Cryobiology* 61 (2010) 38-45.
- [21] L.U. Ross-Rodriguez, J.A.W. Elliott, L.E. McGann, Investigating cryoinjury using simulations and experiments: 2. TF-1 cells during graded freezing (interrupted slow cooling without hold time), *Cryobiology* 61 (2010) 46-51.
- [22] U. Schneider, P. Mazur, Osmotic consequences of cryoprotectant permeability and its relation to the survival of frozen-thawed embryos, *Theriogenology* 21 (1984) 68-79.
- [23] J.K. Sherman, Comparison of in vitro and in situ ultrastructural cryoinjury and cryoprotection of mitochondria, *Cryobiology* 9 (1972) 112-122.
- [24] J.K. Sherman, correlation in ultrastructural cryoinjury of mitochondria with aspects of their respiratory function, *Exp. Cell Res.* 66 (1971) 378-384.

- [25] S. Smiley, M. Reers, C. Mottolahartshorn, M. Lin, A. Chen, T. Smith, G. Steele, L. Chen, Intracellular heterogeneity in mitochondrial membrane potentials revealed by a J-aggregate-forming lipophilic cation JC-1, *Proc. Natl. Acad. Sci. U. S. A.* 88 (1991) 3671-3675.
- [26] P. Steponkus, Role of the plasma membrane in freezing-injury and cold acclimation, *Annu. Rev. Plant Physiol. Plant Mol. Biol.* 35 (1984) 543-584.
- [27] J. Tchir, J.P. Acker, Mitochondria and membrane cryoinjury in micropatterned cells: Effects of cell-cell interactions, *Cryobiology* 61 (2010) 100-107.
- [28] M. Toner, E.G. Cravalho, M. Karel, Thermodynamics and kinetics of intracellular ice formation during freezing of biological cells, *J. Appl. Phys.* 67 (1990) 1582-1593.
- [29] H. Yang, F. Arnaud, L.E. McGann, Cryoinjury in human granulocytes and cytoplasts, *Cryobiology* 29 (1992) 500-510.
- [30] M.A.J. Zieger, E.E. Tredget, L.E. McGann, Mechanisms of cryoinjury and cryoprotection in split-thickness skin, *Cryobiology* 33 (1996) 376-389.

Chapter 5 – General discussion and conclusions

5.1 Review of aim and hypotheses

Current methods of post-thaw cell assessments rely on membrane integrity as a primary determinant of cell viability. Although membrane integrity is a useful assay of cell survival as it gives an upper limit of viability, it gives little insight into the functional and metabolic capabilities of the cell. The aim of this thesis was to probe the occurrence of damage at a different site of cryoinjury for comparison with cell membrane responses when subjected to a particular cooling strategy. One hypothesis had stated that mitochondrial polarization would show an increased susceptibility to interrupted cooling protocols compared to membrane integrity of HUVEC. From this work it was observed that cryoinjury affects two components of the cell differently under the same cryopreservation conditions.

Flow cytometry was used as a tool to identify and assess cells under cryopreservation conditions. The other hypothesis stated that HUVEC were more readily identified from debris with a fluorescence gating strategy compared to traditional light scatter thresholds.

5.2 Summary of thesis results

Interrupted cooling protocols were used to quantify the cryobiological response of HUVEC to low temperatures in the absence of

cryoprotectant. Cells were subjected to a two-step freezing protocol over a range of decreasing temperatures and hold times, as well as a graded freezing protocol at varied cooling rates. According to the “two-factor hypothesis” of freezing injury cells cooled too rapidly have an increased probability of undergoing IIF, and cells cooled too slowly may be affected by solution effects [1]. HUVEC were observed to benefit from longer hold times and slower cooling rates, and to be adversely affected by rapid cooling rates and short hold times. This was an indication that HUVEC may be resistant to the solution effects injury associated with low cooling rates and susceptible to IIF associated with high cooling rates. Based on these results, only slow cooling rates were used as a basis of comparison for further assessments of cryoinjury.

The second study investigated the effectiveness of light scatter and fluorescent gating strategies with flow cytometry in low temperature studies. The stress imposed on cells from freezing at decreasing temperatures causes a decrease in the forward light scatter properties of cells, making them difficult to distinguish from debris. It is difficult to identify cells using traditional light scatter gating strategies that are typically used in flow cytometry studies. Light scatter gating was demonstrated to be ineffective for identifying cryoinjured cells from debris in samples plunged directly into liquid nitrogen. Gating based on intensity of fluorescence was considered as an alternative to light scatter for identification of both healthy and damaged cells. It was found that both

healthy and damaged HUVEC were effectively identified from debris under control and plunged conditions using the fluorescence intensity of membrane integrity (SytoEB) and mitochondrial polarization assays (JC-1). Although the basis of fluorescence for each of these assays was different, they were equally effective at identifying healthy and damaged cells with the flow cytometer under conditions where light scatter was shown to be unreliable. Flow cytometry has the potential to be a valuable tool in studies involving cryo-damage as long as the limitations of traditional methods are taken into account, and the alternatives are considered.

The third study explored the relationship between mitochondrial polarization and membrane integrity throughout the duration of an interrupted cooling protocol. A relatively slow rate of cooling (0.2 °C/min) was used to examine the effects of decreased temperatures on mitochondrial membrane potential (chapter 4) and these results were compared to previous assessments of membrane integrity (chapter 2). Post-thaw assessments showed that for directly thawed cells there was an increasing number of cells with depolarized mitochondria with decreasing temperature, and that cells plunged in liquid nitrogen and subsequently thawed contained few polarized mitochondria. A comparison of mitochondria and membrane integrity showed that mitochondria become depolarized under conditions where the plasma membrane is found to be intact. The difference in cryobiological response between mitochondrial

polarization and membrane integrity may be attributed to different types of damage at each of these sites. As direct damage from solution effects may cause damage to the plasma membrane, an indirect damage may be affecting the polarization state of mitochondria.

5.3 Significance in cryobiology

There are cooling strategies and methods of assessment that have become standard practice in the field of cryobiology. Cells are typically cooled at a set constant cooling rate combined with a variety of cryoprotective agents to freeze and preserve cells and the outcome of preservation is based on the membrane integrity of cells post-thaw. However, it is advantageous to also consider how freezing affects various components of cells and the relationship between physical and functional changes the cell undergoes when subjected to various low temperatures. This thesis provides a comparative analysis of mitochondrial polarization and membrane integrity cryobiological responses to various low temperatures during interrupted cooling. This study was conducted to emphasize the importance of looking at different sites of the cell that are damaged during cryopreservation. This study may contribute to devising theories to explain mechanisms of cell damage and may contribute to novel approaches of cryopreserving cells. It was shown that cells experience different degrees of damage at two sites of cryoinjury, as it was revealed that mitochondria become depolarized under conditions

where integrity of the plasma membrane was maintained. A better understanding of how cells are damaged at low temperatures will lead to approaches to alleviate this damage allowing for the development of new cryopreservation strategies.

This study also used flow cytometry to investigate the responses of cells in suspension. Flow cytometry is a common technique used in cell biology that has been implemented in preservation studies. This thesis showed that flow cytometry has the potential to be an effective tool in cryobiological studies but must be adapted to identify cryoinjured cells from debris. Flow cytometry studies typically identify cells from debris based on their light scatter properties, readily identifying healthy cells from cellular debris. However cryobiological conditions impose stress on cells that alter their light scatter properties, making cryoinjured cells difficult to identify from debris. It was shown that flow cytometry analysis can be properly adapted for use in cryopreservation applications by taking advantage of fluorescence intensity as a means of cell identification.

5.4 References

[1] P. Mazur, S.P. Leibo, E.H.Y. Chu, A two-factor hypothesis of freezing injury. Evidence from Chinese hamster tissue-culture cells, *Exp. Cell Res.* 71 (1972) 345-355.

Appendix A.

A verification of controls: membrane integrity with fluorescence microscopy and flow cytometry

In order to correctly verify that previous fluorescence microscopy results of membrane integrity (chapter 2) could be compared with flow cytometry results of mitochondrial polarization (chapter 4); an evaluation of membrane integrity of controls was conducted with the flow cytometer.

A dual fluorescent assay (SytoEB) consisting of two fluorescent dyes, Syto13 (Molecular Probes, Eugene, OR, USA) and ethidium bromide (Sigma-Aldrich, Mississauga, ON, Canada), was used to assess membrane integrity. Syto is a DNA/RNA binding stain that is permeant to virtually all cell membranes and fluoresces green upon excitation by UV wavelengths. Ethidium bromide (EB) only permeates into cells with damaged plasma membranes, exhibiting red fluorescence upon UV exposure. The combination of these two dyes creates a binary assay where membrane intact cells exhibit green fluorescence and membrane compromised cells exhibit red fluorescence. The SytoEB assay was prepared using 1x phosphate buffered saline (PBS), and aliquots of Syto13 and EB diluted from stock solutions. The final dye combination was comprised of 25 μM of EB and 12.5 μM of Syto13 in a 1 mL solution, where 0.1 mL of dye was added to a 1 mL aliquot of HUVECs in

suspension and incubated for 2 minutes at room temperature before analysis.

Assessments of membrane integrity of HUVEC controls at room temperature and after plunging into liquid nitrogen using flow cytometry is shown in figure A-1. A contour plot of cell events on a diagram of the intensity of green fluorescence (Syto13, x-axis) versus the intensity of red fluorescence (EB, y-axis) was used to assess HUVEC membrane integrity. Contours depict the regions of concentrated events by color; where red, green, blue, and purple contours contain high, moderate, low, and very low densities of cells respectively (figure A-1). Control samples at room temperature (figure A-1A) show a majority of membrane intact cells with high green fluorescence ($82.1 \pm 1.0 \%$), and only a few compromised cells with high red fluorescence ($17.9 \pm 1.0 \%$). These results with the flow cytometer can be compared to results obtained with the fluorescence microscope that also showed control samples having a majority of membrane intact cells ($84.6 \pm 4.8 \%$) and plunged samples having a majority of membrane compromised cells ($15.4 \pm 1.1 \%$). The similarities in the obtained values of membrane integrity under both control conditions with these two different instruments (fluorescence microscopy and flow cytometry) was used as a verification that graded freezing results for HUVEC obtained with the fluorescence microscope and flow cytometer could be directly compared.

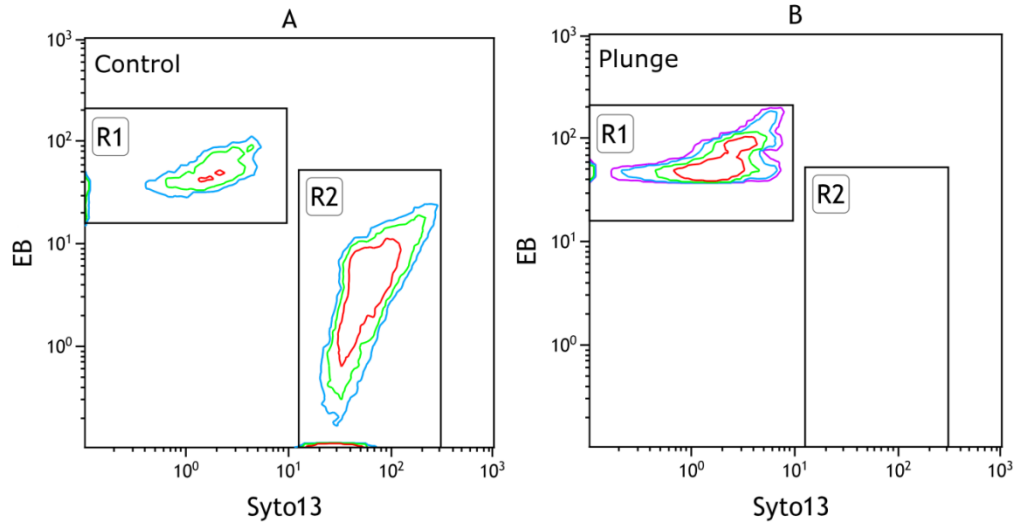


Figure A-1. Contour plots of HUVEC membrane integrity analysis with SytoEB. Showing regions of high (red contours), moderate (green contours), low (blue contours), and very low (purple contours) number of cells measured by flow cytometry

A) Control samples

B) Samples plunged in liquid nitrogen (-196°C)